Estimating Latest Cretaceous and Tertiary Atmospheric CO_2 Concentration from Stomatal Indices

Dana L. Royer

2002

The role of atmospheric CO_2 in determining climate is important for understanding patterns in the geologic record and predicting future climate. Because of the recent anthropogenic rise in temperatures, the role of CO_2 in globally warm periods is particularly important for any predictions of future climate change. Here, I reconstruct the concentration of atmospheric CO_2 using patterns of stomatal index in the plant cuticles of *Ginkgo* and *Metasequoia* for two globally warm intervals, the latest Cretaceous to early Eocene (66-53 Ma) and the middle Miocene (17-15 Ma).

Most vascular C_3 plants show an inverse relationship between the stomatal index in their leaves and the level of atmospheric CO_2. Stomatal index (SI) has been shown experimentally and in the field to be largely independent of every environmental factor (e.g., water stress) except CO_2. There is a potential, then, to use patterns in SI as a proxy for ancient levels of atmospheric CO_2. One drawback to SI-CO_2 relationships is that they are generally species-specific. Modern *Ginkgo* and *Metasequoia* are unusual because both have morphologically identical forms back to the Early and Late Cretaceous, respectively. In addition, at least in the case *Ginkgo*, its sedimentological and floral associations remain stable throughout the Cenozoic. Thus, both *Ginkgo* and *Metasequoia* represent excellent taxa for applying this CO_2 proxy back into the Cretaceous.

Based upon dated herbaria sheets, which document the anthropogenic rise in CO_2, and saplings grown in greenhouses at ambient and elevated CO_2 (350-800 ppmV), the SI-CO_2 relationships for *Ginkgo* and *Metasequoia* were determined. These relationships were then applied to fossil cuticles of *Ginkgo* and *Metasequoia* from 30 sites in order to reconstruct CO_2. The resulting reconstruction indicates near present-day levels of CO_2 (300-450 ppmV) for both the early Paleogene and middle Miocene. This suggests that other radiative forcings were more important during these intervals than they are today, and that these intervals may not serve as good analogs for understanding future climate change.

Estimating Latest Cretaceous and Tertiary Atmospheric CO_2 Concentration from Stomatal Indices

A Dissertation
Presented to the Faculty of the Graduate School
of
Yale University
in Candidacy for the Degree of
Doctor of Philosophy

By
Dana L. Royer

Dissertation Directors: Robert A. Berner and Leo J. Hickey

May 2002

TABLE OF CONTENTS

Appendices

LIST OF FIGURES AND TABLES

ACKNOWLEDGEMENTS

As the old cliché goes, I am standing on the shoulders of giants. Estimates of paleo-CO_2 are not meaningful unless they can be placed into a temporal framework. My work therefore relies upon robust pre-existing stratigraphic frameworks. Secondly, and more obviously, stomatal-based estimates of paleo-CO_2 are not possible unless there are fossil cuticles to be measured. My work therefore also relies upon museum collections of cuticles and well-scouted field areas for which I can visit and have reasonable chances of success for extracting fossil cuticle. Both of these requirements were met in spades in the Bighorn Basin. It is not a coincidence that the bulk of my data come from this basin. I am deeply indebted to the countless workers of stratigraphy, biostratigraphy (vertebrate paleontology, paleobotany, and palynology), magnetostratigraphy, and chronostratigraphy who, over the last 100+ years, have mapped out this basin to a degree perhaps unmatched in the world. I also thank the paleobotanists of the Bighorn Basin (in particular, Leo Hickey and Scott Wing) who have brought back truckloads of plant fossils and detailed fieldnotes to return for more. I think that my study serves as an example of what can been achieved in areas where the stratigraphy and “stamp book collecting” (i.e., the hard stuff, in my opinion) have been well done.

I thank the following people for their help and kindness: Bob Berner for introducing me to the stomatal method, and for keeping me honest along the way; Leo Hickey for balancing the roles of advisor and field assistant, and for valuable discussions about the geology of the Bighorn Basin and the paleoecology of ginkgo; Bill Chaloner, Jenny McElwain, and Dave Beerling for teaching me the proper lab techniques for extracting plant cuticle and measuring stomatal indices; Scott Wing for making both his collections of ginkgo cuticle at the Smithsonian Institution and ginkgo cuticle-bearing field sites available to me for study, for assistance in the field and allowing me to stay at his field camp (summer 2000), for making unpublished paleoecological data available to me, and for thorough and insightful reviews of chapters 2 and 3; Colin Osborne for maintaining the greenhouse experiments at the University of Sheffield; Kirk Johnson for making pre-publication paleoecological data available to me; Bill Rember for guiding Leo Hickey and me to *Ginkgo* and *Metasequoia*-bearing plant fossil sites in the Latah Formation, and for hosting us in his home for several days; Amanda Ash for preparing fossil cuticle from specimens at the Smithsonian Institution, and for (along with the rest of the Scott Wing field crew of 2000) field assistance; Walton Green for field assistance and a helpful review of chapter 2; Ben LePage for his assistance on Axel Heiberg Island, and for his general knowledge of Taxodiaceae; Graeme Berlyn for his useful courses on plant anatomy and plant physiology, of which chapter 1 began as a term paper in one; Steve Wofsy for providing raw CO_2 data from the Harvard Forest; Jay Emerson and Tim Gregoire for statistical help; and Jenny Carroll for useful reviews of chapters 1 and 2, and for emotional support.

I thank the following museum workers for loaning herbarium sheets: James Solomon (Missouri Botanical Garden); Brent Mishler (University of California Herbarium); Kevin Conrad (National Herbarium); Cindy McWeaney and Michael Donoghue (Yale Peabody Museum); Lynn Heilman (Morris Arboretum); and Kerry Barringer (Brooklyn Botanical Garden). Finally, I thank the following museum workers for loaning plant fossil specimens: Scott Wing and Amanda Ash (National Museum of Natural History / Smithsonian Institution); Linda Klise (Yale Peabody Museum); Kirk Johnson and Rich Barclay (Denver Museum of Nature and Science); Franz-Josef Lindem and Svein Manum (Oslo Paleontological Museum); Paul Davis and Paul Kenrick (British Natural History Museum); Heidi Schwab and Ruth Stockey (University of Calgary); Steve Manchester and David Jarzen (Florida Museum of Natural History); and Michael Nowak (University of Wisconsin-Stevens Point).

This work was funded by an NSF Graduate Research Fellowship and Department of Energy grant DE-FGO_2-95ER14522.

NOTE ON FORMATTING

All of my dissertation chapters have been published elsewhere. Care has been taken to balance any standardization of formatting with preserving the content of the chapters. The published references for the chapters are as follows:

Chapter 1

Royer, D.L., 2001. Stomatal density and stomatal index as indicators of paleoatmospheric CO_2 concentration. Review of Palaeobotany and Palynology, 114: 1-28.

Chapter 2

Royer, D.L., Hickey, L.J., Wing, S.L., 2002. Ecological conservatism in the "living fossil" *Ginkgo*. Paleobiology (in review).

Chapter 3

Royer, D.L., Wing, S.L., Beerling, D.J., Jolley, D.W., Koch, P.L., Hickey, L.J., Berner, R.A., 2001. Paleobotanical evidence for near present-day levels of atmospheric CO_2 during part of the Tertiary. Science, 292: 2310-2313.

Chapter 4

Royer, D.L., 2002. Estimating latest Cretaceous and Tertiary PCO_2 from stomatal indices. Geological Society of America Special Paper (in review).

INTRODUCTION

It is the purpose of this study to reconstruct the concentration of paleoatmospheric CO_2 from patterns in the stomatal index (SI) in the fossil cuticles of *Ginkgo adiantoides* and *Metasequoia occidentalis*. CO_2 is an important greenhouse gas, and so understanding the role(s) CO_2 plays in regulating global climate lends insight into understanding the dynamics of the biosphere in the geologic rock record and aids in predicting future climate change.

This study is divided into four discrete chapters. In Chapter One I analyze a compilation of published stomatal responses (both stomatal density and stomatal index) to changes in atmospheric CO_2. Several confounding factors that may influence the stomata-CO_2 relationship have been suggested in the past, and I discuss these in light of this new compilation. The general reliability of this relationship in terms of its application into the geologic past as a CO_2 proxy is discussed in detail. In addition, this chapter serves as a general introduction into stomatal densities and stomatal indices and why they respond to changes in atmospheric CO_2.

Chapter Two is a paleoecological study of Tertiary *Ginkgo*. This ecological dataset includes most of the sites for which I measured stomatal indices from *Ginkgo* cuticle. In addition to some peculiar ecological patterns that may shed light on pre-angiospermous Mesozoic paleoecology, this study provides important constraints on the reliability of *Ginkgo* as a paleo-CO_2 indicator. These constraints are discussed more fully in the final two chapters.

In Chapter Three I present the training sets of *Ginkgo biloba* and *Metasequoia glyptostroboides*. These data stem both from dated herbaria sheets from the last 145 years where CO_2 has risen exponentially from 280 ppmV to (as of 2001) 370 ppmV, and from plant saplings growing in CO_2-controlled greenhouses ranging from 350 ppmV to 800 ppmV. I then inverted the regressions in these training sets and applied them to measurements of SI from fossil *Ginkgo* and *Metasequoia* dating to the early Paleogene (58-53 Ma) and middle Miocene (17-15 Ma). I conclude by discussing the implications of my CO_2 reconstruction for these two intervals, both of which are considered to represent periods of global warmth relative to today.

In Chapter Four I expand on both the data of Chapter Three and its implications for ancient and future climates. I present SI data back to the latest Cretaceous (66 Ma), and then discuss how the combined CO_2 reconstruction bears on the role CO_2 played during these globally warm periods.

CHAPTER 1

Stomatal density and stomatal index as indicators of paleoatmospheric CO_2 concentration

1.1 Introduction

The increase in atmospheric CO_2 concentration since industrialization (Friedli et al., 1986; Keeling et al., 1995) and the predicted continued increase into the near future (Houghton et al., 1995) forces the need to understand how the biosphere operates under elevated (relative to pre-industrial) CO_2 levels. The geologic record affords a wealth of such information. Fundamental to the use of the geologic record, however, is a reliable estimate of CO_2 concentration throughout the intervals of interest. The results of a computer-based model for the Phanerozoic (Berner, 1994; see Fig. 1.1), based on rates of Ca-Mg silicate weathering and burial as carbonates, weathering and burial of organic carbon, CO_2 degassing, vascular land plant evolution, and solar radiation, have gained wide acceptance (e.g., Retallack, 1997; Kump et al., 1999). Proxy data are still crucial, however, for both testing and refining this model. Currently used proxies include $\delta^{13}C$ from pedogenic carbonates (Cerling, 1991, 1992; Mora et al., 1991, 1996; Ekart et al., 1999), $\delta^{13}C$ from trace carbonates contained within goethite (Yapp and Poths, 1992, 1996), $\delta^{13}C$ from phytoplankton (Freeman and Hayes, 1992; Pagani et al., 1999a, 1999b), and $\delta^{11}B$ from planktonic foraminifera (Pearson and Palmer, 1999). To a first approximation, these proxies largely support the model of Berner (1994) (Fig. 1.1). A discrepancy exists during the late Carboniferous and early Permian between the pedogenic carbonate-derived data of Ekart et al. (1999) and the model of Berner (1994). However, this discrepancy disappears if the $\delta^{13}C$ values for marine carbonates of Popp et al. (1986) are used during this time interval instead of those of Veizer et al. (1999) in calculating CO_2 from the data of Ekart et al. (1999) (R.A. Berner, unpublished data; see Fig. 1.1B).

Another emerging proxy relies on the plant species-specific inverse relationship between atmospheric CO_2 concentration and stomatal density and/or stomatal index. Concerns have been raised regarding this method's reliability (Körner, 1988; Poole et al., 1996), and it is the purpose of this chapter to address these concerns via an extensive analysis of the literature. Analysis includes stomatal responses from fossil observations as well as short-term (experimental, natural CO_2 springs, altitudinal transects, and herbaria) observations, as responses from the latter category are often used to generate standard curves for estimating CO_2 from fossil observations (van der Burgh et al., 1993; Beerling et al., 1995; Kürschner, 1996; Kürschner et al., 1996; Rundgren and Beerling, 1999; Wagner et al., 1999). Specifically, the utility of stomatal indices will be examined, an approach not analyzed in previous reviews (Beerling and Chaloner, 1992, 1994; Woodward and Kelly, 1995).

1.2 Mechanism controlling stomatal density

Stomata are pores on leaf surfaces through which plants exchange CO_2, water vapor, and other constituents with the atmosphere. They form early in leaf development, and typically mature by the time the leaf reaches 10-60% of its final leaf size (Tichá,

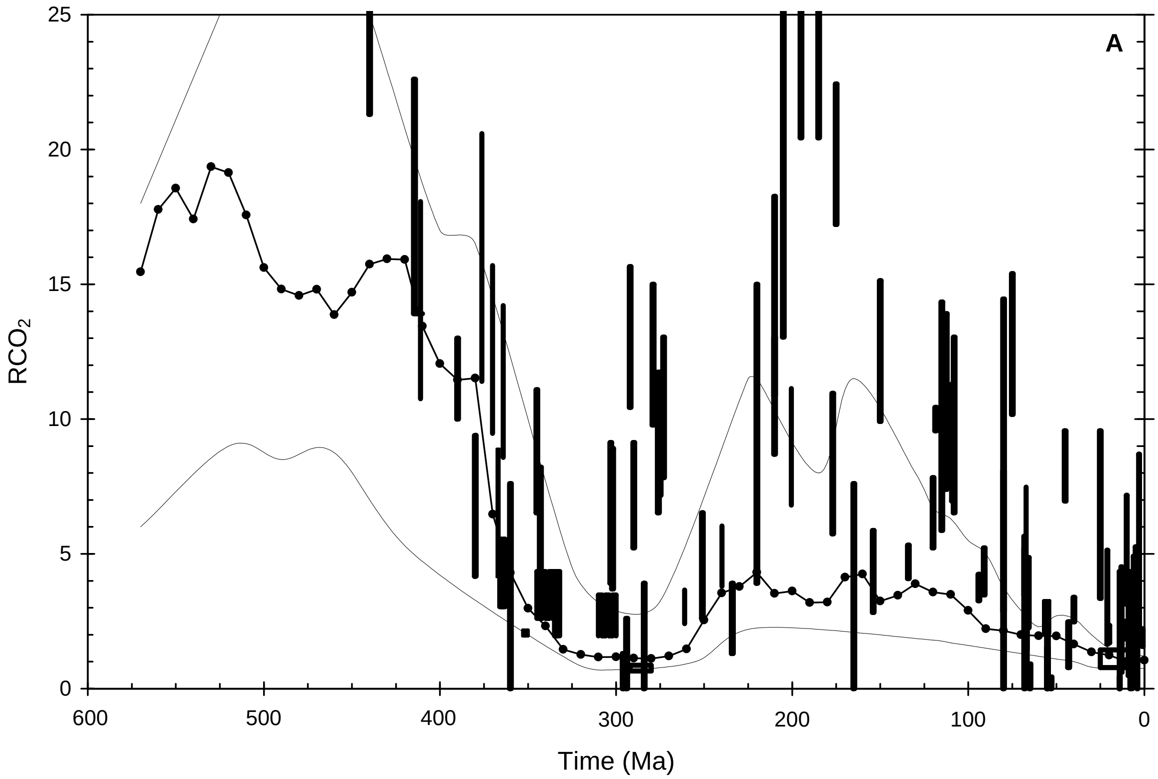

Figure 1.1. Atmospheric CO_2 versus time for the Phanerozoic. RCO_2 = ratio of mass of paleo-CO_2 to time-averaged pre-industrial value (230 ppmV, the mean CO_2 over at least the last 400 k.y. (Petit et al., 1999)). The centerline joining filled circles (10 m.y. time steps) represents the best estimate from the model of Berner (1994, 1998). The two straddling lines represent error estimates based on sensitivity analyses. Boxes in (A) represent 100 non-stomatal-based proxy estimates of varying RCO_2 resolution (data from Suchecky et al., 1988; Platt, 1989; Cerling, 1991, 1992; Freeman and Hayes, 1992; Koch et al., 1992; Muchez et al., 1993; Sinha and Stott, 1994; Andrews et al., 1995; Ghosh et al., 1995; Mora et al., 1996; Yapp and Poths, 1996; King, 1998; Ekart et al., 1999; Elick et al., 1999; Lee, 1999; Lee and Hisada, 1999; Pagani et al., 1999a, 1999b; Pearson and Palmer, 1999; Cox et al., 2001; Ghosh et al., 2001).

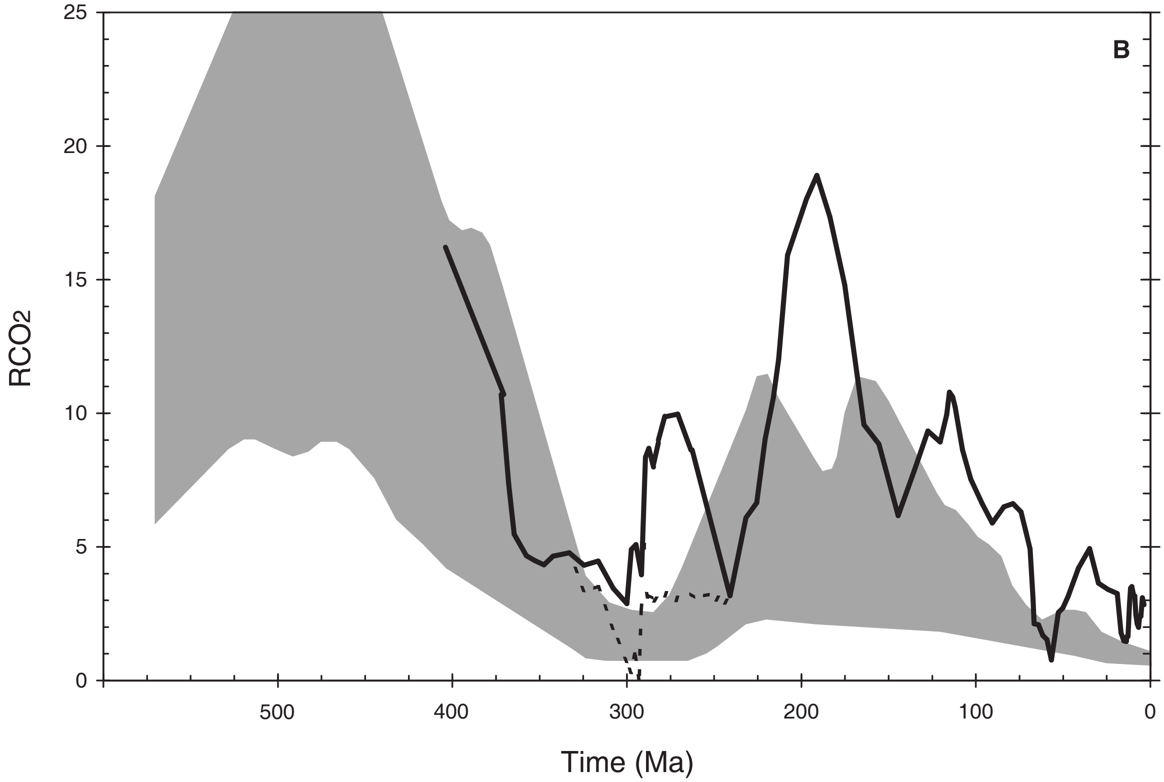

Fig. 1.1 con't. The heavy line in (B) is a five point running average of the mean RCO2 of every box in (A). This approach smoothes short-term CO2 fluctuations and is more directly comparable with the model of Berner (1994, 1998). The dashed line in (B) is a five point running average incorporating a recalculation of Ekart et al. (1999) data during the late Carboniferous and early Permian using the marine carbonate δ13C data of Popp et al. (1986) (see text for details).

1982). Thus, the timing for the mechanism(s) of stomatal initiation lies early in leaf ontogeny (Gay and Hurd, 1975; Schoch et al., 1980). Currently, no mechanism or combination of mechanisms adequately explains the expression of stomatal initiation, although genetic work may provide insights in the near future (e.g., Berger and Altmann, 2000). Proposed mechanisms include irradiance (Gay and Hurd, 1975; Schoch et al., 1980), humidity (Salisbury, 1927), and PCO_2 (Woodward, 1986; Beerling and Chaloner, 1992; Woodward and Kelly, 1995; Beerling and Woodward, 1996).

A common theory for why CO_2 should (partially) control stomatal initiation is as follows (e.g., Woodward, 1987). Water vapor and CO_2 constitute the two main fluxes across the leaf epidermis. It is generally advantageous for plants to conserve water loss while maximizing CO_2 uptake, two typically antithetical processes. As CO_2 rises for a given water budget, for example, a plant can 'afford' to reduce its stomatal conductance without suffering a reduction in carbon assimilation rates. Two main pathways driving this response are smaller stomatal pores (Bettarini et al., 1998) and a reduction in stomatal numbers (Woodward, 1987). Conversely, a drop in CO_2 requires an increase in stomatal conductance to maintain assimilation rates, but at the cost of increased water loss.

1.2.1 Stomatal index

Stomatal density (SD) is a function of both the number of stomata plus the size of the epidermal cells. Thus, SD is affected both by the initiation of stomata and the expansion of epidermal cells. This expansion is a function of many variables (e.g., light, temperature, water status, position of leaf on crown, and intra-leaf position), and can overprint the signal reflective of stomatal initiation. As it turns out, CO_2 plays a stronger role in stomatal initiation than in epidermal cell expansion (this is discussed in detail below). Salisbury (1927) introduced the concept of stomatal index (SI), which normalizes for the effects of this expansion (i.e., density of epidermal cells). It is defined as:

$$\mathrm{SI}(\%) = \frac{\text{stomatal density}}{\text{stomatal density} + \text{epidermal cell density}} \times 100$$

where stomata consist of the stomatal pore and two flanking guard cells.

1.2.2 C_4 plants

The fundamental photosynthetic differences between C_3 and C_4 plants have consequences for stomatal-based CO_2 reconstructions. Carbon in C_3 plants is fixed within the spongy and palisade mesophyll where CO_2 concentrations (c_i) are approximately 70% of the atmospheric value. As atmospheric CO_2 fluctuates, so too does c_i to maintain this ~0.7 ratio (Polley et al., 1993; Ehleringer and Cerling, 1995; Beerling and Woodward, 1996; Bettarini et al., 1997). Thus the stomatal pore area is sensitive to changing atmospheric CO_2 levels. C_4 plants, in contrast, fix carbon within their bundle sheath cells. The endodermis enclosing these bundle sheath cells is highly impervious to CO_2, and consequently CO_2 concentrations within these cells can reach 1000-2000 ppmV (Lambers et al., 1998). One would therefore anticipate, based on the proposed mechanism between CO_2 and stomatal initiation discussed above, that even moderate changes in atmospheric CO_2 have little influence on stomatal pore area and, by extension, stomatal density and stomatal index (Raven and Ramsden, 1988). Of the 9 responses derived from C_4 plants documented here, only 1 inversely responds to CO_2 (see Appendix 1.1). This marked insensitivity in C_4 plants lends indirect support for the proposed mechanism. Because of the above physiological reasons, none of the analyses considered here include responses from C_4 plants.

1.3 Stomatal density and stomatal index as CO_2 indicators

A database consisting of 285 SD responses and 145 SI responses to variable CO_2 concentrations was compiled to elucidate salient patterns (Appendices 1.1-1.3). 176 species are represented. This database is an expansion of previous reviews (Beerling and Chaloner, 1994; Woodward and Kelly, 1995) and includes, for the first time, stomatal indices.

Each response was first placed in one of three categories: experimental, subfossil, and fossil. Experimental responses stem from experimentally controlled CO_2 environments, typically in greenhouses, which last from 14 days to 5 years in length. For studies that measured SD and/or SI at several different times and/or CO_2 levels, typically only the response corresponding to the longest exposure time and highest CO_2 level was used. Most subfossil responses stem from dated herbarium specimens (from the last 240 years), where corresponding CO_2 concentrations are known from ice core data (Neftel et al., 1985; Friedli et al., 1986). Data from altitudinal transects and natural CO_2 springs are also placed in the subfossil category, as this category represents the closest match in terms of CO_2 exposure time. Finally, fossil responses consist of well-dated fossil material. Methods for obtaining reference CO_2 concentrations for the fossil responses are discussed below.

Each response was assigned as either increasing ($P < 0.05$), decreasing ($P < 0.05$), or remaining the same ($P > 0.05$) relative to controls. Where P-values were not reported, a test for overlapping standard deviations was used, which typically yields a conservative estimate for statistical significance (relative to the $\alpha = 0.05$ level).

1.3.1 Experimental responses

127 SD and 74 SI responses from a pool of 68 species are represented here. For stomatal density, 40% of the experimental responses inversely respond (at the $\alpha = 0.05$ level) to CO_2; the proportion for stomatal indices is similar (36%) (Table 1.1).

Plants exposed to subambient CO_2 are more likely to inversely respond than plants exposed to elevated CO_2 for both SD (50% vs. 39%; $P = 0.36$) and SI (89% vs. 29%; $P < 0.001$). These results support previous claims that plants more strongly express the CO_2-SD/SI inverse relationship when exposed to subambient versus elevated CO_2 concentrations (Woodward, 1987; Woodward and Bazzaz, 1988; Beerling and Chaloner, 1993a; Kürschner et al., 1997). A common explanation for this CO_2 'ceiling' phenomenon is that plants today have not experienced elevated CO_2 levels (350+ ppmV) for at least the entire Quaternary and possibly longer (Pagani et al., 1999a; Pearson and Palmer, 1999). Thus, for short time scales where only plant plasticity is tested, plants respond more favorably to CO_2 conditions which they most recently experienced, namely subambient concentrations (Woodward, 1988; Beerling and Chaloner, 1993a). The implication for stomatal-based CO_2 reconstructions is that experimental evidence based on elevated CO_2 treatments may not reflect the reliability of the method. Over 85% of the experimental

Table 1.1
Statistical summary of stomatal responses to changing CO_2 concentrations

	Experimental				Subfossil				Fossil				Combined			
	SD[a]		SI[b]		SD		SI		SD		SI		SD		SI	
	%[c]	(*n*)	%	(*n*)	%	(*n*)	%	(*n*)	%	(*n*)	%	(*n*)	%	(*n*)	%	(*n*)
total	40	(127)	36	(74)	50	(133)	34	(35)	88	(25)	94	(36)	49	(285)	50	(145)
elevated CO_2[d]	39	(109)	29	(65)	-	-	-	-	100	(13)	96	(24)	45	(232)	41	(116)
subambient CO_2	50	(18)	89	(9)	-	-	-	-	89	(9)	89	(9)	75	(40)	88	(25)
opposite response[e]	9	(127)	4	(74)	11	(133)	9	(35)	12	(25)	3	(36)	11	(285)	5	(145)
hypostomatous[f]	59	(27)	65	(17)	50	(80)	38	(24)	-	-	-	-	56	(121)	69	(70)
amphistomatous[g]	36	(90)	27	(55)	49	(49)	25	(8)	-	-	-	-	44	(149)	32	(71)
abaxial	40	(45)	24	(29)	41	(22)	-	-	-	-	-	-	41	(68)	21	(33)
adaxial	29	(42)	31	(26)	55	(22)	-	-	-	-	-	-	38	(65)	33	(30)
experiments using OTCs[h]	13	(31)	13	(24)	-	-	-	-	-	-	-	-	-	-	-	-
experiments using greenhouses	48	(95)	48	(50)	-	-	-	-	-	-	-	-	-	-	-	-
herbarium studies only	-[j]	-	-	-	57	(93)	89	(9)	-	-	-	-	-	-	-	-
repeated species[i]	-	-	-	-	-	-	-	-	-	-	-	-	57	(28)	55	(11)

[a] stomatal density
[b] stomatal index
[c] percentage of responses inversely correlating with CO_2
[d] CO_2 concentrations are higher than controls
[e] percentage of responses positively correlating with CO_2
[f] leaves with stomata only on abaxial (lower) side
[g] leaves with stomata on both surfaces
[h] OTC = open-top chamber; typically cone-shaped with an open top
[i] for species with multiple responses with ≥1 inversely correlating with CO_2, percentage that consistently inversely correlate
[j] not applicable or sample size too small for meaningful comparison

responses analyzed here stem from elevated CO_2 treatments. Another related concern raised with experimental results is that CO_2 is shifted in one step in contrast to the smoother, longer-term trend in nature (Beerling and Chaloner, 1992; Kürschner et al., 1997).

An alternative explanation for the CO_2 ceiling is that while CO_2 is limiting for photosynthesis at CO_2 concentrations below present day levels, it is not limiting at elevated levels. Therefore, for example, if CO_2 decreases in a subambient CO_2 regime (where CO_2 is limiting for photosynthesis), a mechanism exists to increase stomatal pore area and, by extension, CO_2 uptake. The same may not be true at elevated CO_2 concentrations if CO_2 is not limiting for photosynthesis under such conditions (Wagner et al., 1996; Kürschner et al., 1998). Empirical data do not strongly support this alternative hypothesis. While assimilation rates generally decrease at subambient CO_2 levels (Polley et al., 1992; Robinson, 1994), they also typically increase in response to CO_2 concentrations of at least 700 ppmV (Long et al., 1996; Curtis and Wang, 1998). CO_2 therefore usually continues to limit photosynthesis in most plants above present day CO_2 levels, even if the effects of this excess CO_2 are partially mediated by a reduction in photorespiration and enhancement in RuBP regeneration (the primary substrate used to fixed CO_2 in C_3 plants), and so only affect photosynthesis indirectly. Therefore, there is no reason to expect a CO_2 ceiling coincident with current CO_2 levels. It is likely, however, that the rate of change in assimilation rates is reduced at elevated CO_2 concentrations (Farquhar et al., 1980), which could reduce the sensitivity of SD and SI responses under such conditions.

Experimental manipulations are usually conducted in either enclosed greenhouses or open-top chambers (OTCs). Most OTCs have less control over humidity and temperature. Significant ‘chamber effects’ have been detected for stomatal parameters (Knapp et al., 1994; Apple et al., 2000), and results generated here support such claims. Plants in OTCs inversely respond to CO_2 in far fewer cases than greenhouse grown plants for both SD (13% vs. 48%; $P < 0.001$) and SI (13% vs. 48%; $P < 0.01$). Thus, it appears OTCs introduce confounding factors and should be avoided in stomatal density/index work.

Although the proportion of experimental responses inversely responding to CO_2 may appear low (40% and 36% for SD and SI, respectively), in part from the factors discussed above, it is important to note that the percentage of responses showing a positive relationship ($P < 0.05$) is very low (9% and 4% for SD and SI, respectively). Thus, the vast majority of plants either respond inversely to experimental exposure to CO_2 or do not respond at all.

1.3.2 Subfossil responses

133 SD and 35 SI responses from a pool of 95 species are represented here. For stomatal density, 50% of the subfossil responses inversely relate (at the $\alpha = 0.05$ level) to CO_2. Thus, subfossil responses, which are based on longer exposure times, more often inversely relate to CO_2 than do experimental responses (50% vs. 40%; $P = 0.11$). For stomatal index, only 34% of the responses show a significant inverse relationship, however the sample size is disproportionally small ($n = 35$) (Table 1.1).

As outlined above, three types of studies comprise the subfossil responses: altitudinal transects, natural CO_2 springs, and herbaria. If only herbarium responses are analyzed ($n = 93$ and $n = 9$ for SD and SI, respectively), the proportion showing an inverse response to CO_2 improves to 57% and 89%, respectively. Responses from altitudinal transects and natural CO_2 springs may therefore be of less value for paleo-CO_2 reconstructions. This dichotomy in response fidelity may be an expression of the CO_2 ceiling phenomenon discussed above. As CO_2 levels rose to current levels over the last 240+ years, the majority of plants (57% and 89% for SD and SI, respectively) responded with significant decreases in SD and/or SI. At higher CO_2 levels, however, as expressed near natural CO_2 springs, a smaller proportion of plants responded with lower SD (30%; n = 30) and/or SI (16%; n = 25). If, on the other hand, current CO_2 concentrations do *not* represent a true genetic ceiling for plants, than these data show that the majority of plants cannot adapt to CO_2 levels above today's within the special residence time near natural CO_2 springs (10^2-10^3 years?).

In accordance with the experimental responses, a very small proportion of the subfossil observations positively respond to CO_2 (11% and 9% for SD and SI, respectively). Most plants either inversely respond to CO_2 or do not respond at all. If CO_2 exerts any influence on stomatal initiation, it must be of an inverse behavior.

1.3.3 Fossil responses

25 SD and 36 SI responses from a pool of 28 species are represented here. For stomatal density, 88% of the observations show an inverse relationship (at the $\alpha = 0.05$ level) to CO_2; for stomatal index, the proportion is 94% (Table 1.1). Only 12% and 3% of the observations positively respond to CO_2 for SD and SI, respectively. Thus, the robustness of the SD/SI method improves with increased CO_2 exposure time (Fig. 1.2), supporting earlier hypotheses (Beerling and Chaloner, 1992, 1993a).

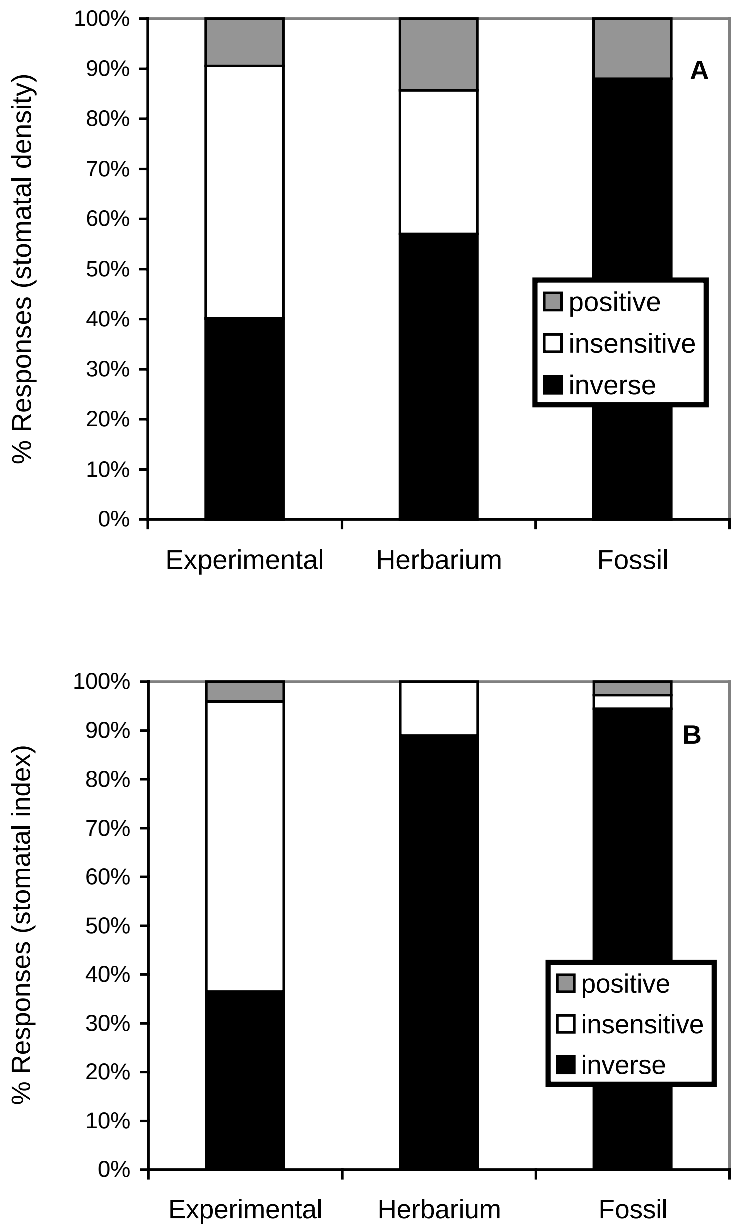

Figure 1.2. The percentage of responses for (A) stomatal density and (B) stomatal index that inversely relate to CO_2 ('inverse'), show no significant change to CO_2 (‘insensitive’), or response positively to CO_2 (‘positive’) in each of three categories. Note that only herbarium responses compose the subfossil category.

Qualitatively, the transition between dominance of stomatal response by plasticity within a given gene pool and genetic adaptation appears to occur for most plants between 10^2 and 10^3 years (i.e., intermediate between CO_2 exposure times typical for subfossil and fossil responses). This conclusion hinges on the assumption that CO_2 exerts a consistent genetic pressure on stomatal initiation, and given sufficient exposure time will overprint the smaller scale plastic responses (including changes in individual stomatal pore size). The fact that the increase in responses showing an inverse relationship to CO_2 as a function of exposure time comes at the expense of insensitive responses (Fig. 1.2) supports this assumption. 10^2 to 10^3 years is slightly longer than previous estimates (Beerling and Chaloner, 1993a), and should give rise to some caution in using experimental and subfossil responses in paleo-CO_2 reconstructions (i.e., comparing responses due mainly to plasticity versus genetic adaptation).

The fossil data cast doubt on the notion that stomata cannot respond to CO_2 concentrations above present day levels. The proportion of fossil responses showing an inverse relationship based on subambient CO_2 exposure are nearly equal to those fossil observations based on elevated CO_2 exposure for both SD (89% and 100%, respectively) and SI (89% and 96%, respectively), although sample sizes are fairly small (Table 1.1). Some groups of plants respond to CO_2 levels of at least 2700 ppmV (McElwain and Chaloner, 1995; Appendix 1.3). This result does not discount, however, that stomatal parameters may be less *sensitive* at elevated than at subambient (relative to today) CO_2 levels. The CO_2 ceiling observed in experimental responses therefore appear to stem from the short-term inability of plants to respond to elevated CO_2, not a long-term genetic limit. Interestingly, Woodward (1988) noted that plants with short generation times (e.g., annuals) are often capable of decreasing their stomatal densities when experimentally exposed to elevated CO_2 levels (for ≥1 year), probably because of their quicker genetic adaptation rates (Woodward, 1988). This suggests that the exposure time required to mitigate the CO_2 ceiling may not be much beyond typical experimental exposure times, and in fact may not exist at all for some plants.

Caution is urged with regard to several features concerning the fossil responses. First, in several studies stomatal comparisons between fossil and modern plants were made with two separate but ecologically equivalent sets of species (McElwain and Chaloner, 1995, 1996; McElwain, 1998; McElwain et al., 1999). In addition to the long-term influence of CO_2 on SD and SI for a given species, it has also been shown, for example, that high CO_2 selects for groups of plants with lower mean stomatal densities/indices (Beerling and Woodward, 1996; Beerling and Woodward, 1997) (Fig. 1.3). Thus, it is not particularly surprising that stomatal densities and indices from times of high CO_2 are lower than for ecologically equivalent modern species. Ideally, these two effects should be kept separate.

Second, estimates of CO_2 for the fossil responses are invariably not as accurate as those estimates for experimental and subfossil responses. Ice core derived data are used for the last 150 k.y., and the model of Berner (1994) or other proxy data are most often used for pre-ice core responses. In particular, estimates from Berner's curve are highly approximate due to its sizable error envelope and coarse 10 m.y. time resolution (see Fig. 1.1); brief but large CO_2 excursions discernable with the various proxy methods are probably too temporally constrained to influence Berner's model (Montañez et al., 1999). In cases where experimental and subfossil responses are used to generate a standard curve upon which CO_2 concentrations are directly calculated from fossil responses, ice core data (Beerling et al., 1995; Wagner et al., 1999; Rundgren and Beerling, 1999) or the presence

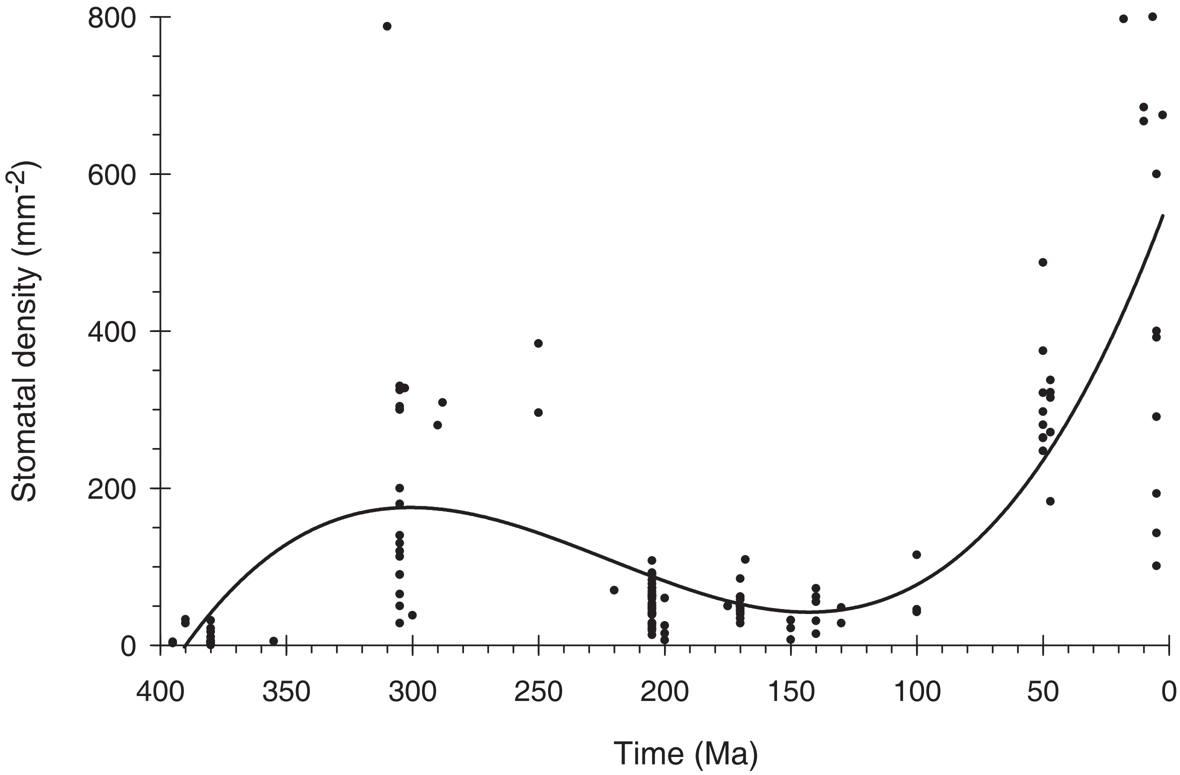

Fig. 1.3. Stomatal density versus time for the Phanerozoic. Redrawn from Beerling and Woodward (1997), with additional data plotted from McElwain and Chaloner (1996), Edwards et al. (1998), McElwain (1998), Cleal et al. (1999), and McElwain et al. (1999). Regression is a third order polynomial (*r2* = 0.57; *n* = 132). Compare trend with Fig. 1.1.

of temperature excursions (van der Burgh et al., 1993; Kürschner, 1996; Kürschner et al., 1996) are used to corroborate the stomatal-based estimates.

1.3.4 Combined data set

Based on the combination of the above three categories, both SD and SI inversely correlate with CO_2 c. 50% of the time (n = 285 and 145, respectively) (Table 1.1). Very rarely do the responses positively correlate with CO_2 (11% and 5% for SD and SI, respectively). For species that have been analyzed repeatedly by different researchers, those that inversely respond to CO_2 tend always to respond in such a way (57% (n = 28) and 55% (n = 11) for SD and SI, respectively). Woodward and Kelly (1995) reported a similar behavior, where 76% of their sensitive species consistently responded.

Thus, although response times differ (see above and Fig. 1.2), CO_2 is highly negatively correlated with stomatal initiation. A scatterplot of all data shows an overall inverse relationship between stomatal density/index and CO_2 (Fig. 1.4A). Although the overall regression is not robust (r^2 = 0.26; n = 420), this principally stems from equivocal experimental and natural CO_2 spring data. The fossil data, when regressed independently, yield an r^2 of 0.68 (n = 59) (Fig. 1.4B). Given the species-specific and probable multi-mechanistic nature of the relationship, this regression is surprisingly robust.

Curiously, based solely on the combined results, it appears SD is equally reliable as SI as a CO_2 indicator (Table 1.1). The implications are tempting, as epidermal cells are often difficult to resolve in fossil material (Beerling et al., 1991; McElwain and Chaloner, 1996). This issue is discussed in the section below.

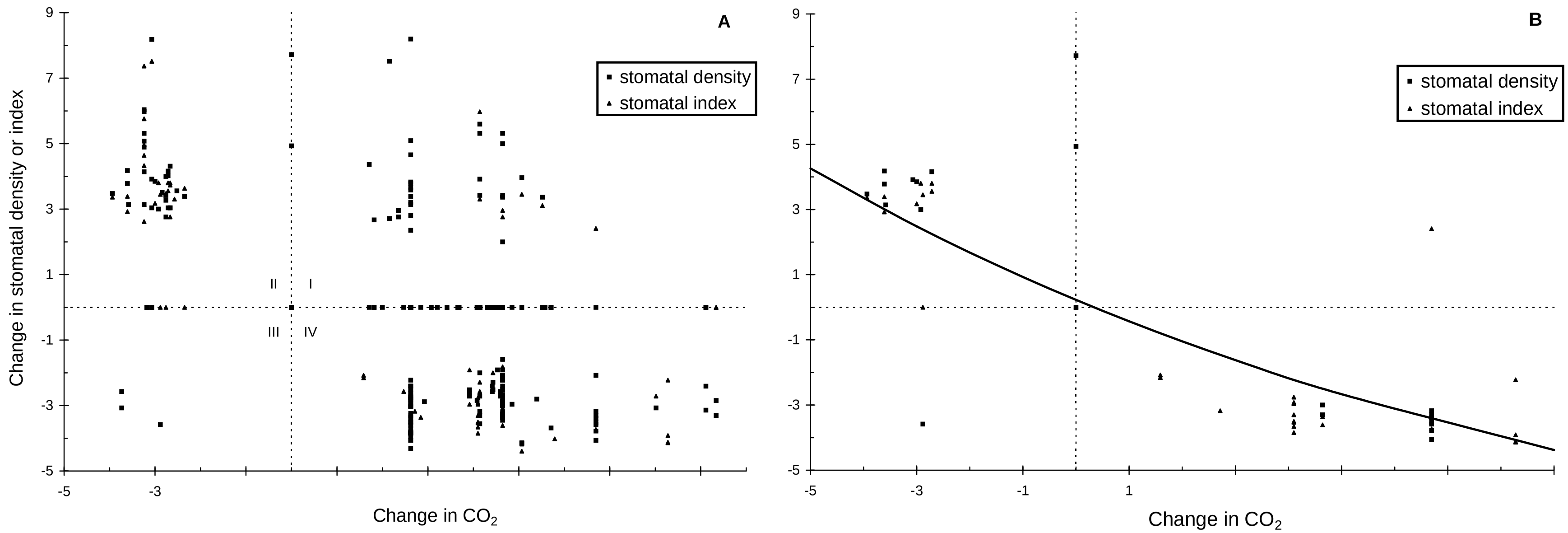

Fig. 1.4. (A) Scatterplot of all data ($r^2 = 0.26$; $n = 420$) showing the cube-root transform of percentage change in stomatal density and stomatal index in response to percentage change in atmospheric CO_2 concentration. Responses in quadrants II and IV inversely relate to CO_2 while responses in quadrants I and III positively relate. (B) Similar scatterplot for fossil data only. Regression equation of untransformed data: $y = 112.43 \times \exp(-0.0026x) - 100$. ($r^2 = 0.68$; $n = 59$).

Most vascular land plants have stomata on either both surfaces (amphistomatous) or only the abaxial (lower) surface (hypostomatous). Woodward and Kelly (1995) reported no strong differences in responses between the two leaf types, although in experimental responses amphistomatous species appeared more likely to inversely relate to CO_2. Results here indicate hypostomatous species more often inversely respond to CO_2 for both SD (56% vs. 44%; $P < 0.03$) and SI (69% vs. 32%; $P < 0.001$). For amphistomatous species, neither the abaxial nor adaxial (upper) surface yield statistically different responses (Table 1.1).

1.4 Potential confounding factors

CO_2 is likely not the sole factor determining stomatal density and stomatal index. As discussed above, SD is sensitive to both stomatal initiation and epidermal cell expansion, while SI is sensitive only to stomatal initiation. The influence of natural variability, water stress, irradiance, temperature, and other factors on stomatal parameters are briefly discussed below. More thorough reviews are given by Salisbury (1927), Tichá (1982) and Woodward and Kelly (1995).

1.4.1 Natural variability

In general, stomatal density increases from leaf base to tip (Salisbury, 1927; Sharma and Dunn, 1968, 1969; Tichá, 1982; Smith et al., 1989; Ferris et al., 1996; Zacchini et al., 1997; Stancato et al., 1999). SD also often increases from leaf midrib to margin (Salisbury, 1927; Sharma and Dunn, 1968; Smith et al., 1989), although sometimes the differences are not significant (Sharma and Dunn, 1969; Tichá 1982). In contrast, very little intra-leaf variation in SI is present (Salisbury, 1927; Rowson, 1946; Sharma and Dunn, 1968, 1969; Rahim and Fordham, 1991), although Poole et al. (1996) found significant intra-leaf variation in *Alnus glutinosa*. For amphistomatous species, the distribution of stomata are generally more uniform on the abaxial surface (Rowson, 1946; Sharma and Dunn, 1968, 1969), and so for all species typically the mid-lamina of the abaxial surface yields the least variation.

Stomatal density also increases from the basal to distal regions of the plant (Salisbury, 1927; Gay and Hurd, 1975; Tichá, 1982; Oberbauer and Strain, 1986; Zacchini et al., 1997), primarily as a consequence of decreased water potential. Decreased water potential stimulates xerophytic traits, which include smaller epidermal cells, which in turn promote closer packing of stomata, and thus increased stomatal density. Little effect is reported for SI (Rowson, 1946), although evergreen species may exhibit a significant gradient (W.M. Kürschner, personal communication, 2000). Conflated with this trend are the differences between sun and shade leaves. Again, SD is consistently higher in sun leaves while SI values remain conservative (Salisbury, 1927; Poole et al., 1996; Kürschner, 1997; Wagner, 1998) with the exception of the study of Poole et al. (1996), who found a small 7% decline in SI for shade versus sun leaves. For fossil studies, since sun leaves in allochthonous assemblages are preferentially preserved (Spicer, 1981), this issue is often not a concern even for SD-based work. For example, Kürschner (1997) observed that 90% of his Miocene *Quercus pseudocastanea* leaves were sun morphotypes.

1.4.2 Water stress

In general, water stress correlates with increased SD (Salisbury, 1927; Sharma and Dunn, 1968, 1969; Tichá, 1982; Abrams, 1994; Estiarte et al., 1994; Clifford et al., 1995; Heckenberger et al., 1998; Pääkkönen et al., 1998). Some studies, however, report no response (Estiarte et al., 1994; Dixon et al., 1995; Pritchard et al., 1998; Centritto et al., 1999). No studies report a decrease. SI consistently appears insensitive to water stress (Salisbury, 1927; Sharma and Dunn, 1968, 1969; Estiarte et al., 1994; Clifford et al., 1995).

Salisbury (1927) proposed humidity as a mechanism for controlling stomatal initiation, and thus SI. Increased humidity slightly increased SI ($P > 0.05$) for *Scilla nutans*, however Tichá (1982) concluded that humidity may actually reduce stomatal index. Sharma and Dunn (1968, 1969) found no effect. Thus, the current data are equivocal.

1.4.3 Irradiance

Not surprisingly, light intensity usually positively correlates with SD (Sharma and Dunn, 1968, 1969; Gay and Hurd, 1975; Tichá, 1982; Oberbauer and Strain, 1986; Solárová and Pospíšilová, 1988; Stewart and Hoddinott, 1993; Ashton and Berlyn, 1994; Furukawa, 1997; Zacchini et al., 1997). This response is driven (partially) by enhanced water stress. Light intensity may also positively affect stomatal index (Sharma and Dunn, 1968, 1969; Furukawa, 1997), although some report no response (Salisbury, 1927; Sharma and Dunn, 1968, 1969) and Rahim and Fordham (1991) observed a small decrease with increasing irradiance. In the case of Sharma and Dunn (1968, 1969), they speculated that the low irradiance levels required to depress SI could not sustain plants in a competitive environment.

In experimental manipulations, photoperiod strongly affects both SD and SI (Schoch et al., 1980; Zacchini et al., 1997). Schoch et al. (1980) observed that even one day of low irradiance levels during the critical period of stomatal initiation could affect SD and SI. Given that SI is typically conservative in deciduous species within a given crown, it is possible the effects of photoperiod on SI observed in experiments are minimal in nature.

1.4.4 Temperature

Temperature appears positively correlated with stomatal density (Ferris et al., 1996; Reddy et al., 1998; Wagner, 1998; but see Apple et al., 2000), a likely consequence of enhanced water stress. Temperature may also affect stomatal index (Ferris et al., 1996; Wagner, 1998), suggesting an influence on stomatal initiation. Reddy et al. (1998), however, found no response. The influence of temperature on stomatal initiation may be inconsequential, though, as most plants partially normalize for fluctuating temperatures by adjusting the timing of leaf development, and so the temperature at which stomata form remains fairly constant (Wagner, 1998).

1.4.5 *Canopy CO_2 gradient*

If CO_2 concentrations within canopies deviate significantly from ambient concentrations, CO_2 estimates based on stomatal parameters could be skewed. Empirical evidence, however, does not suggest such large deviations. Hourly measurements of CO_2 at 8 different heights (0.3, 0.8, 4.5, 7.5, 12.7, 18.3, 24.1, and 29.0 m above the ground surface) have been recorded for several consecutive years from an atmospheric tower in the Harvard Forest (data available at http://www-as.harvard.edu/chemistry/hf/profile/profile.html). This forest, in north central Massachusetts, USA, consists of mixed hardwoods and conifers. As shown in Fig. 1.5A, above 4.5 m, where the bulk of leaves from mature trees form, canopy CO_2 levels are virtually indistinguishable from ambient levels. Furthermore, all deviations diminish during the middle of the day (Fig. 1.5B), a period when cell respiration and division is highest. Thus, CO_2 gradients within canopies are likely not strong enough to influence stomatal initiation rates.

1.4.6 *Paleotaxonomy*

Paleobotanical species identification via morphological comparison with modern representatives is often tenuous, particularly with pre-Neogene material. There are methods, however, to bolster confidence in such morphologically-based species identification. These include comparing the sedimentological and ecological contexts with the proposed extant representative. For example, if a strictly swamp margin fossil species is morphologically identical to a modern representative that is also restricted to swamp

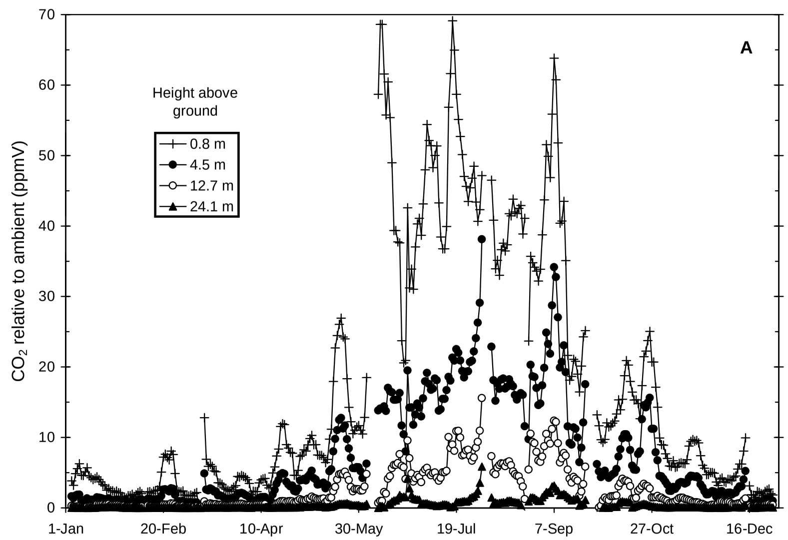

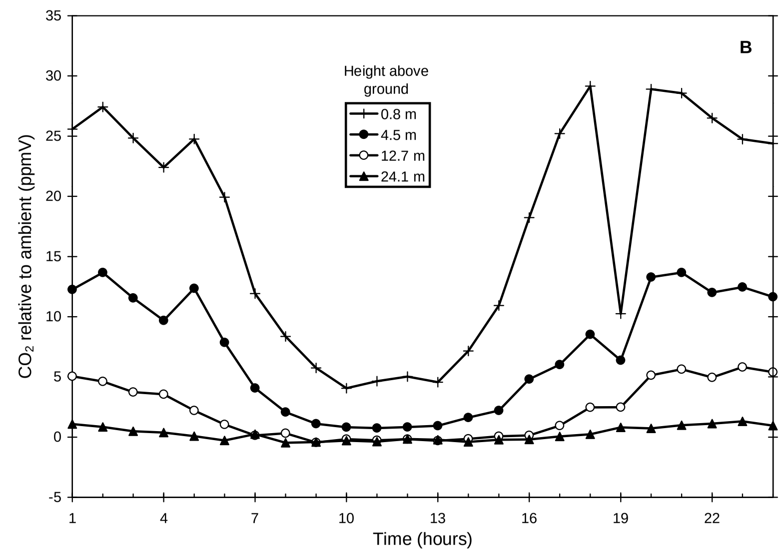

Fig. 1.5. (A) CO_2 relative to ambient concentrations for four heights within a tree canopy in 1996. Canopy height is c. 24 m. Ordinate represents seven day running average of daily averages of hourly measurements at each height (*n* = 5311 for each height). Measurements at 29.0 m height taken as ambient value (mean for time interval at this height = 370 ppmV). (B) Diurnal trend of CO_2 relative to ambient concentrations (data from 9 April-13 July 1996). Ordinate represents mean for each hour at each height (*n* = 1388 for each height). Standard errors approximate size of symbols. Raw data used with permission of S. Wofsy.

margins, then one can be more confident that the two are identical species. Independent of species identification, however, it is also possible that a single species may develop, for example, different stomatal behaviors through time. This, in turn, could affect paleo-CO_2 reconstructions. One way to circumvent this problem is through the study of the species' closest extant sister group (e.g., de Queiroz and Gauthier, 1990). If the stomata in both extant species show a similar response to CO_2, then it can be assumed that this stomatal behavior in both species is conservative in time back to at least when the species branched.

1.4.7 Other potential confounding factors

Through the comparison of 100 species, neither growth form (woodiness vs. non-woodiness; trees vs. shrubs), habitat (cool vs. warm), nor taxonomic relatedness strongly correlated with SD (Woodward and Kelly, 1995). Habitat has also been found not to affect SI (Rowson, 1946). Analysis of the data set presented here shows that for genera represented by >1 species, only 19% (n = 16) and 14% (n = 7) of these genera are internally consistent (α = 0.05) with respect to SD and SI, respectively. These results provide further support for the taxonomic independence of stomatal responses to CO_2.

An increase in ploidy level is associated with lower SD (Rowson, 1946; Mishra, 1997). No clear trend is found in SI (based on two studies), with Rowson (1946) reporting a decrease and Mishra (1997) no change. Given the widespread variability of ploidy levels in the fossil record (Masterson, 1994), this may have important consequences for stomatal-based CO_2 reconstructions.

Elevated levels of ozone increase SD in *Betula pendula* (Frey et al., 1996; Pääkkönen et al., 1998), *Fraxinus excelsior* (Wiltshire et al., 1996) and *Olea europaea* (Minnocci et al., 1999). Effects on SI were not reported.

Although largely untested, atmospheric oxygen may influence SD and SI. Elevated O_2/CO_2 ratios increase photorespiration in C_3 plants, suppressing CO_2 assimilation rates. One pathway to mediate this decline is increasing SD and/or SI. Experimental work on *Hedera helix* and *Betula pubescens* show slightly higher stomatal indices in a 35% versus 21% O_2 atmosphere (Beerling et al., 1998b). If correct, this factor may be particularly important during the Carboniferous and early Permian when O_2 concentrations are modeled to exceed 30% (Berner and Canfield, 1989; Berner et al., 2000).

1.5 Summary

Based on the data presented here, nearly all species appear responsive on the time scales inherent in most fossil CO_2 reconstructions (>10^2 years) (Fig. 1.2; Table 1.1). Only 40-50% of species are responsive over the time scales of experimental and subfossil studies (~10^{-2}-10^2 years), and so those conducting studies requiring such responses must take care in choosing sensitive species (Appendices 1.1-1.2). Another potential weakness in utilizing experimental and subfossil responses is that they are more reflective of plasticity within given gene pools, and may display different behaviors than their respective fossil responses (which are more reflective of genetic adaptation).

SD and SI are both equally likely to inversely relate to CO_2. Stomatal density, however, is sensitive to factors affecting cell expansion such as water stress, temperature, and irradiation. Stomatal index, in contrast, is sensitive only to factors affecting cell initiation, of which CO_2 appears to be one factor. Thus, even if SD and SI show similar responses for a given species (e.g., both positive or negative), stomatal index should yield more accurate CO_2 estimates.

1.5.1 Applications of method

Although experimental work has been carried out for many years, Woodward (1987) was the first to document the inverse CO_2-SD/SI relationship over longer time scales (200 years). Beerling et al. (1991, 1993) extended the applicability of the method to 140 k.y. with *Salix herbacea*, where stomatal densities showed a general inverse relationship with ice core reconstructed CO_2 concentrations. This method has also proven successful with 9.2 ka *Salix cinerea* (McElwain et al., 1995), 13 ka *Betula nana* (Beerling, 1993), and 28 ka *Pinus flexilis* (van de Water et al., 1994).

While the above studies validate the relationship over time scales useful for fossil studies, they do not generate independent estimates of paleo-CO_2. For this, fossil responses must be fitted to a standard curve based on experimental, subfossil, and fossil responses (from the last 400 k.y., for which ice core data exist; e.g., Petit et al., 1999) of the *same* species. This approach has been successful in the Holocene with *Salix herbacea* (Beerling and Chaloner, 1993a; Beerling et al., 1995; Rundgren and Beerling, 1999) and *Betula pubescens* and *B. pendula* (Wagner et al., 1999), and in the Miocene with *Quercus petraea* and *Betula subpubescens* (van der Burgh et al., 1993; Kürschner, 1996; Kürschner et al., 1996). While this approach produces the most accurate CO_2 reconstructions, it is limited by its requirement to compare identical species (or highly similar species within a genus; Wagner et al., 1999). There are, however, single species spanning most or all of the late Cretaceous and Tertiary (e.g., *Ginkgo adiantoides/biloba*, several members of Taxodiaceae), and so CO_2 estimates for this interval are possible.

One clear advantage of the stomatal method over other proxies and models is its high temporal resolution. The temporal resolution of late Quaternary fossil material often exceeds that of ice cores (Beerling et al., 1995; Wagner et al., 1999), and similar high resolution data have been used to document CO_2 excursions across the Allerød/Younger Dryas (Beerling et al., 1995) and Triassic/Jurassic (McElwain et al., 1999) boundaries. Another advantage over other proxies and models is its higher level of precision (compare Fig. 1.1A with Fig. 1.6).

Estimating pre-Cretaceous CO_2 levels proves more difficult. McElwain and Chaloner (1995) developed a technique comparing responses of fossil species to those of their Nearest Living Equivalents (NLEs). NLEs are defined ecologically, not taxonomically, and represent the ecologically closest living analog to the fossil species. SI ratios of the fossils:NLEs were calculated, and in order to estimate CO_2 the Carboniferous:NLE stomatal ratio was normalized to the Phanerozoic CO_2 curve of Berner (1994), with the remainder of the ratios scaled accordingly in a linear fashion. Given that this method assumes a linear response and is not a true independent CO_2 indicator, reconstructed CO_2 concentrations from the Devonian, Carboniferous, Permian, and Jurassic all matched Berner's values remarkably well (McElwain and Chaloner, 1995, 1996). Later (McElwain, 1998), in order to reduce the method's dependence on Berner (1994), data (including new material from the Eocene) were plotted assuming a 1:1

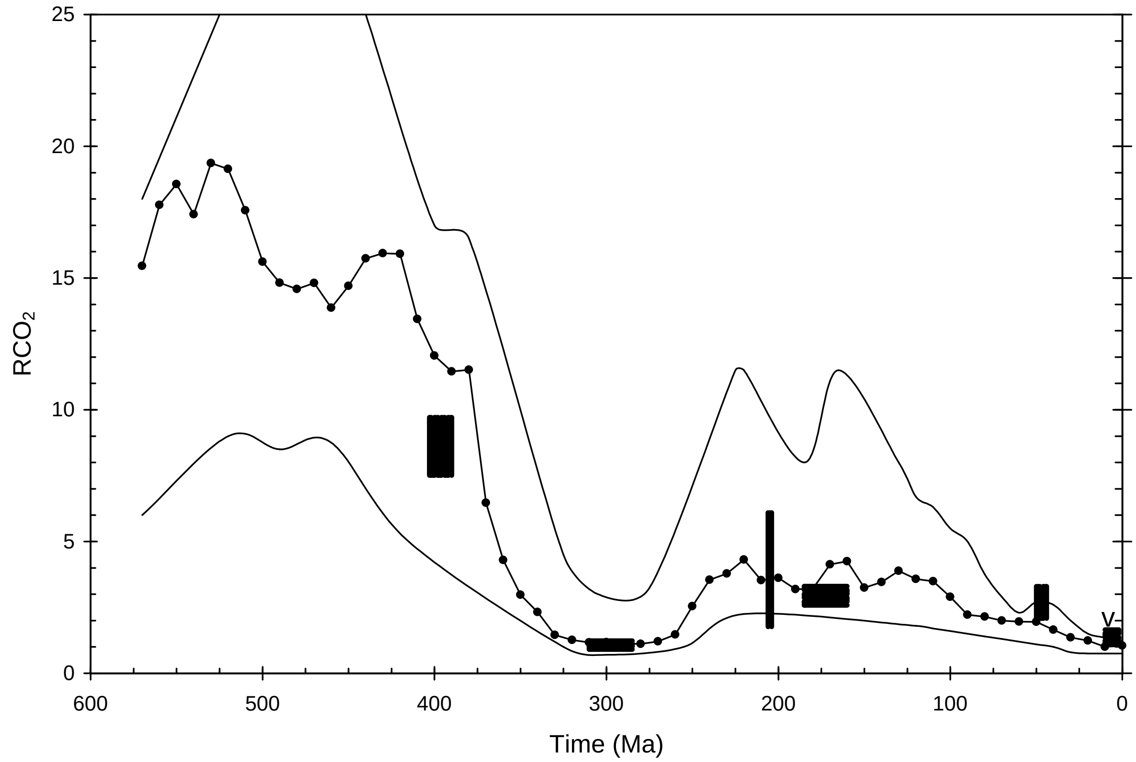

Fig. 1.6. Estimates of CO_2 for the Devonian, Carboniferous-Permian, Triassic, Jurassic, and Eocene (unmarked boxes) calculated from the stomatal ratio technique of McElwain and Chaloner (1995) superimposed over the CO_2 curve and corresponding error envelope of Berner (1994, 1998). Stomatal ratio scale calibrated to RCO_2 scale using a 1:1 correspondence; this is the 'Recent standard' of McElwain (1998). RCO_2 and stomatal ratio defined in Fig. 1.1 and text, respectively. Data from McElwain (1998) and McElwain et al. (1999). Estimates of CO_2 for the Miocene ("v") calculated from a herbaria-based training set. Data from van der Burgh et al. (1993) and Kürschner et al. (1996).

correspondence between stomatal ratios and RCO_2 (RCO_2 = ratio of mass of paleo-CO_2 to pre-industrial value; see Fig. 1.1). Using this more independent technique, all but the Devonian material agreed well with the estimates of Berner (1994). Recent changes in Berner's model, however, have pushed back the sharp drop in Paleozoic CO_2 ~40 m.y. (Berner, 1998), resulting in closer agreement between the two methods for the Devonian (Fig. 1.6).

There is growing interest in quantifying Tertiary CO_2 concentrations (Cerling et al., 1997; Pagani et al., 1999a, 1999b; Pearson and Palmer, 1999), primarily fueled by the question of whether CO_2 and temperature are coupled during this interval. Estimates from stomatal indices have the potential to help resolve this question. As for pre-Cretaceous estimates, the less quantitative stomatal ratio method of McElwain and Chaloner (1995) remains the best option.

CHAPTER 2

Ecological conservatism in the "living fossil" *Ginkgo*

2.1 Introduction

Members of the Ginkgoalean clade remained a moderately important to minor associate of mid- to high latitude paleofloras from the mid-Mesozoic to the mid-Cenozoic (Tralau, 1967, 1968; Vakhrameev, 1991). However, reconstructing the ecology of the group is problematic, given the extreme taxonomic isolation (Chamberlain, 1935; Gifford and Foster, 1989) and highly relictual distribution of what might well be only semi-wild stands of *Ginkgo biloba* Linnaeus, the sole survivor of this once moderately diverse clade (Vasilevskaya, 1963; Tralau, 1968). The objective of this study was to determine whether some aspects of *Ginkgo*'s paleoecology could be recovered from: 1) an interpretation of the sedimentary context in which its fossils occur; 2) the autecology of the modern descendants of its important fossil associates; and 3) a contextual study of the fragmentary ecology of its surviving species.

According to Tralau (1968), the Order Ginkgoales consists of six families and 19 genera. Ginkgoales first appeared in the Permian and achieved maximum diversity during the Jurassic and Early Cretaceous. Its most plausible ancestral group is the pteridosperms ("seed ferns") (Thomas and Spicer, 1987), and especially the Peltaspermales (Meyen, 1987, p. 146). However, the clade is so isolated evolutionarily that efforts to establish its closest extant sister group have remained highly controversial. Nevertheless, there is a growing consensus, favored by molecular data, that cycads are the most plausible closest living relative (Meyen, 1984; Thomas and Spicer, 1987; Raubeson and Jansen, 1992; Chaw et al., 1993, 1997; Rothwell and Serbet, 1994; Boivin et al., 1996; Hickey, 1996; Hasebe, 1997) rather than conifers (Chamberlain, 1935; Pant, 1977; Stewart, 1983; Crane, 1985; Doyle and Donoghue, 1986, 1987).

Undoubted remains of the Genus *Ginkgo* (*G. digitata* [Brongniart] Heer) first appeared in the Early Jurassic (Tralau, 1968: but see Vasilevskaya and Kara-Murza [1963] for a questionable attribution to the Late Triassic), making it the oldest extant genus among seed plants (Arnold, 1947). At least a dozen species have been assigned to *Ginkgo*, which achieved its greatest diversity during the Early Cretaceous (Tralau, 1968). Of particular interest for this study is *G. adiantoides* (Unger) Heer, which is morphologically identical to *G. biloba* (Seward, 1919, p. 29; Shaparenko, 1935; Manum, 1966; Tralau, 1968; Mösle et al., 1998; see Fig. 2.1). These similarities have led some authors to consider *G. adiantoides* conspecific with *G. biloba* (Seward, 1919; Tralau, 1967, 1968, p. 87). *Ginkgo adiantoides* first appeared in the Early Cretaceous and was relatively common during the Late Cretaceous and Paleogene (Tralau, 1968; Vakhrameev, 1991).

Although several additional Northern Hemisphere species of Cenozoic *Ginkgo* have been formally established, all but one of these are morphologically identical, or nearly so, to *G. adiantoides* (and *G. biloba*). One example is *G. beckii* Scott, Barghoorn, & Prakash, a species of Miocene wood associated with *G. adiantoides* foliage, which shows a striking similarity to *G. biloba* wood, with the possible exception of fewer pits per unit length on the radial walls of its tracheids (Scott et al., 1962; Mastrogiuseppe et al., 1970). The only Cenozoic form that possibly merits recognition as a separate species

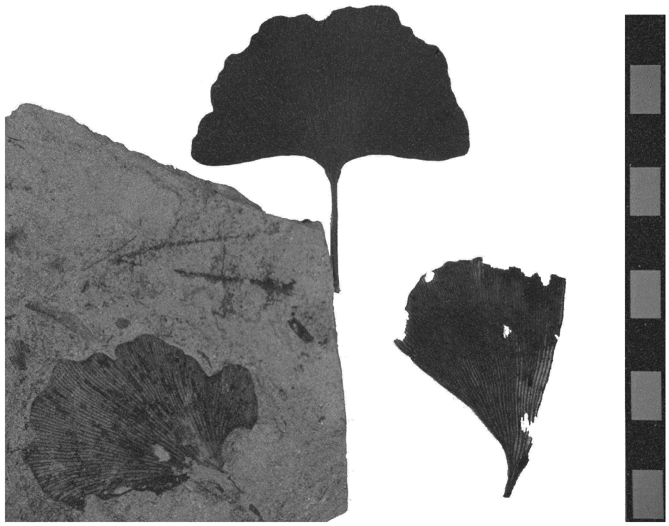

Fig. 2.1. Comparison of the leaves of modern *Ginkgo biloba* (top), middle Miocene *G. adiantoides* (right; only half of leaf present; from site 51), and middle Paleocene *G. adiantoides* (left; from site 18; University of Alberta specimen S51314). Scale bar = 1 cm.

is *G. gardneri* Florin (Tralau, 1968), which has more prominent papillae and less sinuous adaxial epidermal cells than does *G. adiantoides* (Manum, 1966). *G. gardneri* is found only in the late Paleocene deposits on the Isle of Mull, Scotland (e.g., Boulter and Kvaček, 1989). Given this lack of morphological diversity, it is possible that Ginkgoales has been monospecific (or nearly so) in the Northern Hemisphere for the entire Cenozoic. In the Southern Hemisphere a different, more strongly digitate type of *Ginkgo* leaf persists into the Eocene, but we lack data on its occurrence and do not discuss it further here.

A number of Mesozoic species of *Ginkgo* closely match the extant species as well. For example, Mösle et al. (1998) found strong similarities between the cuticles of the Early Cretaceous *G. coriacea* Florin and *G. biloba*. Villar de Seoane (1997) reported similar results for the cuticle of Early Cretaceous *G. tigrensis* Archangelsky from Argentina. Zhou (1993) compared the megaspore membranes of middle Jurassic *G. yimaensis* Zhou & Zhang with *G. biloba*, and noted few morphological differences. Van Konijnenburg-van Cittert (1971) concluded that the pollen of middle Jurassic *G. huttoni* (Sternberg) Heer was morphologically identical to *G. biloba*. Thus, *Ginkgo* is a highly conservative genus morphologically, with the long-ranging fossil species *G. adiantoides* indistinguishable from modern *G. biloba*.

2.1.1 Ecology of Ginkgo biloba

Ginkgo biloba (Fig. 2.2) has been cultivated for more than 2000 years in China and for some 1000 years in Japan as a source of food, shade, and beauty (Li, 1956; He et al., 1997); small stands are sometimes present within the forests customarily preserved adjacent to Buddhist and Taoist temples (Li, 1956). However, the natural ecology of *G.*

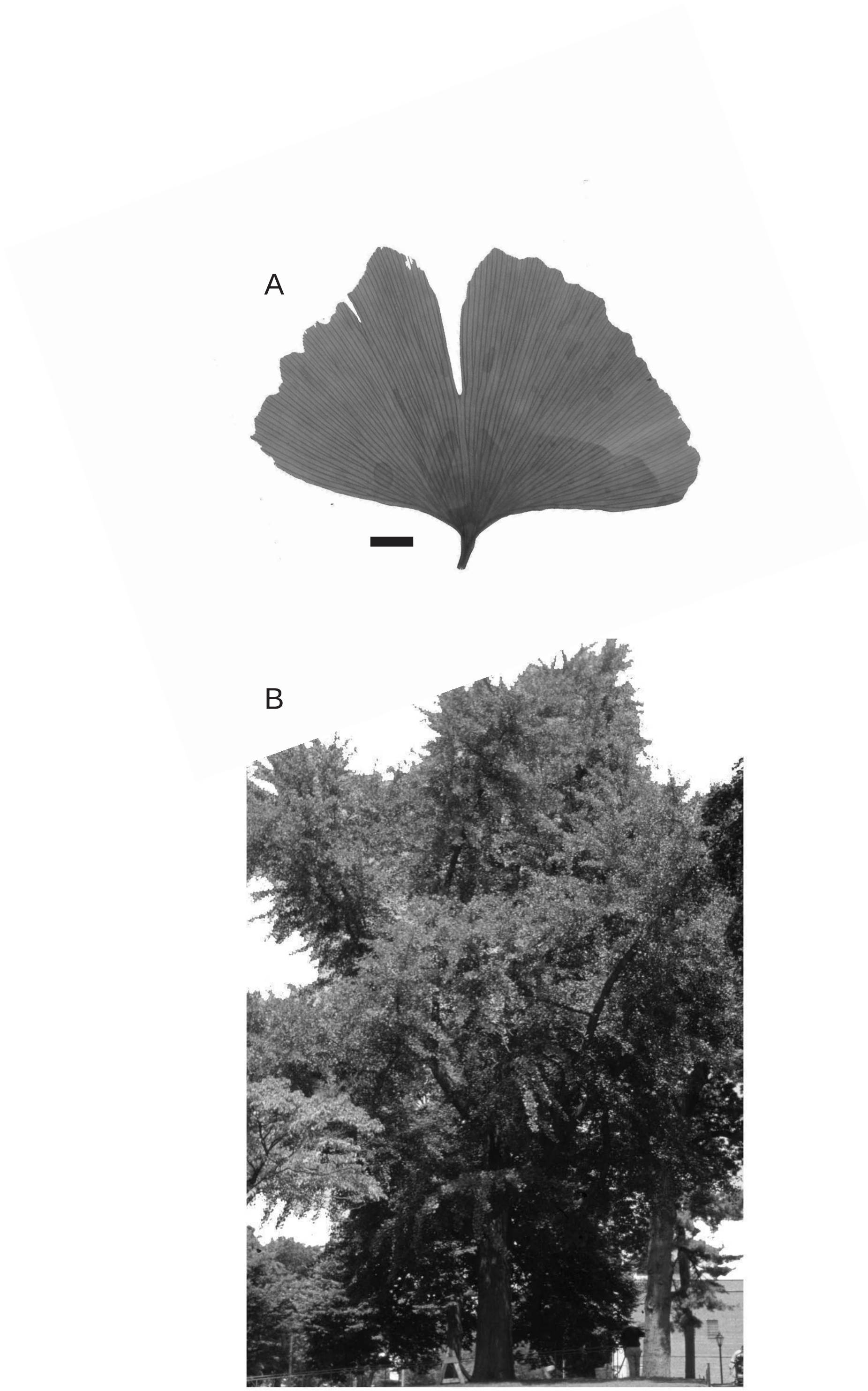

Fig. 2.2. (A) Representative leaf of *Ginkgo biloba* (scale bar = 1 cm) and (B) Mature *Ginkgo biloba* tree growing on Yale University grounds (New Haven, CT).

biloba is largely unknown because no unequivocally natural stands remain today (see discussions in Li, 1956; Franklin, 1959; Del Tredici et al., 1992; He et al., 1997). The last remaining natural populations are (or were) largely in the low coastal and interior mountains straddling the Yangtze River. This is the region where *G. biloba* was first cultivated and also harbors relictual stands of other taxa with long fossil records such as *Cryptomeria*, *Liriodendron*, *Metasequoia*, *Nothotaxus* and *Pseudolarix*. The area lies at about 30 °N and has a warm temperate mesic climate (mean annual temperature = 9-18 °C; mean annual precipitation = 600-1500 mm) (Li, 1956; Del Tredici et al., 1992; He et al., 1997). In cultivation *Ginkgo* tolerates a wide variety of seasonal climates, ranging from Mediterranean to cold temperate, where winter temperature minimums can reach –20 °C. Interestingly, nearly all fossil occurrences of *Ginkgo* lie poleward of 40° and, concomitant with cooling and increased seasonality during the Tertiary, its geographical range progressively constricted towards 40 °N, and it disappeared all together from the southern hemisphere (Tralau, 1967). Thus, both its broad modern range of climatic tolerance and the paleobotanical data suggest that the climatic parameters of its current (semi-)natural range at 30 °N are anomalous in terms of the long-term history of *Ginkgo*.

Ginkgo is a tree of medium height, reaching approximately 30 m (Del Tredici et al., 1992; He et al., 1997), and can live as long as 3500 years (Zhang et al., 1992). Although *Ginkgo* is frequently described as slow growing, under favorable conditions with warm summers it exhibits growth rates of up to 30 cm/yr for the first 30 years or so of its life (Del Tredici, 1989). During this “bolting” phase of their growth, seedlings and saplings have a straight main axis, with sparse, excurrent branches. After that, growth slows markedly—100-year-old trees may have attained only two-thirds of their mature height (Santamour et al., 1983; He et al., 1997)—and the young tree begins to fill out its crown (Del Tredici, 1989). Plants do not produce viable seeds for 20 to 30 years (Wyman, 1965; Santamour et al., 1983; He et al., 1997), but individual trees can remain fertile for more than 1000 years (S.-A. He, personal communication, 2000). *Ginkgo*'s fusiform seeds are large, ranging from 1-2 cm in length.

In addition to sexual reproduction, *Ginkgo* can reproduce clonally from embedded buds, called chichi, that occur near the base of the trunk. If the soil in the immediate environment is disturbed, as by excessive erosion, positive geotropic growth is stimulated within its chichi. Once the apex of a chichi penetrates below ground, it forms rhizomatous tissue that can generate both aerial shoots and adventitious roots (Del Tredici, 1992). In a modern 'semi-wild' stand in the coastal mountains near the Yangtze River studied by Del Tredici et al. (1992), 40% of the larger trees had at least two primary stems but few saplings were present, a clear indication of the reproductive importance of chichi. In older individuals, these buds also form within secondary stems and are called aerial chichi. As with basal chichi, aerial chichi develop in response to a disturbance (e.g., severe crown damage) and can lead to successful clonal reproduction (Fujii, 1895; Del Tredici et al., 1992).

Modern *Ginkgo* is shade intolerant, growing best on exposed sites (He et al., 1997). Del Tredici et al. (1992) observed that seeds of *G. biloba* in a 'semi-wild' stand require an open canopy for growth and development; Jiang et al. (1990) report a similar requirement in another 'semi-wild' stand. Many of the individual trees studied by Del Tredici et al. (1992, p. 202) were growing in disturbed microsites such as "stream banks, steep rocky slopes, and the edges of exposed cliffs." However, Del Tredici (1989) also suggests that *Ginkgo* may play a role as a gap opportunist and persist in the shady understory of the forest until a gap occurs that allows it to shoot up into the canopy.

At least in cultivation, *Ginkgo* grows best in "sandy loam soils…along dams…or at the foot of hill slopes" (He et al., 1997, p. 377), environments that are well-watered and well-drained. *G. biloba* is very successful as an urban street tree (e.g., Handa et al., 1997), owing in part to its tolerance to air pollution (Kim and Lee, 1990, Kim et al. 1997), high resistance to insects (Major, 1967; Kwon et al., 1996; Ahn et al., 1997; Honda, 1997), fungi (Major et al., 1960; Major, 1967; Christensen and Sproston, 1972), bacteria (Mazzanti et al., 2000) and viruses (Major, 1967), as well as its preference for exposed sites. *Ginkgo*'s resistance to disease is due, in part, to its high production of secondary defense compounds (e.g., Yoshitama, 1997).

2.1.2 Implications for fossil Ginkgo

While the close morphological similarity of *Ginkgo adiantoides* to *G. biloba* makes it tempting to infer the paleoecology of the fossil species from what is known of the living, the extreme relictual nature of the modern form suggests that such surmises should be made cautiously and only with corroboration from the fossil record (cf. Hickey, 1977). Uemura (1997) thought that *Ginkgo* was ecologically conservative through time, and required moist environments. Kovar-Eder et al. (1994) studied Neogene occurrences in central Europe, and considered *G. adiantoides* an accessory element in riparian communities. Spicer and Herman (2001) reported similar depositional associations for mid-Cretaceous *G. adiantoides* in northern Alaska. In this chapter, I will provide a quantitative description of the sedimentological contexts and floral associates of fossil *Ginkgo*, concentrating primarily on *G. adiantoides*, the putatative conspecific of *Ginkgo biloba*, and ranging in age from latest Cretaceous to middle Miocene. Through the interpretation of *Ginkgo*'s sedimentological contexts and the modern ecology of the nearest living relatives of its floral associates, two independent lines of evidence will be used to interpret the paleoecology of the genus.

2.2 Methods

2.2.1 Sources of data

Sedimentological and floral data were obtained through field observations and the literature. Most data are from the Fort Union and Willwood Formations (Bighorn Basin) and the Hell Creek Formation (Williston Basin). The geographic extent of our sampling is shown in Fig. 2.3. Data sources are as follows: Williston Basin—Johnson (in press) for sedimentology and floral data, and Hicks et al. (in press) for dating, except for the Almont site, for which all data are taken from Crane et al. (1990); Bighorn Basin—Hickey (1980), Wing et al. (1995) and field observations for sedimentology and floral data, and Gingerich (2000) and Age Model 2 of Wing et al. (2000) for dating; Denver Basin (site DMNH 2360)—R. S. Barclay (unpublished data) for sedimentology, and Raynolds et al. (2001, p. 25) for dating; Basilika site—Manum (1963) for sedimentology and floral data, and Kvaček et al. (1994) for dating; south-central Alberta—Speirs (1982) and Hoffman and Stockey (1999) for sedimentology and floral data, and Fox (1990) for dating; Ardtun Head site—Boulter and Kvaček (1989) for sedimentology and floral data, and Chapter 2 for dating; Stenkul Fiord site—field observations for sedimentology and floral data; Kalkreuth et al. (1996) for dating; Beaver Creek site—K. R. Johnson (unpublished data)

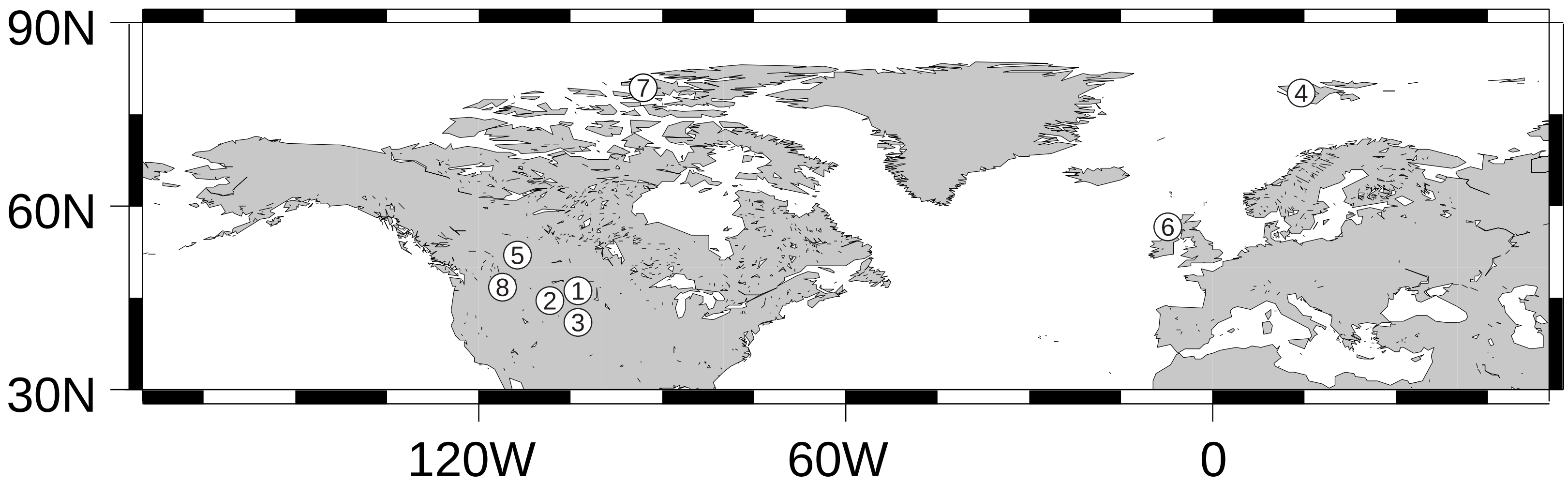

Fig. 2.3. Map showing sampling areas. Numbers refer to the following field areas: 1. Williston Basin; 2. Bighorn Basin; 3. Denver Basin; 4. Spitsbergen; 5. south-central Alberta; 6. Isle of Mull; 7. Axel Heiberg Island; 8. north-central Idaho.

for sedimentology, and C. N. Miller (unpublished data) for dating; Juliaetta site—field observations for sedimentology and floral data, and Reidel and Fecht (1986) for dating.

2.2.2 Recognition of sedimentological contexts

Sites were assigned to environments of deposition based upon the lithology, grain size, primary stratification, overall cross-sectional and plan-view shape of their deposits, along with their organic content and nature of their contacts with surrounding sediments, using criteria developed by J. R. L. Allen (1964, 1965), Hickey (1980), Wing (1984) and Miall (1992). We will use the following terms for the environments of deposition that we recognize here: relief / abandoned channel, crevasse splay, active trunk channel, backswamp, and distal floodplain.

Relief channels are represented by thin, shallow-lenticular, laterally restricted bodies of silt to sand-size sediment that fill minor stream axes used in time of flood. Abandoned channels represent a segment of a stream or river that was intermittently or permanently cut off from its main channel, whose original depth can be reconstructed from the thickness of the total sedimentary package. They often have clay- or mudstone in their axes. The basal contacts of both types of channels are frequently down-cut, concave upward, and veneered with a coarse (often pebble-sized) basal lag deposit. Plant remains within these deposits are typically parautochthonous (Wing, 1984; Gastaldo et al., 1989). These channel deposits are characterized by relatively thin (<5 cm for relief channels and <1 m for abandoned channels) couplets of coarser sandstone and siltstone with finer siltstone and mudstone that represent the alternating periods of flooding or channel reactivation and slackwater or subareal phases (Wing, 1984). Intervals within abandoned channels often show evidence of standing water, such as aquatic plants and invertebrates, and successions of small-scale, fining-upwards sequences (Wing, 1984).

Crevasse splay deposits are floodplain deposits formed by the breaching of a levee, typically during flood events. They are characterized by sand- or silt-size sediments with generally tabular beds that are sometimes cross-bedded or cross-laminated. These often overlie finer-grained, massive floodplain-sediments. Proximal to the break-through point, downcut contacts with concave upward bedding and scour and fill structures are more common, but distal to the break-through point basal contacts tend to be more parallel with one another. Beds of sandstone in splays represent multiple reactivation events and range in thickness from centimeters to more than a meter. Often these grade upward into progressively finer sediments that represent low energy floodplain conditions. The modal grain size of the sediments in these reactivation events usually coarsens upwards due to the progressive lateral shift of the stream axis towards a given point in the crevasse splay (Miall, 1992). Crevasse splay deposits are generally more laterally extensive than relief channels, but are not traceable for long ($>10^2$ m) distances. A detailed microstratigraphic section at a site that we interpret as a crevasse splay is illustrated in Fig. 2.4.

Other sedimentological contexts distinguished here include backswamps, which are dominated by carbonaceous shale; active trunk channels, which are characterized by massive cross-bedded sandstone; and ponds / lakes, which are distinguished by laminated mudstone and the presence of aquatic plants and animals. Because of the convergence of their properties, we assigned large abandoned channels to the pond / lake category.

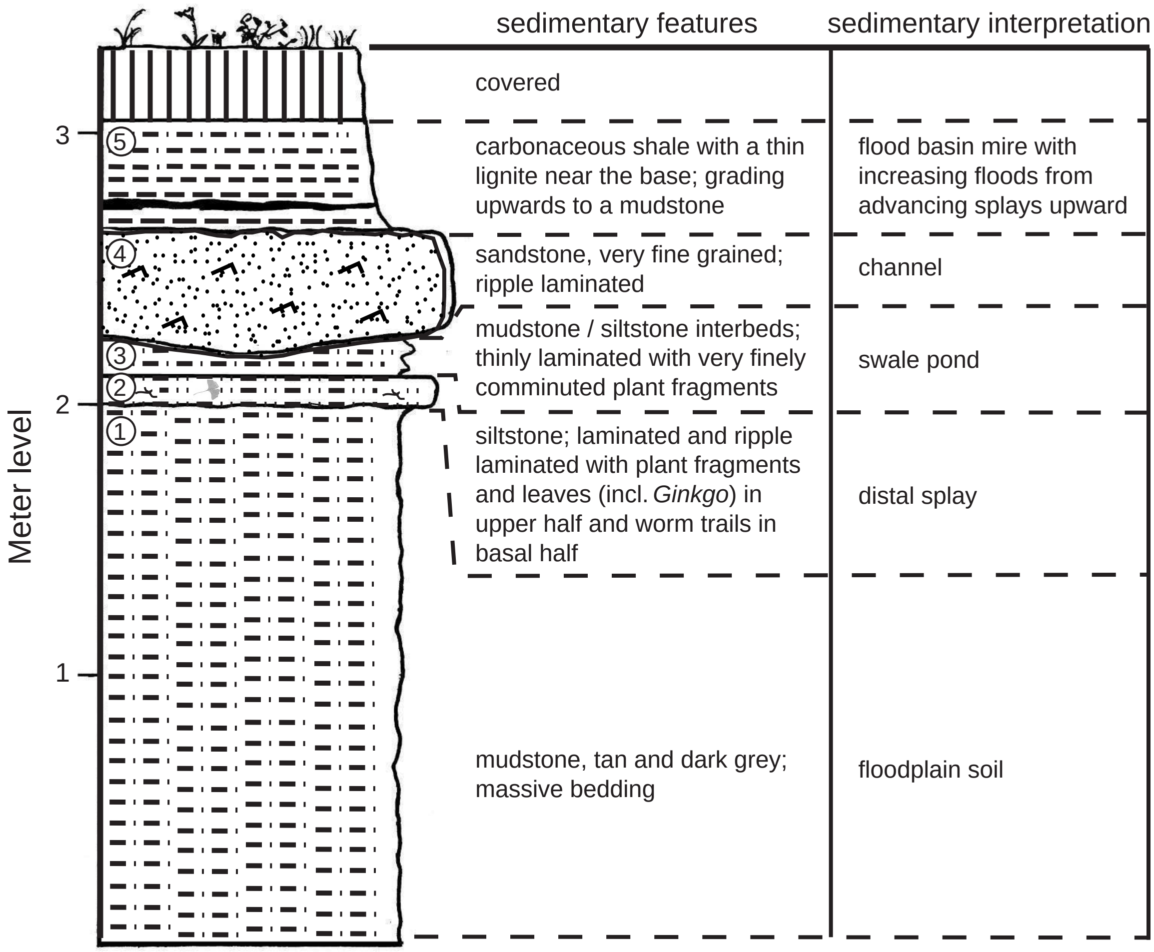

Fig. 2.4. Microstratigraphic section for Chance locality (site 23). Section is near Chance, MT (45^{o} 00' 29.2" N, 109^{o} 04' 53.0" W).

2.2.3 Floral associates

We generated floral lists for most sites. When possible, we limited these lists to the individual beds within a deposit where *Ginkgo* was found. In general, we follow the taxonomic terminology of Wing et al. (1995). In two cases, we combined closely related species of the family Platanaceae into single counting units. The first of these units consists of the broadly trilobed *Platanus raynoldsii* Newberry and *P. guillelmae* Goeppert, and the second of the narrowly five-lobed *Macginitiea gracilis* (Lesquereux) Wolfe & Wehr and *M. brownii* (Berry) Wolfe & Wehr.

All but two of our sites contain *Ginkgo adiantoides*. *G. spitsbergensis*, found at one site, is considered conspecific with *G. adiantoides* by Tralau (1968), while *G. gardneri*, found at one site on the Isle of Mull, may be a distinct species, as discussed above.

2.3 Results

2.3.1 Sedimentological contexts

Based upon our sampling of 48 sites spanning the latest Cretaceous to middle Miocene, *Ginkgo* is most often found in relief / abandoned channels (44% of all sites) and crevasse splays (38%) (Table 2.1; raw data presented in Appendix 2.1). In most relief / abandoned channel deposits, *Ginkgo* occurs within the coarser-grained intervals. *Ginkgo* is rarely preserved in backswamps (4%). Certain depositional environments are preserved

Table 2.1. Summary of the distribution of sedimentological contexts and floral associates. Description of columns are as follows: 1) % occurrence at all *Ginkgo*-bearing sites; 2) % occurrence at *Ginkgo*-bearing sites that overlap with the datasets of Johnson (in review) and Wing et al. (1995); 3) % occurrence at all sites (including *Ginkgo*-bearing sites) from the datasets of Johnson (in review) and Wing et al. (1995); 4) % difference between the two restricted sets (i.e., column [2]-[3]); 5) Level of significance between the two restricted sets (G-test of independence; Sokol and Rohlf, 1995, p. 729). Since the sedimentological contexts are not independent of one another (i.e., columns add up to 100%), these *P*-values were adjusted using the Dunn-Šidák method in the following manner: $a' = 1 - (1 - a)^{1/k}$, where $k = 6$ = the number of significance tests (Sokol and Rohlf, 1995, p. 239).

	Ginkgo sites (%) all	*Ginkgo* sites (%) restricted set	All sites from restricted set (weighted %)	Difference in restricted set (%)	*P*
sedimentological contexts	(*n* = 48)	(*n* = 41)	(*n* = 288)		
relief channel / abandoned channel	43.8	41.5	14.3	27.2	0.004
crevasse splay	37.5	41.5	17.8	23.7	0.012
channel	8.3	9.8	5.5	4.3	0.98
backswamp	4.2	4.9	53.2	-48.4	<0.001
distal floodplain	4.2	4.9	0.8	4.0	0.60
other (mostly stable ponds / lakes)	4.2	0.0	8.4	-8.4	0.08
floral associates	(*n* = 47)	(*n* = 41)	(*n* = 289)		
(*Ginkgo adiantoides*)			8.4		
Cercidiphyllum genetrix	59.6	63.4	32.9	30.5	<0.001
Metasequoia occidentalis	44.7	46.3	27.7	18.7	0.022
Platanus raynoldsii / guillelmae	42.6	48.8	23.3	25.5	0.002
Glyptostrobus europaeus	29.8	31.7	44.3	-12.6	0.19

more commonly than others or are more likely to preserve fossil plants. The high proportion of relief / abandoned channels and crevasse splays might therefore simply reflect the numerical abundance of these plant fossil-containing deposits. To normalize for this potential bias, we determined the distribution of sedimentological contexts for all fossil plant sites (including *Ginkgo*-bearing sites) documented by Johnson (in press) (n = 157 sites) and Wing et al. (1995) (n = 131). Together, these datasets span the interval from the latest Cretaceous to the early Eocene and include the late Cretaceous Hell Creek Formation and earliest Paleocene part of the Fort Union Formation in the Williston Basin and the Paleocene through early Eocene Fort Union and Willwood Formations in the Bighorn Basin. We considered only our *Ginkgo*-bearing sites included in these datasets (n = 41 sites), and weighted the full datasets of Johnson (in press) and Wing et al. (1995) to reflect the distribution of these *Ginkgo*-bearing sites (22% from the Williston Basin, 78% from the Bighorn Basin).

For these two geographic regions, *Ginkgo* is preferentially found in both relief / abandoned channel (42% for *Ginkgo* localities vs. 14% for all plant localities) and crevasse splay (42% vs. 18%) deposits (Table 2.1; Fig. 2.5). Equally striking is that the likelihood of finding *Ginkgo* in a backswamp is far less than the background percentage of backswamp deposits (5% vs. 53%). The differences for all three of these sedimentological contexts are significant at the $\alpha = 0.02$ level (G-test of independence).

2.3.2 Floral associates of Ginkgo

Based upon a sampling of 47 *Ginkgo*-bearing sites spanning the latest Cretaceous to middle Miocene, *Ginkgo* most commonly is fossilized with *Cercidiphyllum genetrix*

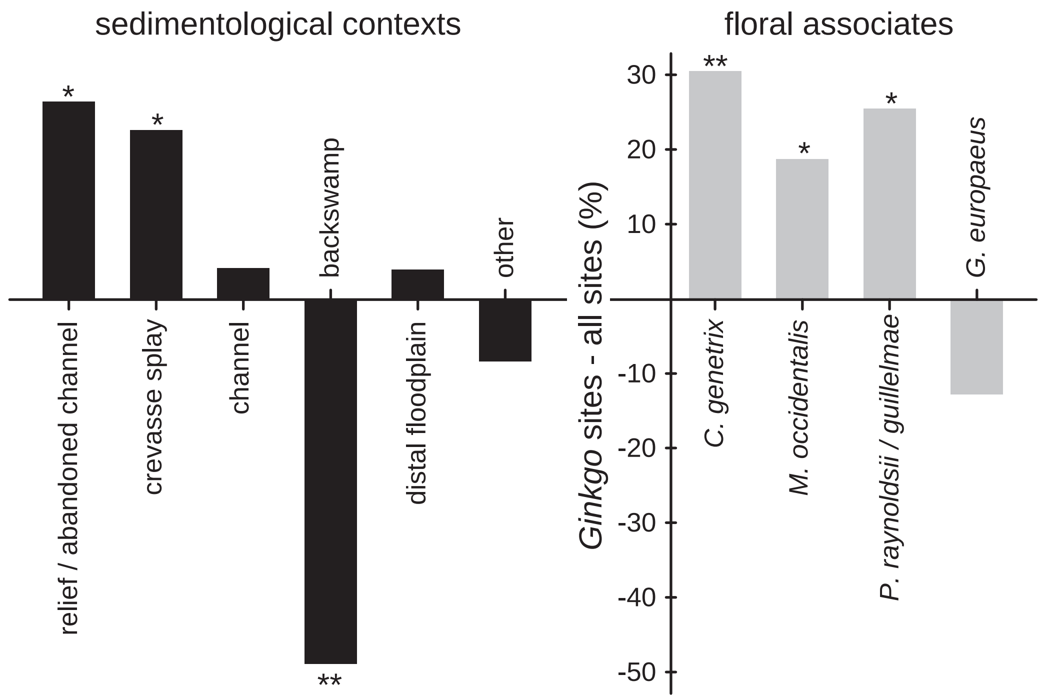

Fig. 2.5. Deviations of the proportion of sedimentological contexts and floral associates at *Ginkgo*-bearing sites from the background occurrence rate of these sedimentological contexts and floral associates. Data taken from second-to-last column in Table 2.1. Methodology of calculation discussed in text. Asterisks represent whether the differences in proportionality are significant at the a = 0.05 level (*) or a = 0.001 level (**) (G-test of independence).

(Newberry) Hickey (co-occurs at 60% of all *Ginkgo* sites), *Metasequoia occidentalis* (Newberry) Chaney (45%), *Platanus raynoldsii* / *guillelmae* (43%), and *Glyptostrobus europaeus* (Brongniart) Heer (30%) (Table 2.1; raw data presented in Appendix 2.2). All four of these associates have temporal ranges that span the latest Cretaceous to middle Miocene. Analogous to the potential sedimentological taphonomic bias, it is possible that these floral associates simply dominate the megafloral record during this interval, which, if true, would diminish the paleoecological significance of our results. As with the data on sedimentary environments, then, we compared a weighted average of the overall floral distribution patterns for the Hell Creek and Fort Union Formations in the Williston Basin (n = 158 sites) (Johnson, in press) and the Fort Union and Willwood Formations in the Bighorn Basin (n = 131) (Wing et al., 1995) with the *Ginkgo*-bearing sites that overlap with these studies (n = 41). *C. genetrix* and *P. raynoldsii* / *guillelmae* occur more often with *Ginkgo* relative to their overall occurrence rate (63% vs. 33% and 49% vs. 23%, respectively) (Table 2.1; Fig. 2.5). These differences are significant at the $\alpha = 0.003$ level (G-test of independence). *Ginkgo* also preferentially associates with *M. occidentalis* (46% vs. 28%; $P = 0.02$; G-test of independence). The background occurrence rate of *G. europaeus*, however, is higher than its co-occurrence rate with *Ginkgo* (44% vs. 32%) (Table 2.1; Fig. 2.5), suggesting that it is not useful in determining the paleoecology of *Ginkgo*.

2.3.3 Microstratigraphy: a detailed example

The Chance locality (site 23) in the Tiffanian portion of the Fort Union Formation of the Bighorn Basin displays sedimentological and floral characteristics common to many *Ginkgo*-bearing sites examined in this study. Here, fossil *Ginkgo* leaves are found in the upper half of a 10 cm-thick unit of interbedded mudstone and siltstone (unit 2 in Fig. 2.4) that is inferred to represent the distal portion of a crevasse splay. In addition to *G. adiantoides*, leaves of *Zizyphoides flabella* Crane, Manchester & Dilcher, *Platanus raynoldsii*, *Acer silberlingii* Brown and *Wardiaphyllum daturaefolia* (Ward) Hickey also occur. The fragmentary nature of many of these leaves and their occurrence in the laminated siltstone of a splay indicate that this flora has been subjected to some transport, in this case inferred to have been from the nearby slopes of the stream levee. The fossil bearing unit overlies a massive, flood-basin mudstone (unit 1) that shows very weakly developed soils features (inceptisol). Following the deposition of the *Ginkgo*-bearing splay siltstone, deposition of a thinly laminated siltstone-mudstone unit indicates that the area became a swale-pond (unit 3). This in turn was replaced by a sandstone lens that is inferred to represent a trunk channel. This is overlain by sediments representing a distal floodplain (units 4 and 5).

2.4 Discussion

2.4.1 Paleoecology of Ginkgo

The sedimentological features at the majority of *Ginkgo* localities indicate that it grew primarily in disturbed environments along stream margins and the distal sides of levees. These environments are typically well-watered (due to a shallow water table and frequent flood events) yet well-drained (due to their primarily coarse-grained substrate).

Due to their high disturbance rate, these environments typically host open-canopy forests. Although *Ginkgo* leaves tend to sort with silt-sand size particles in flume experiments (Spicer and Greer, 1986), this would not explain their distribution in both coarse-grained, typically cross-stratified sediments (representing crevasse splays, relief channels, and rejuvenated abandoned channels) and fine-grained, parallel-laminated sediments (e.g., abandoned channels).

As reported above, *Cercidiphyllum genetrix* and a form of *Platanus* delimited by the pair *P. raynoldsii* and *P.guillelmae* are two of the more common floral associates of *Ginkgo*. *C. japonicum* Siebold & Zuccarini, the nearest living relative (NLR) of *C. genetrix*, grows in the wild today in Japan and China. It usually occurs in small gaps or along stream margins (Seiwa and Kikuzawa, 1996). It is a fast growing pioneer species, often reproduces by sprouting, and prefers mesic, disturbed sites (Ishizuka and Sugawara, 1989). Interestingly, at mid-elevations (1450-3500 m) in the mountains of south-central China, *C. japonicum* occurs on scree slopes (Tang and Ohsawa, 1997) and in other highly disturbed habitats (Wang, 1961). Although plant remains are rarely preserved in alluvial fan facies, at Ardtun Head (Isle of Mull, Scotland) *Ginkgo* is found in fine-grained sediments within an alluvial fan deposit (see Appendix 2.1). As noted above, modern *Ginkgo* has been observed growing on steep rocky slopes and along edges of exposed cliffs (Del Tredici et al., 1992). It is possible, then, that disturbance is the overriding ecological filter for *Ginkgo*, and the fluvial deposits where *Ginkgo* is most commonly preserved represent only a small fraction of its potential habitat range.

The NLR's of *P. raynoldsii* and *P.guillelmae* are *P. occidentalis* Linnaeus, *P. orientalis* Linnaeus, and their hybrid *P.* × *acerifolia* Willdenow. These living species are most commonly found in riparian habitats (Tang and Kozlowski, 1982; Ware et al., 1992;

Thomas and Anderson, 1993; Atzmon and Henkin, 1998; Everson and Boucher, 1998); for example, *P. occidentalis* often grows on the lowest stream terrace (McClain et al., 1993) where flood frequency is highest (Bell, 1980). *P. occidentalis* can develop adventitious roots and lenticels in response to flooding (Tsukahara and Kozlowski, 1985), however it appears to require aerated soils during the growing season (Everson and Boucher, 1998).

Metasequoia occidentalis, another common *Ginkgo* associate (Table 2.1), has remained largely unchanged morphologically throughout the Cenozoic (Chaney, 1951; Christophel, 1976; Liu et al., 1999) and is represented today by *M. glyptostroboides* H. H. Hu & Cheng. Like *Ginkgo*, the geographic range of *Metasequoia* has been severely restricted, however areas of near-natural stands still grow in one mountain valley in south-central China. It occurs there along stream banks and at seepages at the bases of slopes (Chu and Cooper, 1950). These modern observations contrast in part with the paleobotanical observations that show *Metasequoia* most often occurring in swamp, swamp margin and distal splay environments (e.g., Hickey, 1980; Momohara, 1994; Wing et al., 1995; Falder et al., 1999). This discrepancy may result either from the fact that most of the valley floor where *Metasequoia* makes its last stand has been converted to agriculture and habitat space has been lost, or from a shift in the ecological niche of *Metasequoia* during the Cenozoic.

In summary, the sedimentological record strongly indicates that *Ginkgo* most commonly grew along streamsides and on the proximal slope of levees. The ecology of the NLR's of two genera of *Ginkgo*'s common floral associates (*Cercidiphyllum* and *Platanus*) support these sedimentological interpretations. *Ginkgo*'s association with *Metasequoia* proves problematic, however, as the latter most commonly grew in swamps and distal levees during the Tertiary. It is possible then, that either *Ginkgo* also grew in more stable distal floodplain settings or that *Metasequoia* was a minor associate in disturbed levee and riparian-type environments. This latter option is supported, albeit weakly, by modern ecological observations of *Metasequoia*.

In general, NLR-derived paleoecological interpretations are less reliable than sediment-derived interpretations because a given lineage of plants can shift its ecological tolerances over geologic time (e.g., Hickey, 1977; Wolfe, 1977), and because few late Cretaceous and early Tertiary plants have close modern relatives. In contrast, the sedimentology of an autochthonous fossil plant site retains a primary paleoecological signal. Only recently have paleobotanists begun to analyze the sedimentological contexts of their assemblages in an effort to extract paleoecological information (e.g., Hickey, 1980; Spicer, 1980; DiMichele and Wing, 1988; Burnham, 1994; Wing et al., 1995; Spicer and Herman, 2001). The results of this study highlight the potential of applying sedimentological data from a large number of fossil plant sites, and we hope that the application of such data becomes more common in the future.

2.4.2 Implications for the relationship between G. biloba *and* G. adiantoides

Analysis of our data indicate that there were no striking changes in the sedimentological context of *Ginkgo* during the latest Cretaceous to early Eocene (Fig. 2.6A). *Ginkgo* consistently associated with unstable crevasse splay and relief / abandoned channel environments. Although there is a shift to more relief / abandoned channel localities in the early Eocene, this is driven by a drying trend in the Bighorn Basin that

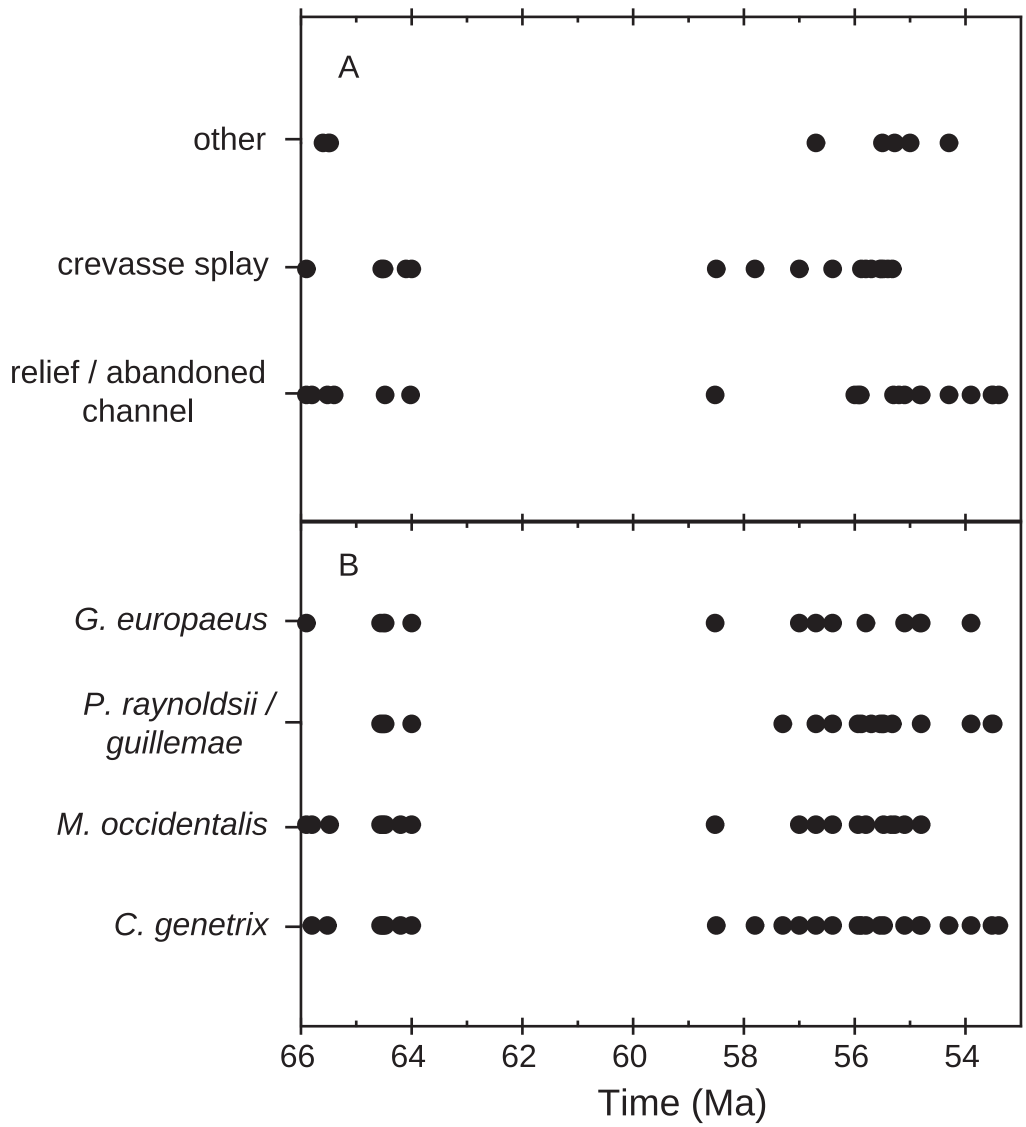

Fig. 2.6. Temporal distribution of (A) sedimentological contexts and (B) principle floral associates for latest Cretaceous-early Eocene *Ginkgo*-bearing sites.

restricted the preservation of fossil plants to these environments and to tabular carbonaceous layers representing swampy floodbasins (Wing, 1984).

Ginkgo's floral associates also remain stable through the early Paleogene (Fig. 2.6B). This stability is striking considering the large number of factors that influence plant migrations and evolution. The one minor change in this time series is the lack of *Metasequoia* during the early Eocene, although this may be due to the paucity of early Eocene backswamp deposits relative to the late Paleocene in the Bighorn Basin (Wing et al., 1995). If correct, this observation provides additional support for inferring *Ginkgo*'s preference for streamside and levee habitats.

Data are generally lacking for the Neogene. However, at the middle Miocene Juliaetta site in Idaho, *Ginkgo* occurs in sandy delta foreset beds (Appendix 2.1). Although the overall depositional setting is lacustrine, *Ginkgo* is only found in this high-energy delta environment, and so perhaps grew in a nearby riparian setting and was carried by the river to the lakeshore. *Amentotaxus gladifolia* (Ludwig), Ferguson, Jähnichen, & Alvin is the single floral associate of *Ginkgo* at the Juliaetta site. *A. gladifolia* is also present in the late Paleocene Ardtun Head site, some forty million years earlier. Its nearest living relative, *A. formosana* Li, grows along streams on mountain flanks (Page, 1990).

On the basis of our sedimentological and floral data, *Ginkgo* appears to have been ecologically conservative throughout the Cenozoic. The environmental preferences of the modern *G. biloba* match the paleoecological interpretations generated here. This marked stability in environmental preferences supports previous work, based upon morphology alone, that *G. adiantoides* and *G. biloba* are conspecific.

2.4.3 The ecological paradox of Ginkgo *and a possible mechanism for its decline*

Woody plants successful in highly disturbed habitats today usually share a suite of traits described as the competitive-ruderal strategy, sensu Grime (2001). These may include an early successional habit, shade intolerance, high growth rates, ability for clonal reproduction (Everitt, 1968; Eriksson, 1993), early reproductive maturity, small seed size (Harper et al., 1970; Westoby et al., 1992), the production of few secondary defense compounds (Coley et al., 1985), short life span, and a rapid rate of evolution (Eriksson and Bremer, 1992). *Ginkgo* shares some of these characteristics, namely shade intolerance, rapid early growth, and a clonal habit, but many of its life history traits counter those considered beneficial in disturbed environments. *Ginkgo* requires > 20 years to reach reproductive maturity, produces large seeds needing a protracted period for fertilization and embryo development, manufactures an impressive array of secondary defense compounds, can live for > 3000 years, and has an extremely slow rate of evolution.

Ginkgo therefore represents an ecological paradox: it appears to favor disturbed habitats, and has likely done so for more than 65 million years, yet the living species has few of the life history traits typical of plants that prosper in disturbed settings. One solution to this paradox is to accept a non-uniformitarian view that plants in the geologic past operated in a different ecological regime. Angiosperms dominate the canopy today in most riparian and crevasse splay-type environments, and are the principle taxon from which modern ecological concepts for disturbed habitats are derived. The Ginkgoalean clade first appeared in the Permian and the Genus *Ginkgo* in the early Jurassic, making it possible that, prior to the radiation of angiosperms early in the Early Cretaceous (Doyle and Hickey, 1976), certain competitive-ruderal ecological strategies were less highly developed than in the present.

It is difficult to test this hypothesis directly because detailed sedimentological data for pre-angiospermous Mesozoic plant fossil-bearing sites are rare, and many lineages that may have dominated these disturbed habitats are extinct. However, from at least the Jurassic, the Ginkgoales show a strong tendency to be associated with sandy channel deposits (Hughes, 1976; Falcon-Lang et al., 2001; Spicer and Herman, 2001; L. J. Hickey, unpublished field data from the Jurassic in Yorkshire, England). In the subtropical Lower Cretaceous Wealden beds of northwest Germany, *Baiera* F. Braun is restricted to barrier sands, while *Ginkgoites* Seward is found in environments ranging from muddy floodplains to backswamps (Pelzer et al., 1992).

Prior to the flowering plants, ferns dominated the early seral stages in unstable, fluvial settings (Hughes, 1976; Hickey and Doyle, 1977; Taylor and Hickey, 1996) and probably provided the chief competition for *Ginkgo* from germination to the young sapling stage. In competition with the ferns, *Ginkgo*'s large seed reserves and "bolting" habit are inferred to have been sufficient to carry it beyond the herbaceous pteridophyte canopy. Among arborescent plants, *Ginkgo*'s chief competitors for crown space before the rise of the angiosperms were probably Bennettitales and various pteridosperms and tree ferns, plants whose sedimentary context, growth-habit, wood, and leaf structure suggest that they produced a relatively low, open canopy on disturbed sites (Hughes, 1976; Crane, 1985). The growth strategy of living *Ginkgo*, which undergoes rapid vertical elongation to a height of 10 m before elaborating lateral branches, would have been adaptive in such a situation.

Many of the early flowering plant lineages appear to have evolved in disturbed riparian habitats (Taylor and Hickey, 1996), and so could have been directly competing with *Ginkgo* for resources. For example, studies of the mid-Cretaceous (Albian-Cenomanian) of northern Alaska (Spicer and Herman, 2001) and the Antarctic Peninsula (Falcon-Lang et al., 2001) both indicate ginkgo-angiosperm-fern communities in riparian depositional environments. If the combination of rapid life cycles, high dispersal potential, and abundant foliage production in angiosperms was sufficient to out-compete *Ginkgo* in these settings, then it is possible that they played a role in the decline of *Ginkgo*.

There is also a striking temporal correlation between the rise of relative diversity in angiosperms (Ligard and Crane, 1990; Lupia et al., 1999) and the decline in Ginkgoalean diversity (Tralau, 1968) (Fig. 2.7). This comparison is not ideal as one must assume that all Ginkgoales possessed adaptive strategies similar to those of *G. adiantoides*. However, even within the genus *Ginkgo* there is a large drop in diversity between the Early and Late Cretaceous (Tralau, 1968). The relative diversity of 'other seed plants' (see Fig. 2.7), consisting of Ginkgoales, Bennettitales, Caytoniales, Cycadales, Czekanowskiales and Gnetales, but not conifers, also declines concomitantly with the rise of angiosperm diversity (Fig. 2.7; Ligard and Crane, 1990). The relative diversity of ferns, some of which preferred disturbed streamside environments (Taylor and Hickey, 1996), drops sharply as well in the mid-Cretaceous, while the diversity of conifers, which preferred backswamp environments, remains largely unchanged (Ligard and Crane, 1990; Lupia et al., 1999). These observations further suggest that angiosperms restructured the ecology of disturbed floodplain environments during the Cretaceous.

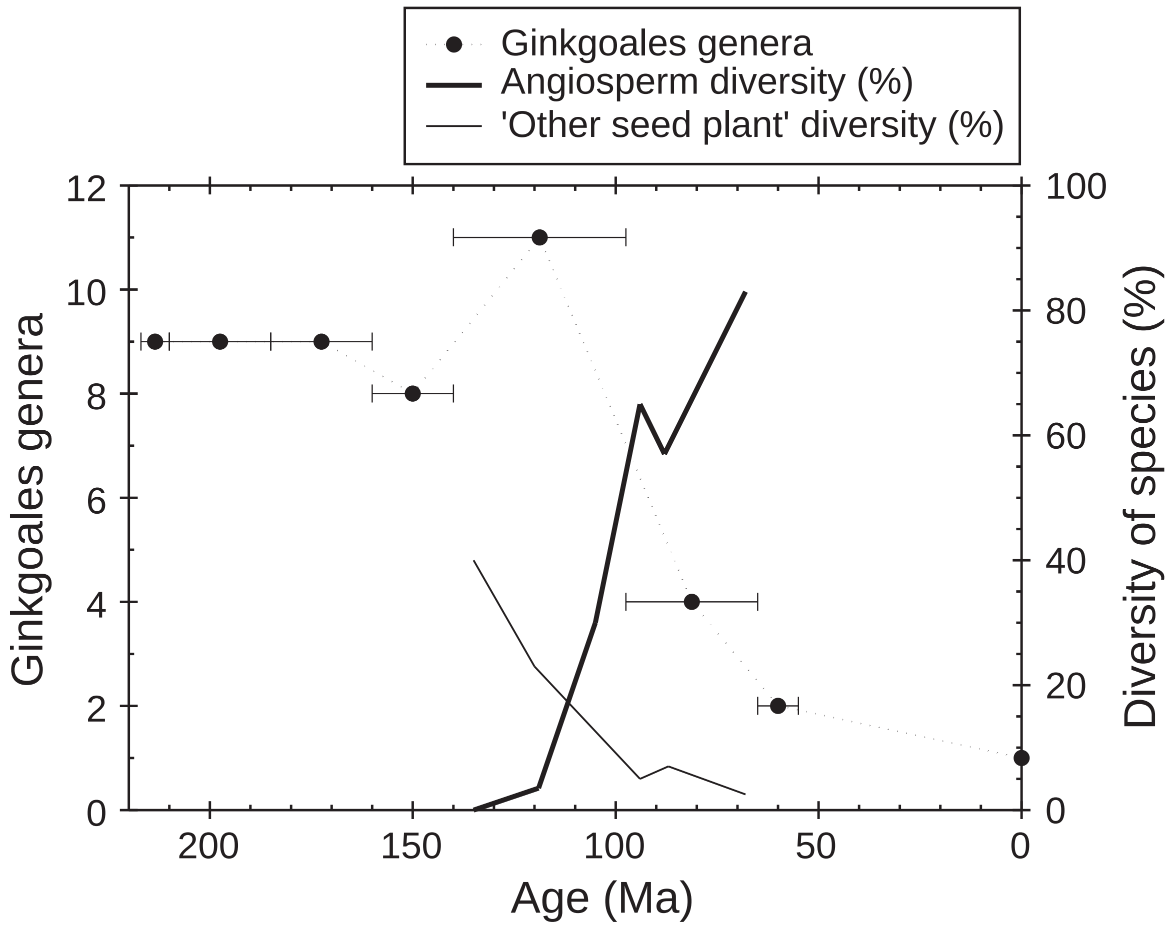

Fig. 2.7. Temporal trend of the number of Ginkgoales genera and the percent of total plant species that are angiosperms and 'other seed plants' (Ginkgoales, Bennettitales, Caytoniales, cycads, Czekanowskiales and Gnetales). Ginkgoales data from Tralau (1968); other data from Ligard and Crane (1990).

Perhaps the most surprising fact is that *Ginkgo* survives to the present at all. The persistence of the *Ginkgo* lineage may relate to its occurrence in mid- and high latitude areas. Wing and Boucher (1998) argued that lower temperatures and less light at higher latitudes make it more difficult for fast-growing competitive-ruderal trees to prosper, and that this explained the delayed increase in angiosperm diversity and dominance at higher latitudes during the Cretaceous (e.g., Lupia et al., 1999). If so, *Ginkgo* may have persisted because it was a mid- to high-latitude lineage for most of its existence; with growth limited by light and temperature, a relatively slow-growing competitive-ruderal such as *Ginkgo* could persist in the face of angiosperm competitors with the potential for faster rates of growth.

2.5 Conclusions

Ginkgo is an extreme example of a geologically long-lived genus, with its one living species arguably having a temporal range of > 100 Myr. A quantitative survey of sedimentological and floral data from 51 *Ginkgo*-bearing fossil sites, spanning the latest Cretaceous to middle Miocene, indicate that *Ginkgo* was largely confined to disturbed stream margin and levee environments. Furthermore, the stability of *Ginkgo*'s sedimentological and floral associations through the time series parallels the morphological identity of the fossil species, *G. adiantoides*, and the living *G. biloba*. As many of *Ginkgo*'s life history traits (e.g., long life-span, large seeds, and late sexual maturity) are not considered advantageous today in highly disturbed habitats, it is possible that *Ginkgo* represents the survival of a pre-angiospermous strategy for growth in well-drained, disturbed habitats.

CHAPTER 3

Paleobotanical evidence for near present-day levels of atmospheric CO_2 during part of the Tertiary

Understanding the link between the greenhouse gas carbon dioxide (CO_2) and Earth's temperature underpins much of paleoclimatology and our predictions of future global warming. Here, we use the inverse relationship between leaf stomatal indices and the partial pressure of CO_2 in modern *Ginkgo biloba* and *Metasequoia glyptostroboides* to develop a CO_2 reconstruction based on fossil *Ginkgo* and *Metasequoia* cuticles for the middle Paleocene to early Eocene and middle Miocene. Our reconstruction indicates that CO_2 remained between 300 and 450 parts per million by volume for these intervals with the exception of a single high estimate near the Paleocene/Eocene boundary. These results suggest that factors in addition to CO_2 are required to explain these past intervals of global warmth.

Atmospheric CO_2 concentration and temperature have been tightly correlated for the past four Pleistocene glacial-interglacial cycles (Petit et al., 1999). Various paleo-CO_2 proxy data (Ekart et al., 1999; Royer et al., 2001) and long-term geochemical carbon cycle models (Tajika, 1998; Berner and Kothavala, 2001; Wallmann, 2001) also suggest that CO_2-temperature coupling has, in general, been maintained for the entire Phanerozoic (Crowley and Berner, 2001). Recent CO_2 proxy data, however, indicate low CO_2 values during the mid-Miocene thermal maximum (Pagani et al., 1999; Pearson and Palmer, 2000), and results for the middle Paleocene to early Eocene, another interval of known global warmth relative to today, are not consistent, ranging from ~300 to 3000 parts per million by volume (ppmv) (Ekart et al., 1999; Pearson and Palmer, 2000). Here we address this problem by developing and applying an alternative CO_2 proxy based on the inverse correlation between the partial pressure of atmospheric CO_2 and leaf stomatal index (SI), with the aim of reconstructing CO_2 for both intervals to determine its role in regulating global climate.

Most modern vascular C_3 plants show an inverse relationship between the partial pressure of atmospheric CO_2 and SI (Woodward, 1987; Woodwards and Bazzaz, 1988; Chapter 1), a likely response for maximizing water-use efficiency (Woodward, 1987). SI is calculated as: SI (%) = (SD / [SD + ED])×100, where a stoma is defined as the stomatal pore and two flanking guard cells, SD = stomatal density and ED = non-stomatal epidermal cell density. Since SI normalizes for leaf expansion, it is largely independent of plant water stress, and is primarily a function of CO_2 (Woodward, 1987; Chapter 1). This plant-atmosphere response therefore provides a reliable paleobotanical approach for estimating paleo-CO_2 levels from SI measurements on Quaternary (Rundgren and Beerling, 1999) and pre-Quaternary fossil leaves (van der Burgh et al., 1993). Because stomatal responses to CO_2 are generally species-specific (Chapter 1), one is limited in paleo-reconstructions to species that are present both in the fossil record and living today. Fossils morphologically similar to living *Ginkgo biloba* and *Metasequoia glyptostroboides* extend back to the Early and Late Cretaceous, respectively, and many workers consider the living and fossil forms conspecific (Chaney, 1951; Tralau, 1968). In this study, we use *G. adiantoides* and *M. occidentalis*, the forms most closely resembling *G. biloba* and *M. glyptostroboides*, and also *G. gardneri*, which has more prominent papillae and less sinuous upper epidermal cells than *G. biloba* (Tralau, 1968).

Measurements of SI made on fossil *Ginkgo* and *Metasequoia* were calibrated with historical collections of *G. biloba* and *M. glyptostroboides* leaves from sites that developed during the anthropogenically driven CO_2 increase of the past 145 years and with saplings of *G. biloba* and *M. glyptostroboides* grown in CO_2-controlled greenhouses[1]. These data show a strong linear reduction in SI for both species between 288 and 369 ppmv CO_2 and a nonlinear response at CO_2 concentrations above 370 ppmv (Fig. 3.1). Because SI responds to partial pressure, not mole fraction (Woodward and Bazzaz, 1988), the effects of elevation must be considered. All of the leaves measured for the training set grew at elevations <250 m where concentration ≅ partial pressure, so a correction is not needed. Both nonlinear regressions are highly significant (Fig. 3.1); however, a discontinuity exists for *Ginkgo* between the experimental results above 350 ppmv and the rest of the calibration set. Many species require >1 growing season for SI to adapt to high CO_2 (Chapter 1), and so these experimental results likely represent maxima for a given CO_2 level. Nevertheless, due to this discontinuity as well as the small sample

[1] Training sets were largely derived from herbarium sheets, where three fields of view (0.1795 mm^2 each) from each of five leaves were measured using epifluorescence (for *Ginkgo*) and transmitted light (for *Metasequoia*) microscopy. Geographic origins of herbarium sheets range from the United States, Japan and China. During the growing seasons of 1999 (*Ginkgo* and *Metasequoia*) and 2000 (*Ginkgo*), measurements were made on living trees. Reference CO_2 values were taken from the Siple Station ice core (Friedli et al., 1986) for the period 1856-1957 and from direct Mauna Loa measurements for the period 1958-2000 (Keeling et al., 1995). Measurements were also made on *Ginkgo* saplings growing in CO_2-controlled greenhouses after two growing seasons at 350 and 560 ppmv (Beerling et al., 1998) and after one growing season for 6- (*Ginkgo*) and 1-year-old (*Ginkgo* and *Metasequoia*) saplings at 430 and 790 ppmv [see Beerling et al. (1998) for experimental methodology]. Fields of view were concentrated near the centers of leaves in the intercostals, which have been shown in other species to yield the least variation in SI (Chapter 1). Although stomata occur in rows in *Metasequoia*, the field of view chosen (0.1795 mm^2) nearly spanned the distance between the midrib and margin, and thus the stomatal bands should not confound our results.

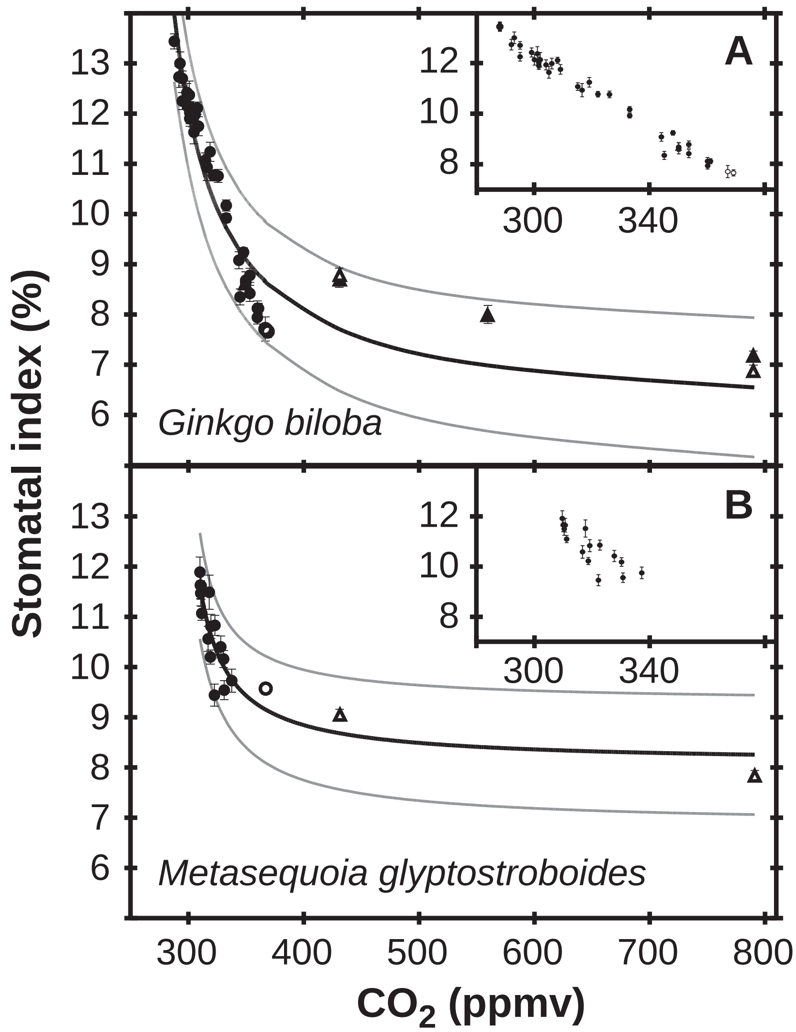

Fig. 3.1. Training sets for (A) *Ginkgo biloba* (n = 40) and (B) *Metasequoia glyptostroboides* (n = 18). Thick black lines represent regressions {*Ginkgo*: r^2 = 0.91, $F(1, 37)$ = 185, P < 0.0001, $SI = [CO_2 - 194.4] / [(0.16784) \times CO_2 - 41.6]$; *Metasequoia*: r^2 = 0.85, $F(1,15)$ = 41, P < 0.0001, $SI = [CO_2 - 274.5] / [(0.12373) \times CO_2 - 35.3]$}. Gray lines represent ±95% prediction intervals. Inset graphs show the linear portions of both response curves in greater detail. Stomatal index determined from herbarium sheets (●), fresh samples from living trees (◎), and 6- (▲) and 1-year-old (△) saplings growing in CO_2-controlled greenhouses. Error bars represent standard errors.

size and decreased sensitivity at high CO_2 for both *Ginkgo* and *Metasequoia*, paleo-CO_2 estimates >400 ppmv should be considered semi-quantitative.

To reconstruct atmospheric CO_2 changes, we measured the SI of fossil *Ginkgo* and *Metasequoia* cuticles from 24 localities in western North America and one from the Isle of Mull (Scotland), and then calibrated these data against the modern training set (Fig. 3.1) using inverse regression[2]. Although not tightly constrained, the paleoelevations for all of the sites were probably <1000 m. This elevation difference could increase our estimates of CO_2 concentration by at most 10%, and so our conversion from partial pressure to concentration excludes any correction. Except for a single high CO_2 value near the Paleocene/Eocene boundary, all of our reconstructed CO_2 concentrations lie between 300 and 450 ppmv (Fig. 3.2; Table 3.1). These contrast with two other *Ginkgo*-based CO_2 estimates for the late Paleocene and middle Miocene that are very high (4500 and 2100 ppmv, respectively) (Retallack, 2001; see Footnote 3).

---

[2] Measurements of SI were made on fossil cuticles on each of 5 to 22 leaves per site (Table 1) using epifluorescence (for *Ginkgo*) and transmitted light (for *Metasequoia*) microscopy, with count replication and field sizes as in footnote 1. Inverted regression for *Ginkgo*: $CO_2 = [1 - (0.1564)\times SI] / [0.00374 - (0.0005485)\times SI]$, $r^2 = 0.84$, $F(1,37) = 91$, $P < 0.0001$; and for *Metasequoia*: $CO_2 = (SI - 6.672) / [(0.003883)\times SI - 0.02897]$, $r^2 = 0.98$, $F(1,15) = 336$, $P < 0.0001$. Standard errors in SI for fossil sites are ~0.20%. Fossil *Ginkgo* leaves preserved in environments that today host well-watered, open canopy forests (Chapter 2). Such conditions should minimize both the influence of confounding variables in the SI-CO_2 signal and the environmental differences between the training and fossil datasets. It is possible a species effect on SI exists between *G. gardneri* at Ardtun Head and *G. adiantoides* at the other sites, however a difference in SI of 6 (Table 1) is highly unlikely based on studies of intra-generic SI variation in modern plants (Chapter 1). All Bighorn Basin sites are dated using Age Model 2 of Wing et al. (2000), while the Ardtun Head site is dated assuming it is stratigraphically near the latest Paleocene carbon isotope excursion (55.2 Ma using Age Model 2). For details of dating methods for the other sites, see Chapter 4.

[3] These two CO_2 estimates are based upon small sample sizes ($n = 4$ cuticle fragments each) and an extrapolation of a training set calibrated only up to 560 ppmv.

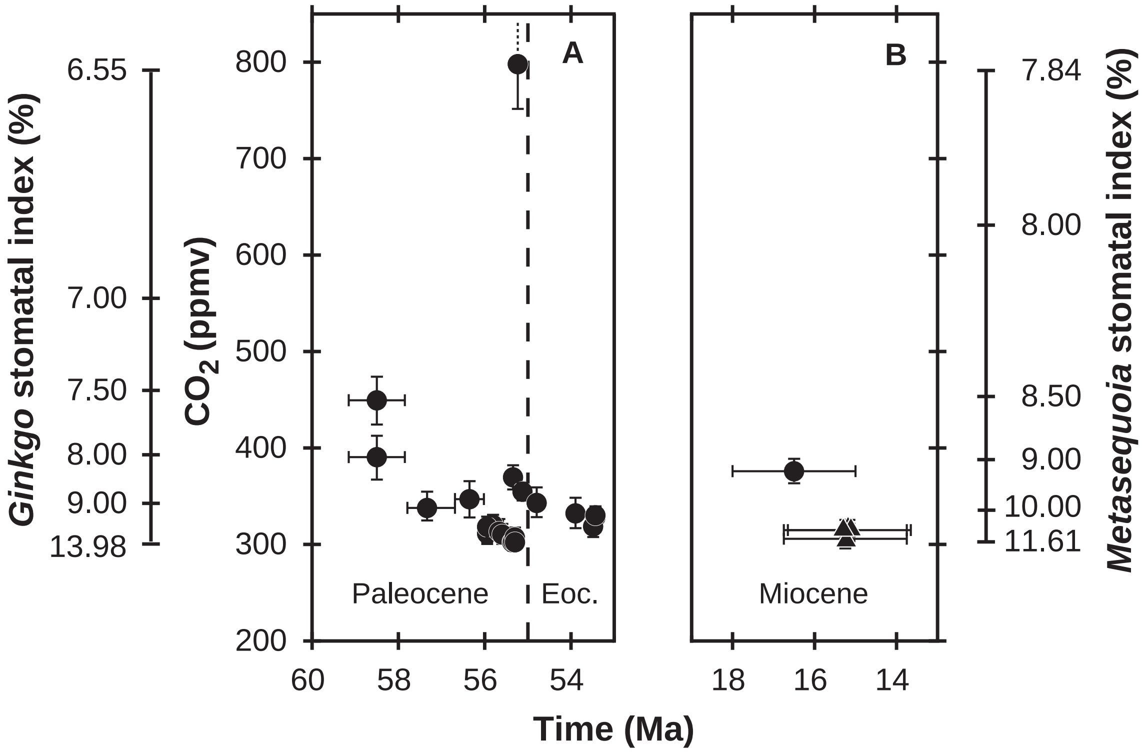

Fig. 3.2. Reconstruction of paleo-CO_2 for the (A) middle Paleocene to early Eocene and (B) middle Miocene based on SI measurements from *Ginkgo* (●) and *Metasequoia* (▲) fossil cuticles. Errors represent ±95% confidence intervals.

Table 3.1. Summary of fossil data. *n* = number of leaves measured for calculation of SI. A = south-central Alberta (Canada), BHB = Bighorn Basin (Wyoming and Montana, USA), M = Isle of Mull (UK), I = north-central Idaho (USA). Dashes indicate that no analyses were performed. BOM = bulk organic matter. $\delta^{13}C_{om}$ = $\delta^{13}C$ of organic matter. See Footnote 4 for $\delta^{13}C$ methodology.

Site	Location	Age (Ma)	*n*	SI (%)	CO_2 (ppmv)	$\delta^{13}C_{om}$ (V-PDB)
		Ginkgo				
Burbank	A	58.5	7	7.55	450	–
Joffre Bridge	A	58.5	5	7.96	391	–
SLW 0025	BHB	57.3	7	9.01	340	–
LJH 7132	BHB	56.4	5	8.75	348	-23.91
SLW 991	BHB	55.9	5	10.97	314	–
SLW 992	BHB	55.9	8	10.80	316	-25.66
SLW 993	BHB	55.9	8	11.43	311	–
LJH 72141–1	BHB	55.8	12	10.63	317	–
SLW 9155	BHB	55.7	10	11.21	313	-29.80
SLW 9411	BHB	55.6	8	11.50	311	-23.77
SLW 9434	BHB	55.4	7	12.23	307	-22.53
SLW 9715	BHB	55.3	12	8.23	371	-24.17
SLW 9050	BHB	55.3	5	12.18	308	-26.99
SLW 9936	BHB	55.3	15	11.77	310	–
SLW 8612	BHB	55.3	7	12.41	307	–
Ardtun Head	M	55.2	13	6.54	798	-24.68
AR-2 (BOM)						-24.56
AR-6 (BOM)						-25.82
AR-8 (BOM)						-24.17
AR-10 (BOM)						-24.26
AR-15 (BOM)						-24.54
SLW 9812	BHB	55.1	22	8.53	356	-24.49
SLW 9915	BHB	54.8	8	8.83	345	–
SLW LB	BHB	53.9	5	9.29	334	–
SLW H	BHB	53.5	9	10.22	321	-26.93
LJH 9915	BHB	53.4	15	9.38	332	-26.33
Juliaetta (P6)	I	16.5	14	8.14	377	–
		Metasequoia				
Clarkia (P33a)	I	15.3	6	11.59	307	–
Clarkia (P33b)	I	15.3	10	10.94	316	–
P37a	I	15.2	10	10.95	316	–

We have *Metasequoia*-derived CO_2 estimates only from the warm interval of the middle Miocene, but these are similar to coeval estimates derived from *Ginkgo* cuticles. The convergence of these two independent estimates increases our confidence that both species are reliably recording paleoatmospheric CO_2 levels. In addition, the measured SI values from most sites fall well inside the region of high CO_2 sensitivity in the training sets (Fig. 3.1; Table 3.1), and the 95% confidence intervals (±50 ppmv or less) are over an order of magnitude lower than the errors associated with early Tertiary CO_2 estimates from geochemical models (Tajika, 1998; Berner and Kothavala, 2001; Wallmann, 2001) and other proxies (Ekart et al., 1999; Pearson and Palmer, 2000). Furthermore, middle Paleocene to early Eocene CO_2 reconstructions based on pedogenic carbonate (Ekart et al., 1999; see Footnote 4) and marine boron isotopes (Pearson and Palmer, 2000) show

---

[4] In addition to the published estimates compiled in Ekart et al. (1999), we also made seven new CO_2 estimates based on our record of cuticle $\delta^{13}C$ (Table 3.1) and the $\delta^{13}C$ of pedogenic carbonate ($\delta^{13}C_{cc}$) from sites stratigraphically within 15 m (~30 ky) of our cuticle-bearing sites. This affords the rare opportunity to apply multiple CO_2 proxies to sediments in close geographic and stratigraphic proximity.

Stable carbon isotope analyses were conducted on *Ginkgo* cuticle fragments at all sites, as well as on bulk organic matter at Ardtun Head. Cuticle fragments were separated from host rock with either tweezers or by placing drops of 52% HF along the cuticle edges. Bulk organic matter was prepared by reacting finely ground host rock with 38% HCl for 6 hours, centrifuging, reacting with fresh HCl for an additional 24 hours, then repeating with 5:1 52% HF:38% HCl. Carbon dioxide was generated for isotopic analysis by combustion in sealed, evacuated VYCOR tubes at 910 °C for 1 hour in the presence of CuO and Cu metal. After cryogenic distillation, CO_2 was analyzed on a gas source mass spectrometer. Data are reported relative to V-PDB. Replicate analyses of a laboratory gelatin standard analyzed with these samples had a standard deviation of 0.05‰ (n = 9).

CO_2 calculated using Equation 1 in Ekart et al. (1999) and a planktonic foraminifera-derived atmospheric $\delta^{13}C$ value of –5.6‰, and assuming the concentration of CO_2 contributed by soil = 5000 ppmv and soil temperature = 25 °C (Ekart et al., 1999). At sites SLW 826, 882, and 8822, we analyzed bulk cuticle, not just *Gingko* cuticle. The site names from which the cuticle and corresponding pedogenic carbonate were collected, $\delta^{13}C_{cc}$ values, and CO_2 estimates (± ~500 ppmv) are as follows: LJH 7132, SC 85 & 185, -7.95‰, 1185 ppmv; SLW 992, SC 92, -7.82‰, 2041 ppmv; SLW 9715, SC 22, -7.69‰, 1448 ppmv; SLW 9812, SC 4, -8.36‰, 1217 ppmv; SLW 826 (54.8 Ma, $\delta^{13}C_{om}$ = -

large changes in CO_2 (≥2000 ppmv) over geologically brief periods of time [<1 million years (My)] (Fig. 3.3) that cannot be readily explained. In contrast, the highly constrained error ranges and consistency among near time-equivalent estimates suggest that our SI-derived CO_2 reconstruction is presently the most reliable, particularly for the middle Paleocene to early Eocene.

A period of rapid climatic warming (~2 °C global mean rise within 10^4 years that lasted 10^5 years) near the Paleocene/Eocene boundary has been extensively documented (Kennett and Stott, 1991; Koch et al., 1992; Huber and Sloan, 1999). Although the leading hypothesis for the cause of most of this warming is the rapid release of methane from marine gas hydrates and its subsequent oxidation to CO_2 in the atmosphere and ocean (Dickens et al., 1995; Norris and Röhl, 1999), all previous attempts to resolve this possible atmospheric CO_2 spike have failed (Koch et al., 1992; Stott, 1992; Sinha and Stott, 1994). Our single high CO_2 estimate is based on *G. gardneri* cuticle from Ardtun Head, Isle of Mull. Anomalously low $\delta^{13}C_{om}$ values (-30‰), an influx of the marine dinocyst *Apectodinium*, and a thermophyllic flora (including *Caryapollenties veripites* and *Alnipollenites verus*) occur in stratigraphically equivalent sediments elsewhere on Mull. Together, these indicate a possible correlation with a section of a Paris Basin borehole that has been calibrated to this event (Thiry et al., 1998). At Ardtun Head, however, we failed to capture the negative carbon isotope excursion globally associated with this event, which ranges from 2.5‰ in the deep ocean (Kennett and Stott, 1991; Norris and Röhl,

---

28.65‰), YPM 200+4m, -11.88‰, 1152 ppmv; SLW 882 (53.5 Ma, $\delta^{13}C_{om}$ = -27.71‰) & SLW H & LJH 9915, YPM 320 & D1217+10m, -11.96‰, 577 ppmv; SLW 8822 (52.8 Ma, $\delta^{13}C_{om}$ = -28.71‰), Fern Q lower, -10.01‰, 2034 ppmv.

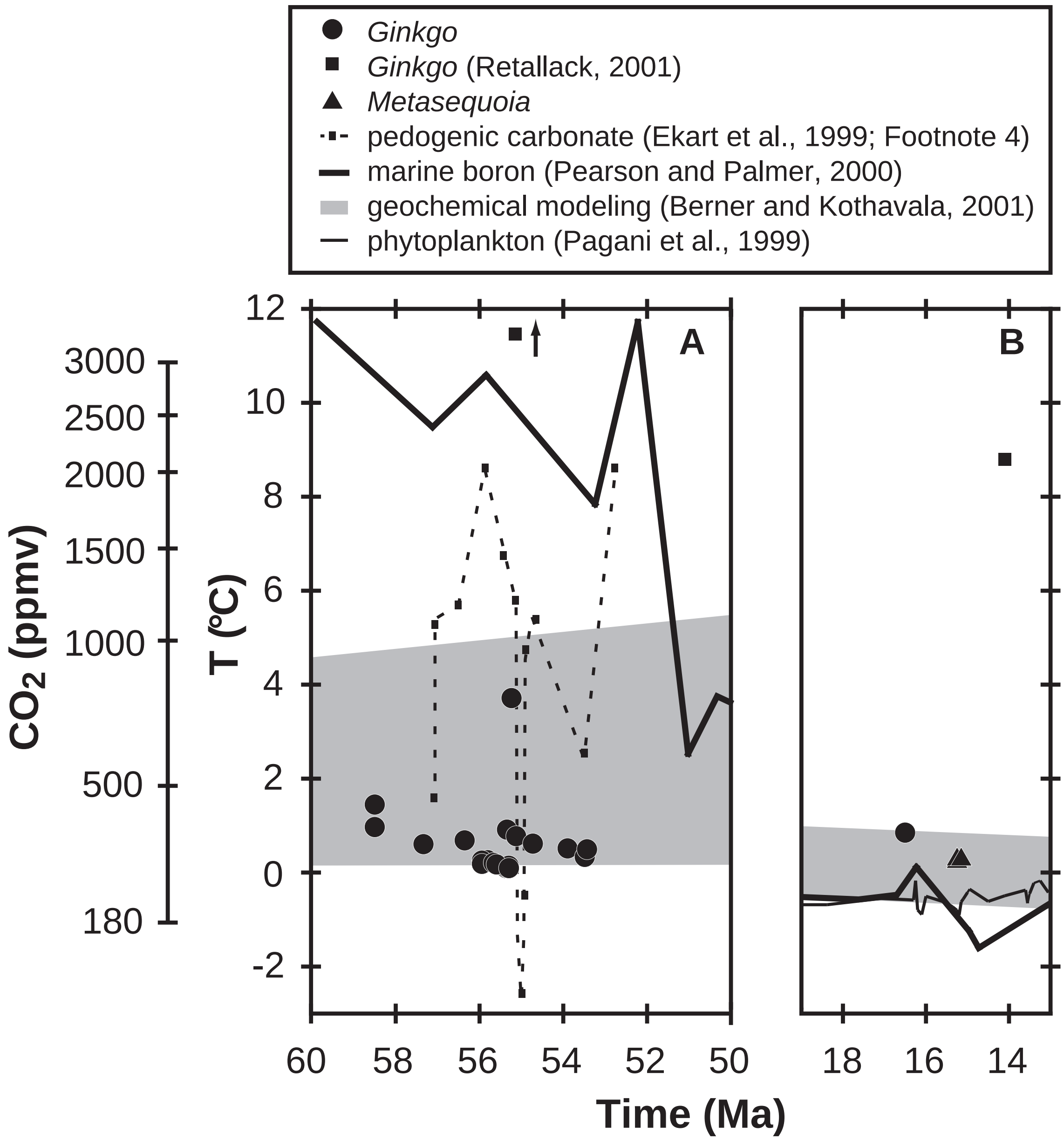

Fig. 3.3. Estimates of paleo-CO_2 concentration derived from a variety of methods and their corresponding model-determined temperature departures (T) of global mean surface temperature (GMST) from present day for the (A) middle Paleocene to early Eocene and (B) middle Miocene. Paleo-GMST calculated from paleo-CO_2 estimates using the CO_2-temperature sensitivity study of Kothavala et al. (1999). Present-day reference GMST calculated using the pre-industrial CO_2 value of 280 ppmv (14.7 °C). The error range of GMST predicted from the geochemical modeling-based CO_2 predictions of Berner and Kothavala (2001) corresponds to the model's sensitivity analysis

1999) to as much as 6‰ on land (Koch et al., 1992) (Table 3.1). Although the precise age of the Ardtun Head site remains uncertain, using a global carbon isotope mass balance model calibrated to Paleocene/Eocene conditions (Beerling, 2000), our reconstructed CO_2 increase (500 ppmv) is consistent with a release of 2522 Gt of methane-derived carbon, a value close to the estimate (2600 Gt C) calculated to account for the marine carbon isotopic excursion using methane as the carbon source (Dickens, 2001).

Carbon dioxide is an important greenhouse gas, and its effect on global mean surface temperature (GMST) can be quantified with general circulation models (GCMs) [e.g., Kothavala et al. (1999)]. Using the model output of Kothavala et al. (1999) we predicted GMST from our CO_2 results. The GCM used by Kothavala et al. is calibrated to the present day, which allows us to test the effect of CO_2 on GMST independent of any paleogeographic or vegetational changes. With the exception of the single value near the Paleocene/Eocene boundary, all predictions lie within 1.5 °C of the pre-industrial GMST (Fig. 3.3). These predictions contrast sharply with most paleoclimatic interpretations for these time intervals. For example, based on a synthesis of global late Paleocene and early Eocene δ^{18}O-derived sea surface temperature data, Huber and Sloan (1999) estimated that GMST was 3° to 4 °C higher than today at this time, and δ^{18}O-derived temperature estimates for the mid-Miocene thermal maximum [17 to 14.5 million years ago (Ma)] indicate that deep and high-latitude surface ocean temperatures were as much as 6 °C warmer than today (Savin et al., 1975).

As a cross-check on our results, we compared our GMST predictions with those based on a geochemical carbon cycle model and other CO_2 proxies for these same time periods. With the exception of the one stomatal-based CO_2 estimate by Retallack (2001), there is very good agreement among the methods for the middle Miocene (Fig. 3.3), strongly suggesting that factors in addition to CO_2 are required to explain this brief warm period. In contrast, a large disagreement (10 °C or greater) exists for the middle Paleocene to early Eocene (Fig. 3.3). This discrepancy is largely driven by the high CO_2 estimates derived from marine boron isotopes (Pearson and Palmer, 2000); however, this proxy is probably less accurate than the other methods (Lemarchand et al., 2000; Royer et al., 2001). Nevertheless, even if the boron-based predictions are discounted, a large range still exists among the remaining three methods. This is striking considering that many of the pedogenic carbonate-derived CO_2 estimates are based on the same sediments as our stomatal-based estimates (Footnote 4); however, these estimates show a large temporal variability (-60 to 2040 ppmv) and are associated with relatively large error ranges (± 500 ppmv). If our low SI-based temperature predictions are correct, additional factors such as paleogeography, enhanced meridional heat transport, and high latitude vegetation feedbacks are required to explain this warm period, and new constraints for CO_2 levels are established for middle Paleocene to early Eocene and middle Miocene GCMs [e.g., Sloan and Rea (1995)]. Understanding the mechanisms of climate change will become increasingly important in the near future as atmospheric CO_2 levels climb to levels perhaps unprecedented for the last 60 My.

CHAPTER 4

Estimating Latest Cretaceous and Tertiary Atmospheric CO_2 Concentration from Stomatal Indices

4.1 Introduction

Globally averaged surface temperatures have risen sharply in the last century (~1 °C in the Northern Hemisphere) (Mann et al., 1998, 1999), concomitant with a 30% increase in the concentration of the greenhouse gas CO_2 (Friedli et al., 1986). It is now clear that CO_2 is largely responsible for this warming (Mann et al., 1998; Crowley, 2000; Barnett et al., 2001; Harries et al., 2001; Levitus et al., 2001; Mitchell et al., 2001). On the longer timescale of 10^5 years, temperature and atmospheric CO_2 have been tightly coupled for at least the last four glacial-interglacial cycles (Petit et al., 1999), and it appears that CO_2 has also been driving these temperature variations (Shackleton, 2000).

On multimillion year timescales, proxy- and modeling-based estimates of CO_2 over the Phanerozoic largely correlate with geologic indicators of continent-scale glaciations, which are the most reliable index for the presence of 'greenhouse' or 'icehouse' climates (Crowley and Berner, 2001). This correlation is not present, however, during certain intervals. Proxy-based CO_2 estimates for the mid-Miocene thermal maximum (17-14.5 Ma), a brief interval of global warmth relative to today, suggest concentrations largely lower than the pre-industrial value of 280 ppmV (Pagani et al., 1999; Pearson and Palmer, 2000). In addition, CO_2 estimates derived from multiple proxies for other time periods are not consistent. For example, early Tertiary (65-50 Ma) CO_2 estimates range from <300 ppmV to >3000 ppmV (Ekart et al., 1999; Pearson and Palmer, 2000).

Here I apply a CO_2-calibrated set of stomatal indices from *Ginkgo biloba* and *Metasequoia glyptostroboides* to reconstruct paleo-CO_2 levels for the very latest Cretaceous to early Eocene (66-53 Ma) and the middle Miocene (~15.5 Ma). This study expands on the data presented in Chapter 3 and Beerling et al. (2002).

4.2 The stomatal index method

Most modern vascular C_3 plants show an inverse relationship between the partial pressure of atmospheric CO_2 and stomatal index (Woodward, 1987; Beerling, 1999; Lake et al., 2001; Chapter 1). Stomatal index (SI) is the percentage of epidermal cells that are stomatal packages (guard cells + stomatal pore), and is defined as the following (Salisbury, 1927):

$$SI = \frac{SD}{SD + ED} \times 100$$

where *SD* = stomatal density (mm^{-2}) and *ED* = non-stomatal epidermal cell density (mm^{-2}). The mechanism(s) linking CO_2 to SI is not fully understood, but probably involves the strong selective pressure to maximize carbon fixation per unit of water transpired (water-use efficiency) (e.g., Woodward, 1987). For example, in a rising CO_2 regime plants can increase their water-use efficiency by reducing their stomatal conductance, thereby reducing water loss. Stomatal conductance is largely a function of stomatal pore area, which in turn is controlled by the size of individual stomatal pores and the density of those pores. On the timescale of several growing seasons or longer, stomatal density is typically more sensitive to changes in atmospheric CO_2 than individual pore size (e.g., Chapter 1). Furthermore, on multimillion year timescales stomatal density and SI across all plant taxa inversely respond to CO_2 (Beerling and Woodward, 1997; McElwain, 1998; Chapter 1).

In contrast to stomatal density, SI is area independent, which normalizes for the effects of cell expansion. Stomatal index is essentially a measure of the number stomatal packages that develop per unit of non-stomatal epidermal cells. Since plant water-potential strongly influences cell expansion [e.g., water stressed plants generally reduce the size of their epidermal cells (Chapter 1)], but not the rate of stomatal initialization, changes in a plant water budget can affect stomatal density, but not stomatal index. Experimental studies show that SI is largely independent of water potential, irradiance, and temperature, and is primarily a function of CO_2 (e.g., Beerling, 1999; Chapter 1).

Stomatal indices (and stomatal densities) have been experimentally shown to respond to the partial pressure of CO_2, not mole fraction (Woodward and Bazzaz, 1988). This finding is corroborated by a positive correlation in many plants between elevation and stomatal density (Körner and Cochrane, 1985; Woodward, 1986; Woodward and Bazzaz, 1988; Beerling et al., 1992) and SI (Rundgren and Beerling, 1999). It is important, therefore, to control for elevation when estimating CO_2 from stomatal properties. The relationship between elevation and partial pressure in the lower atmosphere is roughly as follows:

$$P = -10.6E + 100$$

where E = elevation in kilometers and P = the percentage of partial pressure relative to sea level. If one does not control for elevation (i.e., assumes concentration = partial pressure), CO_2 concentration estimates will be underestimated by 3% for plants growing at 250 m elevation, for example, and 11% for plants at 1000 m.

4.2.1 Choice of species

Stomatal responses to atmospheric CO_2 are usually species-specific (Woodward and Kelly, 1995; Beerling and Kelly, 1997; Chapter 1). For example, based upon genera represented by >1 species in the compilation in Chapter 1 (n = 7), only one is internally consistent (α = 0.05; chi-squared test) with respect to SI. In order to quantitatively reconstruct paleo-CO_2, then, the SI-CO_2 relationship in an extant species must be applied in the fossil record to the same species. This requirement has previously hindered the applicability of this method for fossil leaves pre-dating the late Miocene (10 Ma) (van der Burgh et al., 1993; Kürschner et al., 1996). Here I use the lineages represented today by *Ginkgo biloba* and *Metasequoia glyptostroboides*, which greatly extends the temporal applicability of the method.

Morphologically indistinguishable forms of *G. biloba* extend back to the early Cretaceous, leading many authors to consider the fossil and modern forms conspecific (Tralau, 1968; see Chapter 2). This fossil form is most commonly identified as *G. adiantoides*, however many other designations are considered equivalent, e.g., *G. spitsbergensis* (Tralau, 1968). In fact, the only Tertiary-aged ginkgo form that may deviate sufficiently from the *adiantoides-biloba* form to warrant a separate species class is *G. gardneri* (Manum, 1966; Tralau, 1968), which occurs at one early Paleogene site on the Isle of Mull, Scotland (e.g., Boulter and Kvaček, 1989). Further evidence for conspecificity of the Tertiary-aged and modern forms comes from a paleoecological study of *Ginkgo* (Chapter 2). Based primarily upon the localities used in this study, the distribution of *Ginkgo*'s sedimentological contexts (e.g., stream margin, crevasse splay, backswamp) and floral associates remain largely unchanged throughout the Tertiary, suggesting a conservative phylogeny.

Chen et al. (2001) report that the SI in modern *G. biloba* is statistically independent of leaf size, long vs. short shoots, and male vs. female trees, and only minor differences (<5%) due to canopy position and the timing of leaf development are present. These results further suggest that the SI's in *Ginkgo* are reliable indicators of atmospheric CO_2 concentration.

Ginkgo foliage is very distinctive and readily identified. A *Ginkgo* leaf consists of a petiole and fan-shaped dichotomously veined lamina (Fig. 4.1). The veins only very rarely anastomose (Arnott, 1959). Vein spacing is typically ~1 mm. Stomata are found only on the abaxial side of the leaf (hypostomatous), and are distributed randomly in the intercostal regions. Subsidiary cells are moderately papillose, which partially cover the stomatal pore. The leaf is usually divided into two lobes, whose margins are wavy. The petiole consists of two vascular strands, each of which vascularize one of the lobes (Chamberlain, 1935; Gifford and Foster, 1989). Mucilage cavities are common and conspicuous, even in fossils. They are 1-5 mm in length, and are oriented parallel to venation (Chamberlain, 1935). The *adiantoides-biloba* form is differentiated from other ginkgo-forms (which largely occur earlier in the rock record) by its less dissected lamina (Tralau, 1968), however deeply lobed leaves do occur occasionally in *G. biloba* (Critchfield, 1970). The only other plants with open dichotomizing venation and bilobed

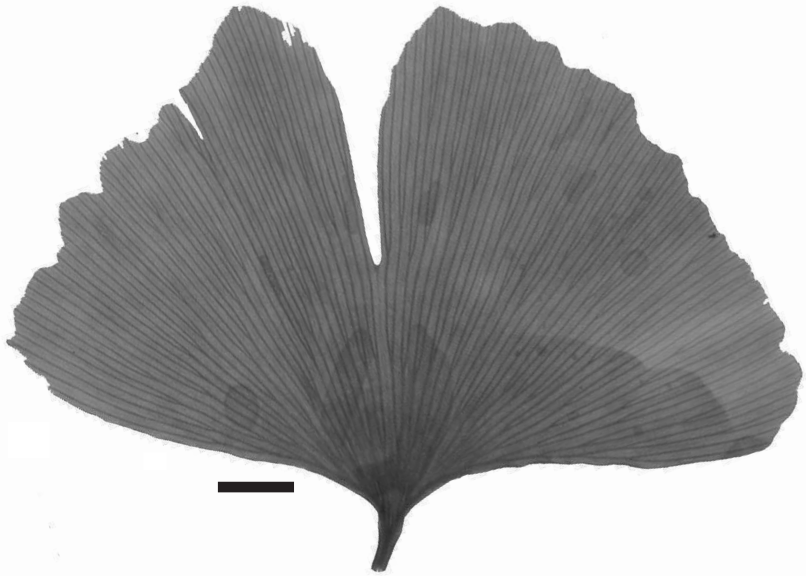

Fig. 4.1. A leaf of *Ginkgo biloba*. Collected from New Haven, Connecticut (USA). Scale bar = 1 cm.

lamina are ferns such as *Adiantum* (e.g., Gifford and Foster, 1989). These can be distinguished from *Ginkgo* by the single vascular strand in their petioles, the presence of sori abaxially near the tips of their leaves, and their more closely spaced veins.

Metasequoia also has a long fossil record of indistinguishable forms back to the Late Cretaceous (Liu et al., 1999). Many workers consider this fossil form, *M. occidentalis*, very closely related to, or conspecific with the modern *M. glyptostroboides* (Chaney, 1951; Christophel, 1976; Liu et al., 1999). *Metasequoia* needles are flat and ~15-20 mm in length and ~2 mm in width. The leaf morphology of *Metasequoia* is very similar to *Sequoia* and *Taxodium*, however *Metasequoia* needles are arranged decussately opposite while the needles in the other two genera are spirally alternate. *Metasequoia* also tends to have more rounded tips, a higher angle of divergence between the leaf and shoot (~90°), and a more highly twisted base than *Sequoia* and *Taxodium* (Chaney, 1951).

The fossil records of *Ginkgo* and *Metasequoia* indicate that both were components of mid- to high latitude temperate forests (Tralau, 1967; Mai, 1994). In contrast to multi-story tropical forests, intracanopy CO_2 gradients are small in temperate forests and should not bias stomatal-based CO_2 estimates (Chapter 1).

4.2.2 Construction of training set

Leaves from dated herbarium sheets of *Ginkgo biloba* and *Metasequoia glyptostroboides* were used to assess the response of their SI's to the anthropogenic rise in atmospheric CO_2 concentration over the last 145 years. Because both *Ginkgo* and *Metasequoia* have deciduous leaf habits, all leaves are assumed to have grown only during the year recorded on the sheets. The CO_2 concentrations that the leaves developed in were taken from ice core-derived (Friedli et al., 1986) and direct atmospheric (Keeling et al., 1995) measurements. The geographic origins of the leaves for both species range from the United States, China, and Japan. Most material came from cultivated individuals. All trees grew at <250 m in elevation, with 84% of them growing at elevations <75 m. Therefore, no correction is needed to convert CO_2 partial pressure to concentration. For each herbarium sheet, five mature leaves were randomly selected. Stomatal index was calculated for three fields of view (0.1795 mm^2 each) on every leaf. Measurements were made in the intercostal regions near the centers of the leaves, which in other species show the least variation in SI (Salisbury, 1927; Chapter 1). A combination of acetate peels and cleared leaves using light microscopy, and unaltered leaf tissue using epifluorescence microscopy was employed. No systematic variation in SI among the three preparation techniques was noted. During the growing season of 1999 (and 2000 for *Ginkgo*), SI was measured from trees growing in New Haven (Connecticut, USA), Ann Arbor (Michigan, USA), and London (UK). Sampling details are given in Table 4.1.

Stomatal indices were also measured on saplings growing in greenhouses at four discrete CO_2 concentrations. For each CO_2 treatment, three potted saplings were placed in each of four independent greenhouses [see Beerling et al. (1998) and Beerling and Osborne (2002) for details]. For the 430 / 445 ppmV and 790 / 800 ppmV treatments, SI was measured after a CO_2 exposure time of both one and two growing seasons. The *Metasequoia* saplings were one-year-old after their first season of CO_2 treatments. Two sets of *Ginkgo* saplings were used, aged one- and six-years-old after their first season of CO_2 treatments. For the 350 and 560 ppmV treatments, SI was determined from three-year-old *Ginkgo* saplings after a CO_2 exposure time of two growing seasons (Beerling et al., 1998). Sampling details are given in Table 4.1.

TABLE 4.1. DETAILS OF SAMPLING FOR TRAINING SETS

A. HISTORICAL COLLECTIONS

Species	Year(s) Collected	CO_2 (ppmV)	Mode of Preparation*	Trees†	Leaves†	Field of views†
G. biloba	1856-1996	288-361	E	1	5	15
	1999	367	A	6	13	46
	2000	369	C	3	10	30
M. glyptostroboides	1947-1980	310-338	A, C	1	5	15
	1999	367	A	4	21	46

B. GREENHOUSE EXPERIMENTS

Species	Exposure to CO_2 (years)	CO_2 (ppmV)	Mode of Preparation*	Trees†	Leaves†	Field of views†
G. biloba	2	350§	A	8	16	160
	1	430#	C	8	16	48
	1	430**	C	8	8	24
	2‡	445#	C	8	8	24
	2‡	445**	C	8	8	24
	2	550§	A	8	16	160
	1	790#	C	8	16	48
	1	790**	C	7	7	21
	2‡	800#	C	8	8	24
	2‡	800**	C	8	8	24
M. glyptostroboides	1	430**	C	8	16	48
	2‡	445**	C	7	7	21
	1	790**	C	8	16	48
	2‡	800**	C	8	8	24

* A = acetate peels (light microscopy); C = cleared leaves (light microscopy); E = unaltered leaves (epifluorescence microscopy).

† Total number per CO_2 value or herbarium sheet.

§ From Beerling, McElwain, and Osborne (1998). Three year old saplings.

\# Six-year-old (for 430 and 790 ppmV treatments) and seven-year-old (for 445 and 800 ppmV treatments) saplings.

** One-year old (for 430 and 790 ppmV treatments) and two-year-old (for 445 and 800 ppmV treatments) saplings.

‡ Includes the exposure time from the previous growing season (either 430 or 790 ppmV).

4.2.3 Application of fossil cuticles

Stomatal indices were calculated from 27 very latest Cretaceous to middle Miocene-aged *Ginkgo* cuticle-bearing sites and three middle Miocene-aged *Metasequoia* cuticle-bearing sites. The application of both *Ginkgo* and *Metasequoia* cuticles from near coeval middle Miocene-aged sites provides a check on the reliability of the method. As with the training set material, SI was determined for three field of views on each fossil leaf. At least five leaves were measured per site (see Table 4.2). This ensures that at least as many leaves per site were used to reconstruct paleo-CO_2 than were used per herbarium sheet to establish the training sets. For *Ginkgo*, epifluorescence microscopy on unaltered cuticle was employed. Fossil *Metasequoia* cuticle failed to fluoresce, and so leaves were first cleared and then analyzed using light microscopy. Voucher specimen information for both the training and fossil datasets are available from the author.

The paleoelevations of all regions sampled in this study are most likely <1000 m. For example, the late Cretaceous Hell Creek Formation in the Williston Basin contains marine and brackish facies (Frye, 1969; Murphy et al., 1999), indicating paleoelevations near sea level. In the Bighorn Basin, which produced the largest number of fossil cuticle sites, there are few constraints on paleoelevation [see discussion in Chase et al. (1998)]. The most liberal estimates for the basin during this time range from 1500 to 2500 m (Chase et al., 1998), however other workers consider these estimates to be too high because they think it unlikely that climate at these higher elevations would be warm enough to support the large number of subtropical and frost intolerant plants that are known from basinal deposits (S. L. Wing, personal communication, 2001). Due to the lack of reliable estimates for the Bighorn Basin, and the inferred low paleoelevations for

TABLE 4.2. SAMPLING DETAILS AND CO_2 RECONSTRUCTION FOR FOSSIL DATA

A. *GINKGO*

Site	Location*	Depository†	Age (Ma)	*n*§	SI (%)	CO_2 (ppmV)
DMNH 566	ND	DMNS	65.5	31	8.32	385
LJH 7423	BHB	USNM	64.5	5	9.48	339
LJH 7659	BHB	YPM	64.5	15	9.32	344
DMNH 2360	DB	DMNS	64.1	5	9.90	329
Basilika	S	PMO	64.0	8	9.42	341
Burbank	A	UA	58.5	7	7.55	451
Joffre Bridge	A	UA	58.5	5	7.96	409
SLW 0025	BHB	USNM	57.3	7	9.01	353
LJH 7132	BHB	YPM	56.4	5	8.75	363
SLW 991	BHB	USNM	55.9	5	10.97	312
SLW 992	BHB	USNM	55.9	8	10.80	314
SLW 993	BHB	USNM	55.9	8	11.43	307
LJH 72141–1	BHB	USNM,YPM	55.8	12	10.63	317
SLW 9155	BHB	USNM	55.7	10	11.21	309
SLW 9411	BHB	USNM	55.6	8	11.50	306
SLW 9434	BHB	USNM	55.4	7	12.23	299
SLW 9715	BHB	USNM	55.3	12	8.23	390
SLW 9050	BHB	USNM	55.3	5	12.18	300
SLW 9936	BHB	USNM	55.3	15	11.77	303
SLW 8612	BHB	USNM	55.3	7	12.41	298
Ardtun Head	M	BNHM, PMO,YPM	55.2	13	6.54	826
SLW 9812	BHB	USNM	55.1	22	8.53	373
SLW 9915	BHB	USNM	54.8	8	8.83	360
SLW LB	BHB	USNM	53.9	5	9.29	345
SLW H	BHB	USNM	53.5	9	10.22	323
LJH 9915	BHB	YPM	53.4	15	9.38	342
Juliaetta (P6)	I	YPM	16.5	14	8.14	396

B. *METASEQUOIA*

Site	Location*	Depository†	Age (Ma)	*n*§	SI (%)	CO_2 (ppmV)
Clarkia (P33a)	I	YPM	15.3	6	11.59	310
Clarkia (P33b)	I	YPM	15.3	10	10.94	316
Emerald Creek (P37a)	I	YPM	15.2	10	10.95	316

* ND = southwestern North Dakota (Williston Basin); BHB = Bighorn Basin; DB = Denver Basin; S = south-central Spitsbergen; A = south-central Alberta; M = Isle of Mull; I = north-central Idaho.

† Depository for cuticle preparates: DMNS = Denver Museum of Nature and Science; USNM = National Museum of Natural History, Smithsonian Institution; YPM = Yale Peabody Museum; PMO = Oslo Paleontological Museum; UA = University of Alberta; BNHM = British Natural History Museum.

§ Number of leaves measured for calculation of SI.

the other sites used in this study, no corresponding corrections were applied to the CO_2 estimates.

Most (88%) *Ginkgo*-bearing sites used in this study have been interpreted as representing streamside and crevasse splay environments (Chapter 2). These highly disturbed environments usually host well-watered, open canopy forests. Mesic conditions should only improve the fidelity of the SI-CO_2 signal, while open canopies should remove any potential intra-canopy CO_2 gradients and provide a closer analog to the open grown trees used to construct the training set.

The following sources were used to date the fossil sites: Williston Basin (Hell Creek Formation)—Hicks et al. (2002); Bighorn Basin (Fort Union and Willwood Formations)—Wing et al. (1995) and Age Model 2 in Wing et al. (2000); Denver Basin (Dawson Formation)—Raynolds et al. (2001, p. 25); Spitsbergen (Firkanten Formation)—Manum (1963) and Kvaček et al. (1994); Alberta (Paskapoo Formation)—Fox (1990); Isle of Mull (Staffa Group)—Chapter 3; Idaho (Latah Formation)—Reidel and Fecht (1986).

4.2.4 Stomatal ratio method

An alternative, semi-quantitative, stomatal-based CO_2 proxy compares the SI in a fossil species to its nearest living equivalent (NLE) (McElwain and Chaloner, 1995, 1996; McElwain, 1998; McElwain et al., 1999). NLE's are defined ecologically and structurally, not taxonomically. The stomatal ratios of the extant:fossil species are directly translated into CO_2 estimates in an inverse linear fashion, such that a stomatal ratio of three equates to a CO_2 estimate of 1050 ppmV (assuming the leaves of the extant trees grew in a 350 ppmV CO_2 atmosphere). This method is not species-specific, and so can be applied to sediments dating back to the early Devonian (McElwain and Chaloner, 1995), however it assumes that the SI's in the related sets of species respond to CO_2 in the following hyperbolic fashion: $CO_2 \propto (SI)^{-1}$.

To provide an independent check on the early Paleogene *Ginkgo*-derived CO_2 estimates, the stomatal indices of *Platanus guillelmae* from the *Ginkgo*-bearing site SLW H were compared to modern *P. occidentalis* and *P. orientalis* (and their hybrid *P.* × *acerfolia*) using the stomatal ratio method. *P. occidentalis* and *P. orientalis* are morphologically similar to the broadly trilobed *P. guillelmae*, and both the modern and fossil species prefer disturbed streamside environments (Chapter 2).

4.3 Results and discussion

The stomatal indices in both *Ginkgo* and *Metasequoia* show a strong linear response to the anthropogenic increases in atmospheric CO_2 over the last 145 years (r^2 = 0.98, $P < 0.001$ for *Ginkgo*; r^2 = 0.68, $P < 0.001$ for *Metasequoia*). For CO_2 concentrations above present-day levels, the responses are nonlinear (Fig. 4.2; Table 4.3). This type of nonlinear response is predicted by plant physiological principles (Kürschner et al., 2001) and supported by recent genetic work (Gray et al., 2000). Overall, both nonlinear regressions are highly significant (see Fig. 4.2).

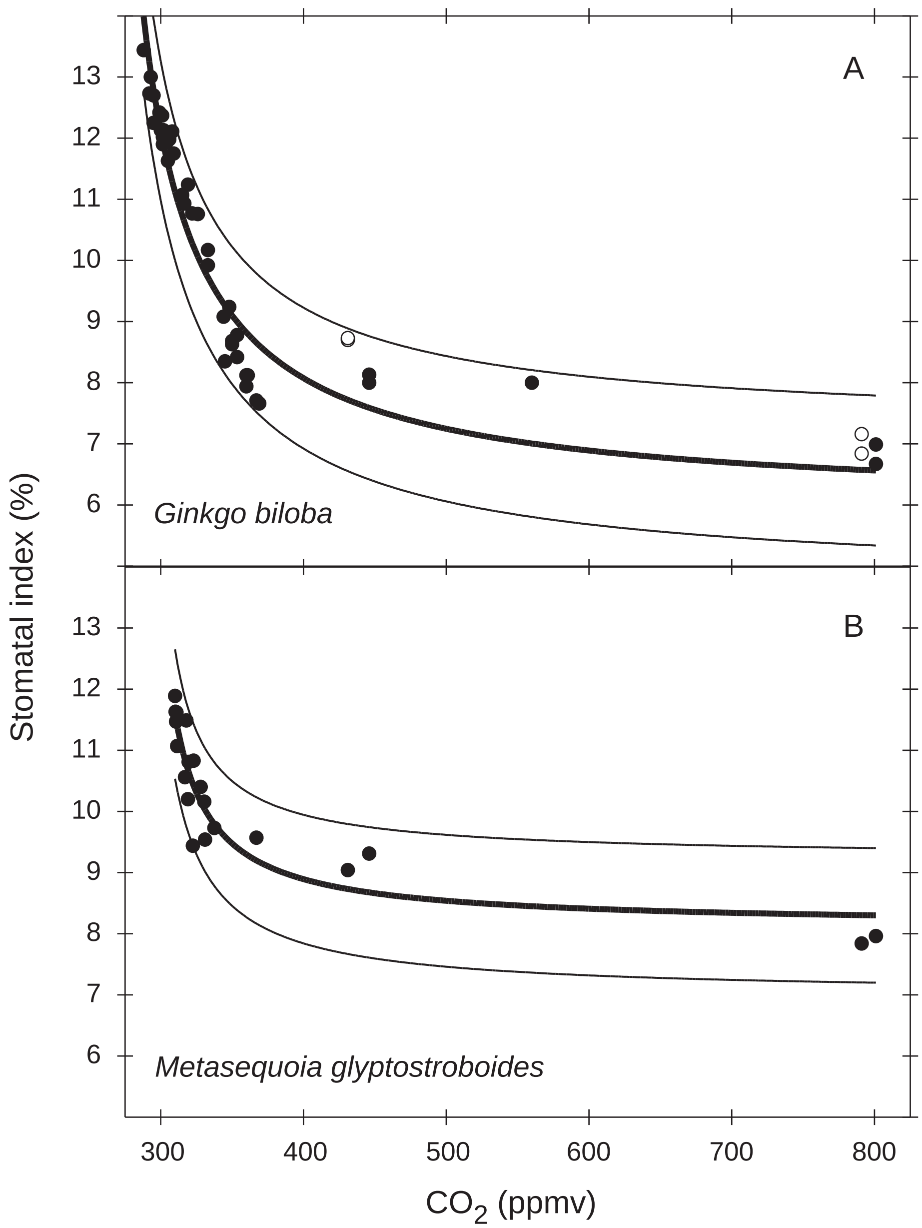

Fig. 4.2. Training sets (● ,○) for (A) *Ginkgo biloba* (n = 44) and (B) *Metasequoia glyptostroboides* (n = 20). Thick lines represent regressions {*Ginkgo*: $r^2 = 0.93$, $F(1,37) = 243$, $P < 0.0001$, $SI = 2000 \times [CO_2 - 196.1] / [333.7 \times CO_2 - 83000]$; *Metasequoia*: $r^2 = 0.86$, $F(1,17) = 54$, $P < 0.0001$, $SI = 10000 \times [CO_2 - 273.7] / [1230.1 \times CO_2 - 350000]$}. Thin lines represent ±95% prediction intervals. For *Ginkgo*, experimental results based upon a CO_2 exposure time of one growing season (○) were not used in regression (see text).

TABLE 4.3. RAW DATA FOR TRAINING SETS

A. *GINKGO*

Date	CO_2 (ppmV)	SI (%)	Herbarium*	Source
1856	288	13.44	YPM	N.D.
1880	292	12.73	YPM	Hartford, CT
1883	293	13.00	MBG	Botanic Garden, Cambridge, MA
1900	295	12.25	NA	Washington, DC
1900	295	12.70	YPM	Yale Forestry School, New Haven, CT
1910	299	12.42	BBG	Orange, NJ
1915	300	12.13	MBG	Hannibal, MO
1918	301	12.37	BBG	Arnold Arboretum, Boston, MA
1920	302	11.90	MGB	Nanking, Kiangsu Province, China
1921	302	12.02	MGB	Missouri Botanical Garden, St. Louis, MO
1922	302	12.13	BBG	Purdys, NY
1928	304	11.93	NA	Maymont Park, Richmond, VA
1932	305	11.63	MA	Arnold Arboretum?, Boston, MA
1937	306	11.98	MBG	Japan
1942	308	12.11	NA	Berkeley, CA
1943	309	11.75	MBG	Japan
1958	315	11.07	MBG	Tower Grove Park, St. Louis, MO
1960	317	10.93	MBG	Peking, China
1965	319	11.24	MA	Arnold Arboretum, Boston, MA
1968	322	10.77	NA	Arnold Arboretum, Boston, MA
1971	326	10.76	MA	Knox College, Galesburg, IL
1977	333	9.92	NA	U.S. Capitol, Washington, DC
1977	333	10.17	NA	Blandy Experimental Farm, Boyce, VA
1984	344	9.08	MBG	China (Yellow Plateau Team)
1985	345	8.35	BBG	Brooklyn Botanical Garden, NYC, NY
1987	348	9.24	NA	Morton Arboretum, Lisle, IL
1988	350	8.68	MBG	Clemson University, Clemson, SC
N.A.	350	8.63	exp	3 year old saplings in greenhouses† (2§)
1990	354	8.42	MBG	Missouri Botanical Garden, St. Louis, MO
1990	354	8.78	MBG	Oomoto Kameyama Botanical Garden; Kyoto, Japan
1995	360	7.94	YPM	Yale Peabody Museum, New Haven, CT
1995	360	8.12	MBG	Missouri Botanical Garden, St. Louis, MO
1996	361	8.12	MBG	Oomoto Kameyama Botanical Garden; Kyoto, Japan
1999	367	7.71	modern	New Haven, CT
2000	369	7.66	modern	New Haven, CT
N.A.	431	8.70	exp	6 year old saplings in greenhouses (1§)
N.A.	431	8.73	exp	1 year old saplings in greenhouses (1§)
N.A.	446	8.13	exp	7 year old saplings in greenhouses (2§)
N.A.	446	8.00	exp	2 year old saplings in greenhouses (2§)
N.A.	560	8.00	exp	3 year old saplings in greenhouses† (2§)
N.A.	791	7.16	exp	6 year old saplings in greenhouses (1§)
N.A.	791	6.84	exp	1 year old saplings in greenhouses (1§)
N.A.	801	6.99	exp	7 year old saplings in greenhouses (2§)
N.A.	801	6.67	exp	2 year old saplings in greenhouses (2§)

TABLE 4.3 CONTINUED. RAW DATA FOR TRAINING SETS
B. *METASEQUOIA*

Date	CO_2 (ppmV)	SI (%)	Herbarium*	Source
1947	310	11.89	UC	E Szechuan / NW Hubei, China
1948	310	11.63	UC	E Szechuan / NW Hubei, China
1949	311	11.47	UC	Berkeley, CA
1950	311	11.62	UC	Bar Harbor, ME
1953	312	11.07	UC	San Rafael, CA
1961	317	10.56	UC	Tallahassee, FL
1962	318	11.49	YPM	Bethany, CT
1964	319	10.20	MA	PA
1965	320	10.81	UC	Washington, DC
1968	323	9.44	UC	Fukuchiyama-city, Japan
1969	323	10.83	BBG	Brooklyn Botanical Garden, NY
1973	328	10.40	NA	Turlock, CA
1975	331	10.16	UC	University of Oregon, Eugene, OR
1976	331	9.54	UC	University of Oregon, Eugene, OR
1980	338	9.73	UC	Western Hubei, China
1999	367	9.57	modern	New Haven, CT; London, UK
N.A.	431	9.04	exp	1 year old saplings in greenhouses (1§)
N.A.	446	9.31	exp	2 year old saplings in greenhouses (2§)
N.A.	791	7.84	exp	1 year old saplings in greenhouses (1§)
N.A.	801	7.96	exp	2 year old saplings in greenhouses (2§)

Notes: N.D. = no data; N.A. = not applicable.

* YPM = Peabody Museum of Natural History (Yale University); MGB = Missouri Botanical Gardens; NA = U.S. National Arboretum; BBG = Brooklyn Botanic Gardens; MA = Morris Arboretum (University of Pennsylvania); UC = University Herbarium (University of California, Berkeley); modern = collections of fresh leaves; exp = collections from greenhouses.

† From Beerling, McElwain, and Osborne (1998).

§ Number of growing seasons saplings were exposed to CO_2 treatments.

A discontinuity exists in the *Ginkgo* training set between the experimentally-derived SI measurements at elevated CO_2 (>370 ppmV) and the rest of the training set (which includes one experimentally-derived measurement at 350 ppmV) (Fig. 4.2). Plants often require >1 growing season for their SI's to respond to CO_2 concentrations above present-day levels (Chapter 1). The stomatal indices in *Ginkgo* saplings exposed to CO_2 treatments for two growing seasons are indeed slightly lower than the same plants after one growing season (see Fig. 4.2; Table 4.3), and in the case of the 440 ppmV CO_2 treatment the difference is significant [$F(1,118) = 10.61$; $P < 0.001$; one-way ANOVA]. While not conclusive, this suggests that the discontinuity is an artifact of insufficient CO_2 exposure time.

The CO_2 reconstruction based upon 30 *Ginkgo*- and *Metasequoia*-bearing fossil sites is shown in Fig. 4.3 and Table 4.2. Except for one estimate near the Paleocene/Eocene boundary, all reconstructed CO_2 concentrations (300-450 ppmV) are close to present-day values. Estimates based upon <5 cuticle fragments are less reliable (Beerling and Royer, 2002a), however in general they conform with their more reliable coeval estimates (Table 4.4). It is interesting to note that the estimates from the two oldest very latest Cretaceous sites both suggest CO_2 levels in excess of 500 ppmV, and Upper Pliocene cuticles register CO_2 concentrations of 300 ppmV (Table 4.4).

There is some stratigraphic evidence that the site associated with the one high CO_2 estimate (Ardtun Head, Isle of Mull, Scotland) dates to the Paleocene/Eocene Thermal Maximum (PETM; previously known as LPTM) (Chapter 3). The PETM was brief (~10^5 years; Kennett and Stott, 1991; Bains et al., 1999; Norris and Röhl; 1999) but significant [global mean surface temperatures rose ~2 °C (Huber and Sloan, 1999)]. Concomitant with warming, there was a worldwide negative excursion in $\delta^{13}C$, ranging in magnitude

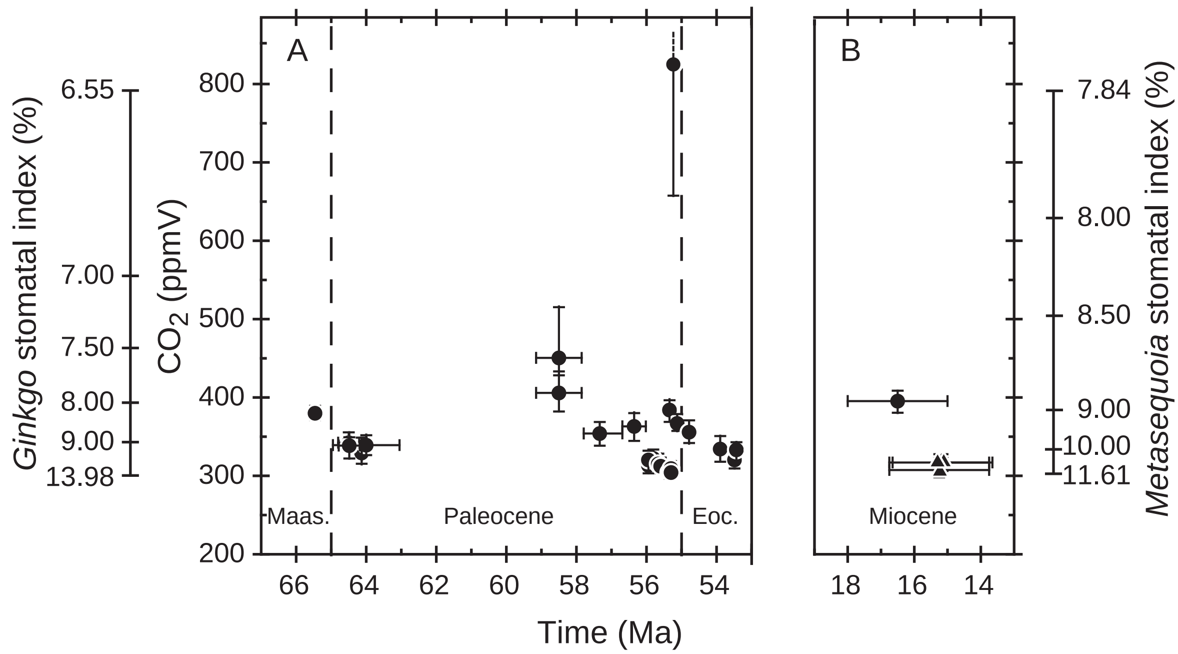

Fig. 4.3. Reconstruction of paleo-CO_2 for the (A) very latest Cretaceous to early Eocene and (B) middle Miocene based upon SI measurements of *Ginkgo* (●) and *Metasequoia* (▲) fossil cuticles. Errors represent ±95% confidence intervals. Regressions used to solve for CO_2 were rewritten from the training set-derived regressions [*Ginkgo*: $CO_2 = 2000 \times (415 \times SI - 1961) / (3337 \times SI - 20000)$; *Metasequoia*: $CO_2 = 70000 \times (50 \times SI - 391) / (12301 \times SI - 100000)$]

TABLE 4.4. SAMPLING DETAILS AND CO_2 RECONSTRUCTION FOR FOSSIL *GINKGO* DATA BASED UPON SITES WITH <5 CUTICLE FRAGMENTS

Site	Location*	Depository†	Age (Ma)	*n*§	SI (%)	CO_2 (ppmV)
DMNH 571	ND	DMNS	65.9	1	7.03	554
KJ 87134	ND	YPM	65.8	3	7.09	536
DMNH 1489	ND	DMNS	65.4	2	8.42	379
N.D.	BHB	YPM	~63	3	8.60	370
UF 18255	PRB	FMNH	~58	3	11.24	309
DMNH 907	ND	DMNS	56	2	8.89	358
LJH 8411	E	YPM	55	2	8.29	386
Klärbecken	G	BNHM	~ 2	3	12.29	299

Notes: N.D. = no data.

* ND = southwestern North Dakota (Williston Basin); BHB = Bighorn Basin; PRB = Powder River Basin; E = Ellesmere Island; G = Germany.

† Depository for cuticle preparates: DMNS = Denver Museum of Nature and Science; YPM = Yale Peabody Museum; FMNH = Florida Museum of Natural History; BNHM = British Natural History Museum.

§ Number of leaves measured for calculation of SI.

from –2.5‰ in the benthic marine record (Kennett and Stott, 1991; Bains et al., 1999) to –6‰ in the terrestrial record (Koch et al., 1992; Sinha and Stott, 1994; Bowen et al., 2001). The leading hypothesis to explain this event involves the dissociation of isotopically light (~ –60‰) methane hydrates along continental margins (Dickens et al., 1995; Bains et al., 1999; Katz et al., 1999) and their subsequent oxidation to carbon dioxide. However, all previous attempts to discern this hypothesized atmospheric CO_2 spike using other CO_2 proxies have failed (Koch et al., 1992; Stott, 1992; Sinha and Stott, 1994). While it is tempting to correlate Ardtun Head and its corresponding 500 ppmV spike in atmospheric CO_2 to the PETM, further stratigraphic work is required to resolve this issue. If it is not of PETM age, then it is recording another high CO_2 event that is probably not associated with massive methane hydrate dissociation.

4.3.1 Ginkgo *and* Metasequoia *cuticle as reliable recorders of atmospheric* CO_2

There are numerous factors indicating that the CO_2 reconstruction presented here is accurate. As discussed above, both genera are restricted in the fossil record to mid- and high latitude temperate forests, and, in addition, *Ginkgo* prefers disturbed riparian settings. These characteristics should strengthen the applicability of the fossil cuticles to their respective training sets. Also, both *Ginkgo* and *Metasequoia* are very phylogenetically conservative, and in the case of *Ginkgo* the slope of the response in experimental treatments after one growing season is similar to that derived from a multimillion year sequence of fossil SI measurements and coeval pedogenic carbonate-derived CO_2 estimates (Beerling and Royer, 2002b). This suggests that: 1) The SI-CO_2 relationships in *Ginkgo* and *Metasequoia* have remained unchanged throughout the Cenozoic; and 2) The short-term (largely phenotypic) stomatal responses to CO_2 captured in the training sets are similar to the long-term (largely genotypic) responses reflected in the fossils.

At least as many leaves per fossil site were used to reconstruct CO_2 as were used per data point to construct the bulk of the training sets (compare Table 4.1 with Table 4.2). This contrasts with other studies, where <5 fossil leaves are commonly measured per fossil site (e.g., Retallack, 2001). In addition, it is likely that fossil cuticles measured for a given site stemmed from multiple trees, whereas SI's from only one tree were normally measured per data point in the training sets. In this sense, then, the sampling methodology for the fossil cuticles was at least as conservative than for the modern cuticles.

I have measured *Metasequoia* cuticles from only the middle Miocene, but these CO_2 estimates agree reasonably well with their near-coeval *Ginkgo*-based estimates (Fig. 4.3; Table 4.2). This provides further support that both species are reliably recording atmospheric CO_2. As a cross-check on the early Paleogene *Ginkgo*-derived estimates, I compared the SI's of *Platanus guillelmae* from site SLW H with the SI's of its nearest living equivalents *P. occidentalis* and *P. orientalis* using the stomatal ratio method (see above). While this method can only generate semi-quantitative estimates of CO_2, all of the estimates for this site fall between 350 and 390 ppmV (Table 4.5). This range compares favorably with the *Ginkgo*-derived CO_2 estimate (323 ppmV), indicating, again, that *Ginkgo* faithfully records CO_2.

The SI's of nearly all the measured fossil material fall within the range of high CO_2 sensitivity in the training sets (Fig. 4.2; Table 4.2). This contrasts with the study of Retallack (2001), where the stomatal indices in 82% of the fossil sites fall outside the range captured in his training set, and so these CO_2 estimates are less reliable. In addition, I have intensively sampled several intervals, for example 12 sites from the last 1 m.y. of

TABLE 4.5. CO_2 RECONSTRUCTION FROM STOMATAL RATIOS IN *PLATANUS*

A. FOSSIL *PLATANUS*

Species	Site	Age (Ma)	*n**	SI (%)
P. guillelmae	SLW H	53.5	7	12.89

B. MODERN *PLATANUS*

Species	Site	Date	*n**	SI (%)	Stomatal ratio†	Paleo-CO_2 (ppmV)§
P. occidentalis	North Carolina, USA	1891	6	15.35	1.19	350
P. orientalis	Iraq	1975	5	15.22	1.18	390
P. acerfolia	Connecticut, USA	2001	5	13.28	1.03	381
P. occidentalis	Connecticut, USA	2001	6	13.44	1.04	386

* Number of leaves measured for calculation of SI.

† Stomatal ratio = SI_{modern} / SI_{fossil}

§ CO_2 reconstructions for site SLW H. These estimates should be considered semi-quantitative only. Values calculated by multiplying the stomatal ratio by the corresponding CO_2 concentration in which the leaves developed. See text for details.

the Paleocene. These characteristics allow for more precise determinations of paleo-CO_2 relative to other CO_2 proxies, and, because SI's respond to CO_2 on the timescale of 10^0-10^2 years, the ability to discern rapid shifts in atmospheric CO_2 (Royer et al., 2001).

A few of the fossil SI's fall outside the densely sampled regions in the training sets, and in the case of the Ardtun Head site, nearly outside the range captured in the entire *Ginkgo* training set. This suggests that the SI's in *G. biloba* and *G. adiantoides* are not constrained to a limited range (8-12%) irrespective of atmospheric CO_2 levels. Additional evidence that the SI's in *Ginkgo* are highly adaptable comes from Paleozoic and Mesozoic studies where SI's in *Ginkgo* are as low as 2.6% (McElwain and Chaloner, 1996; McElwain et al., 1999; Chen et al., 2001; Retallack, 2001).

The only possible confounding factor that I have discerned in my fossil dataset is latitude (Fig. 4.4). Except for the Spitsbergen site, there is a negative correlation between latitude and the SI in *Ginkgo*. Even within the densely sampled Bighorn Basin, there is a small (slope = -2.2 using SI as the dependent variable) but moderately significant (r^2 = 0.43; P = 0.002) correlation. Differences in irradiance (Lake et al., 2001) or temperature (Wagner, 1998) may be driving this response, however more data are required before any firm conclusions can be drawn.

4.3.2 Paleoclimatic implications

Fig. 4.5 is a compilation of most published proxy- and modeling-based CO_2 estimates for the last 66 m.y. There is very good agreement among the methods for the Neogene, strongly indicating that CO_2 levels were not much different from the present-

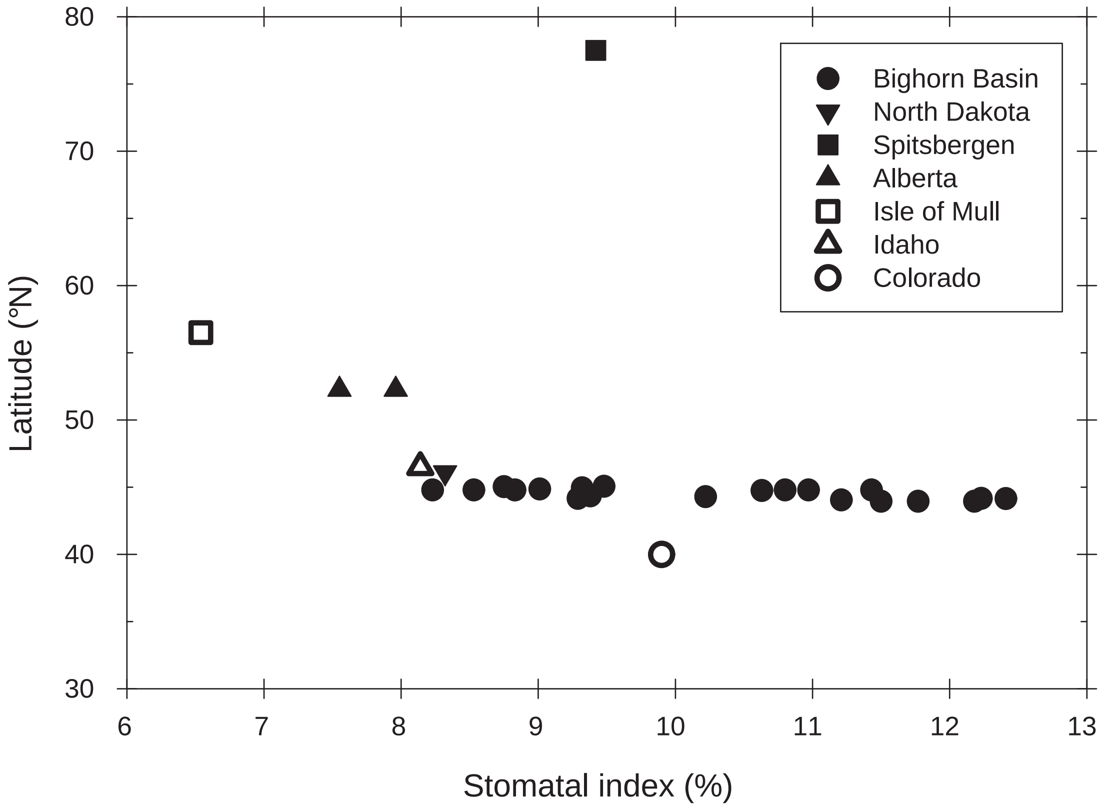

Fig. 4.4. Correlation between latitude and stomatal index for fossil sites. Present-day latitudes are plotted, but should reflect their corresponding paleolatitudes to within 5° (Schettino and Scotese, 2001).

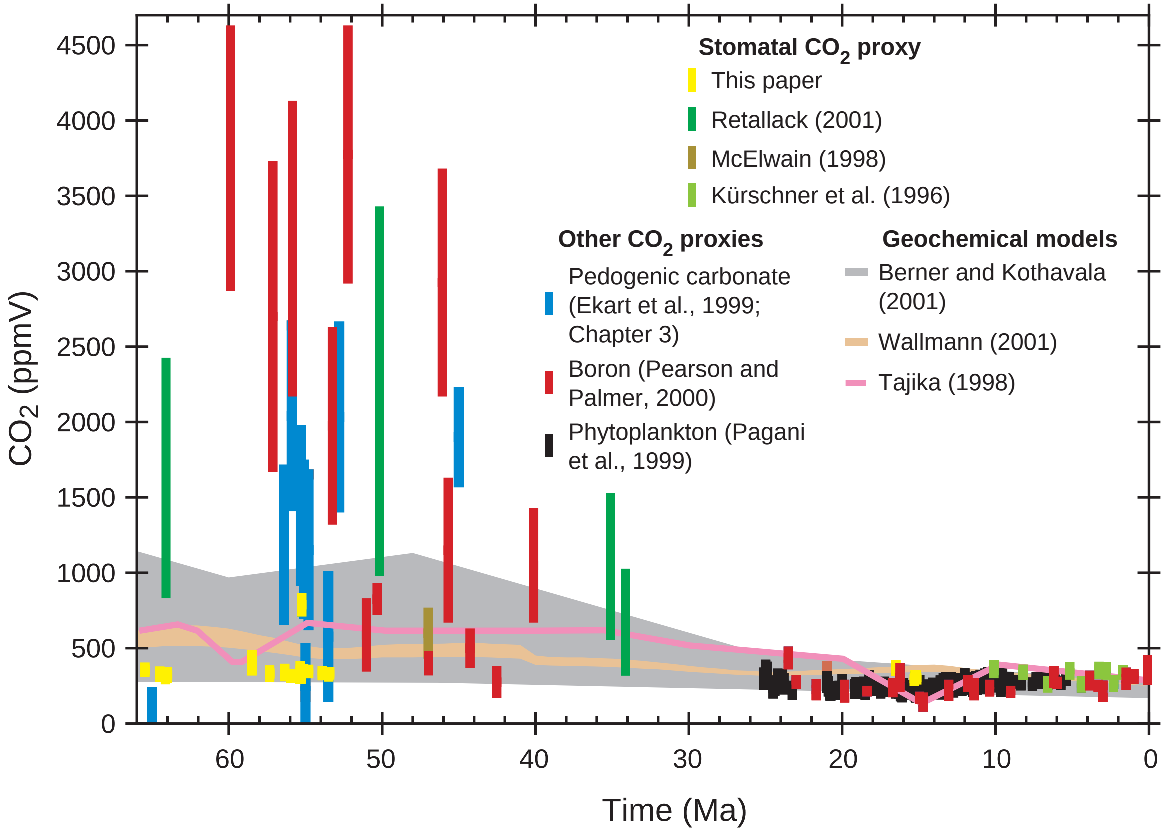

Fig. 4.5. A compilation of CO_2 reconstructions for the Tertiary. In the case of Retallack (2001), only those sites for which > 4 cuticle fragments were counted are plotted. No pedogenic carbonate-derived estimates are plotted for the Neogene because their margins of error are much larger relative to the other methods (Royer et al., 2001).

day. CO_2 reconstructions for the Paleogene, however, are inconsistent, ranging from <300 ppmV to >3000 ppmV. These inconsistencies are largely stratified by method, with the highest CO_2 estimates derived from the boron proxy and the lowest from this stomatal study (Fig. 4.5).

What do these CO_2 reconstructions mean in terms of paleoclimate? Assuming that we understand the role of CO_2 as a greenhouse gas in regulating global temperature, it is possible to convert a given concentration of atmospheric CO_2 into a prediction of global mean surface temperature (GMST). I have done this for the late Cretaceous to early Paleogene (69-50 Ma) and middle Miocene (19-13 Ma) CO_2 reconstructions, the two intervals for which I have stomatal data, using the general circulation model (GCM)-based CO_2-GMST sensitivity study of Kothavala et al. (1999). This GCM study was calibrated to present-day conditions. While it may be instructive to use sensitivity studies calibrated to early Paleogene and middle Miocene conditions, the CO_2-GMST relationship is most accurately known for present-day conditions, and applying a sensitivity study calibrated to the present-day allows testing the sole effects of CO_2 on GMST. In other words, if the CO_2-derived GMST predictions do not match the geologic indictors of GMST for a given period, then factors in addition to CO_2 such as paleogeography and vegetative feedbacks are required to explain the GMST for that period.

The CO_2-derived GMST predictions are shown in Fig. 4.6. As with the raw CO_2 data, there is general agreement for the middle Miocene, with most predictions within 1 °C of the present-day GMST. Predictions for the early Paleogene are not consistent, ranging from near present-day values to over 10 °C warmer than the present-day GMST.

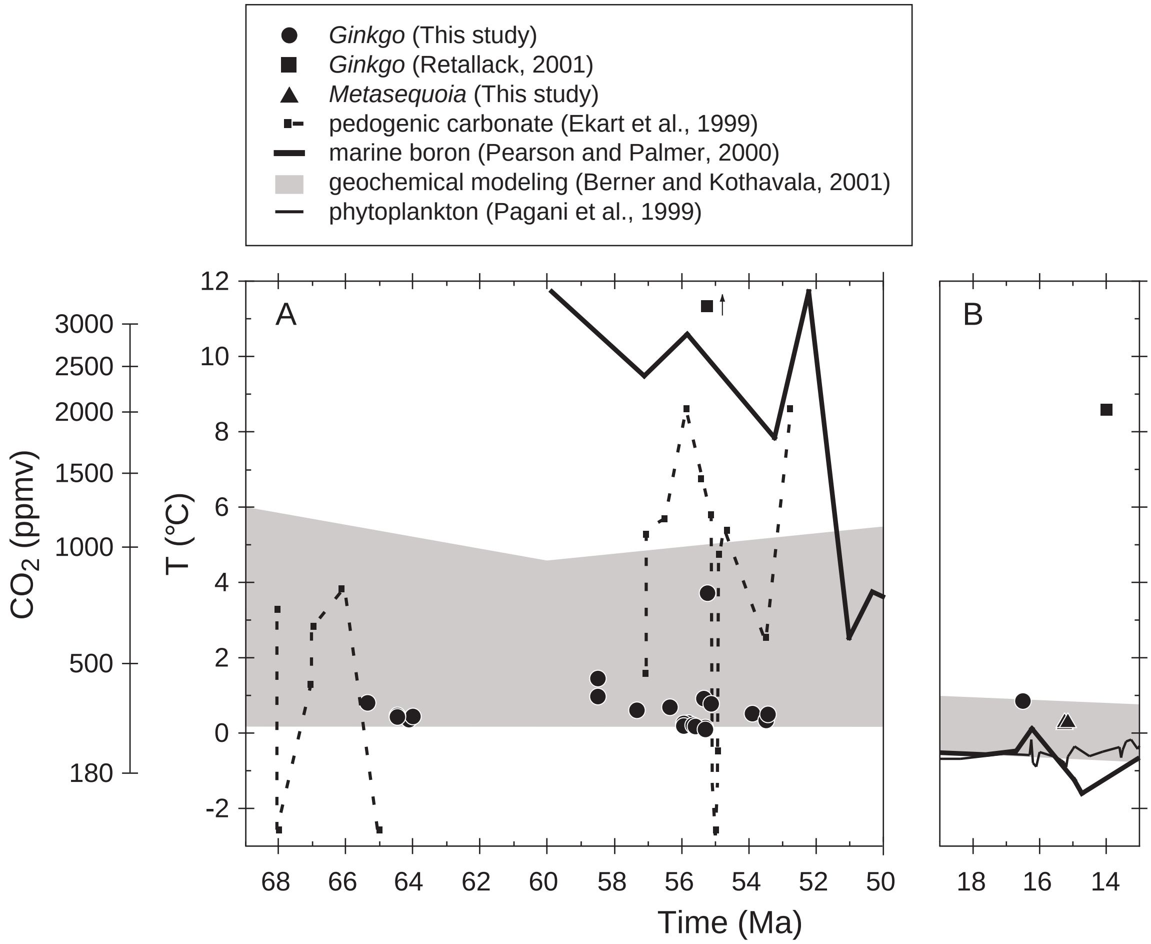

Fig. 4.6. Estimates of CO_2 from Fig. 4.5 and their corresponding model-determined temperature departures (T) of global mean surface temperature (GMST) from present day for the (A) very latest Cretaceous to early Eocene and (B) middle Miocene. Paleo-GMST calculated using the CO_2-temperature sensitivity study of Kothavala et al. (1999). Present-day reference GMST calculated using the pre-industrial CO_2 value of 280 ppmv (14.7 °C). The error range of GMST predicted from the geochemical modeling-based CO_2 predictions of Berner and Kothavala (2001) corresponds to the model's sensitivity analysis.

Both the early Paleogene and middle Miocene are intervals of global warmth relative to today. The physiognomic characters of early Paleogene fossil floras indicate temperatures much higher than today at mid and high latitudes (e.g., Hickey 1980; Spicer and Parrish, 1990; Wing and Greenwood, 1993; Wolfe, 1994; Greenwood and Wing, 1995; Wilf, 2000). The comparison of these fossil plants with their Nearest Living Relatives (NLRs) also indicates warmer temperatures (e.g., Hickey, 1977; Spicer and Parrish, 1990). For example, frost intolerant palms occur at paleolatitudes up to 20° north of their current northern limit in North America (Greenwood and Wing, 1995). Animals also yield paleoclimatic information; for example, the early Paleogene distributions of large tortoises (Hutchison, 1982) and crocodilians (Markwick, 1994, 1998) in the United States indicate temperatures higher than the present-day.

While the above data constrain continental temperatures, $\delta^{18}O$ data from calcitic marine shells provide temperature information for the oceans. Oceans are the largest reservoirs of heat in the biosphere, and therefore provide the best proxy for globally averaged temperatures. Based upon the $\delta^{18}O$ compilations of Zachos et al. (1994) and Zachos et al. (2001), benthic temperatures were 8-12 °C warmer than the present-day during the early Paleogene, and high latitude near surface temperatures were upwards of 15 °C warmer. Using late Paleocene near surface paleotemperature data and present-day levels of atmospheric CO_2 as input into a GCM, O'Connell et al. (1996) calculated a GMST 3 °C warmer than the present-day. During the mid-Miocene thermal maximum (~17-14.5 Ma), benthic waters warmed 1-2 °C to temperatures 6 °C warmer than the present-day (Lear et al., 2000; Zachos et al., 2001). Plant distributions (White et al., 1997) and leaf physiognomic characters (Wolfe, 1994) also indicate substantial warming in

North America. If my stomatal-based CO_2 reconstruction is correct, then, factors in addition to carbon dioxide are required to explain these two intervals of global warmth, and these intervals may not serve as good analogs for understanding future climate change. It is crucial to emphasize that low concentrations of atmospheric CO_2 during intervals of global warmth do not counter the theory of the greenhouse effect (for this, high CO_2 levels are required during globally cool intervals); instead, they indicate that additional forcings are required.

Traditionally, GCM modelers interested in warm climates have struggled to match their output with the geologic data (Barron, 1987; Sloan and Barron, 1990, 1992; Sloan et al., 1995), particularly when using low CO_2 levels (Sloan and Rea, 1995). Recent work, however, has begun to resolve these discrepancies (Otto-Bliesner and Upchurch, 1997; Sloan and Pollard, 1998; DeConto et al., 1999; Upchurch et al., 1999; Sewall et al., 2000; Sloan et al., 2001). It will be crucial to understand the various roles CO_2 plays during globally warm periods, particularly as atmospheric CO_2 rises to levels in the very near future that are perhaps unprecedented for the past 65 m.y.

APPENDIX 1.1

Experimental Stomatal Responses

Experiment Length (days)	CO_2 Levels (relative to controls[a])	Species Used	Side of Leaf	Stomatal Density Response	Stomatal Index Response	Source
?	↑ 300%	*Phaseolus vulgaris*	abaxial	*↓ 9%	-	O'Leary and Knecht, 1981[b]
			adaxial	↔	-	
14	↑2067%	*Marsilea vestita*	abaxial	*↓ 91%	-	Bristow and Looi, 1968[b]
			adaxial	↔	-	
	↑~10^5%	*Marsilea vestita*	abaxial	*↓ 99%	-	
			adaxial	↔	-	
15	↑ 100%	*Populus euroamericana*	-	↑ 38%	↔	Gaudillère and Mousseau, 1989[b]
20	↑ 80%	*Phaseolus vulgaris*	abaxial	↔	↔	Ranasinghe and Taylor, 1996[b]
			adaxial	↔	↔	
21	↑ 86%	*Tradescantia (fluminensis?)*	abaxial	↔	↔	Boetsch et al., 1996[b]
21	↓ 29%	*Vaccinium myrtillus*	abaxial	↔	↔	Woodward, 1986[b]
			adaxial	*↑ 548%	*↑ 424%	
	↑ 29%	*Vaccinium myrtillus*	abaxial	↔	↔	
			adaxial	↔	↔	
21	↓ 34%	*Acer pseudoplatanus*	abaxial	*↑ 220%	*↑ 122%	Woodward and Bazzaz, 1988[b]
		Geum urbanum	abaxial	*↑ 31%	*↑ 18%	
			adaxial	*↑ 214%	*↑ 191%	
		Quercus robur	abaxial	*↑ 131%	*↑ 81%	
		Rhamnus catharticus	abaxial	*↑ 117%	*↑ 100%	
		Rumex crispus	abaxial	*↑ 71%	*↑ 31%	
			adaxial	*↑ 150%	*↑ 400%	
	↑ 100%	*Amaranthus retroflexus*	abaxial	*↓ 35%	*↓ 23%	
			adaxial	*↓ 38%	*↓ 26%	
		Ambrosia artemisiifolia	abaxial	*↓ 11%	↔	

Experiment Length (days)	CO_2 Levels (relative to controls[a])	Species Used	Side of Leaf	Stomatal Density Response	Stomatal Index Response	Source
			adaxial	*↓ 24%	*↓ 25%	
		Setaria faberii	abaxial	↔	*↓ 21%	
			adaxial	*↓ 22%	*↓ 21%	
21-35	↑ 94%	*Lolium perenne*	adaxial	↔	-	Ryle and Stanley, 1992[b]
26	↑ 86%	*Lycopersicon esculentum*	abaxial	*↓ 17%	↔	Madsen, 1973[b]
			adaxial	*↓ 14%	↔	
	↑ 814%	*Lycopersicon esculentum*	abaxial	*↓ 23%	↔	
			adaxial	*↓ 36%	↔	
~28	↑ 33%	*Lolium temultentum*	adaxial	↔	-	Gay and Hauck, 1994[b]
28	↑ 100%	*Phaseolus vulgaris*	abaxial	↔	↔	Radoglou and Jarvis, 1992[c]
			adaxial	↔	↔	
~40	↑ 91%	*Raphanus raphanistrum*	abaxial	↔	↔	Case et al., 1998[b]
45	↑ 71%	*Anthyllis vulneraria*	abaxial	*↓ 32%	*↓ 17%	Ferris and Taylor, 1994[b]
			adaxial	↔	↔	
		Lotus corniculatus	abaxial	↑ 60%	↔	
			adaxial	↑ 40%	↔	
		Plantago media	abaxial	*↓ 20%	↔	
			adaxial	*↓ 36%	*↓ 12%	
		Sanguisorba minor	abaxial	↑ 175%	↑ 36%	
			adaxial	↑ 150%	↑ 213%	
45	↑ 100%	*Vicia faba*	abaxial	↔	↔	Radoglou and Jarvis, 1993[c]
			adaxial	↔	↔	
45	↑ 168%	*Glycine max*	abaxial	↑ 38%	↔	Thomas and Harvey, 1983[c]
			adaxial	↔	↔	
		Liquidambar styraciflua	abaxial	↔	↑ 30%	
		Zea mays (C_4)	abaxial	↔	↔	
			adaxial	↔	↔	

Experiment Length (days)	CO_2 Levels (relative to controls[a])	Species Used	Side of Leaf	Stomatal Density Response	Stomatal Index Response	Source
~50	↑ 68%	*Anthyllis vulneraria*	abaxial	*↓ 23%	↔	Bryant et al., 1998[c]
		Sanguisorba minor	abaxial	↔	↔	
		Bromopsis erecta	abaxial	↔	↔	
50	↓ ~32%	*Avena sativa*	abaxial	↔	-	Malone et al., 1993[b]
			adaxial	↔	-	
		Prosopis glandulosa	abaxial	↔	-	
			adaxial	↔	-	
		Schizachyrium scoparium (C_4)	abaxial	↔	-	
		Triticum aestivum	abaxial	↔	-	
			adaxial	↔	-	
54	↑ 93%	*Boehmeria cylindrica*	-	↔	-	Woodward and Beerling, 1997[b]
56	↑ 100%	*Coleus blumei*	abaxial	*↓ 9%	*↓ 4%	Beerling and Woodward, 1995[b]
		Tropaeolum major	abaxial	*↓ 4%	*↓ 10%	
59	↑ 186%	*Pelargonium hortorum*	abaxial	↔	-	Kelly et al., 1991[b]
			adaxial	*↓ 50%	-	
60	↓ 29%	*Salix herbacea*	combined	*↑ 28%	-	Beerling et al., 1995[b]
	↑ 100%		combined	*↓ 41%	-	
60	↑ 93%	*Ochroma lagopus*	abaxial	↔	-	Oberbauer et al., 1985[b]
			adaxial	↔	-	
63	↑ 157%	*Panicum tricanthum*	abaxial	*↓ 22%	-	Tipping and Murray, 1999[b]
		Panicum antidotale (C_4)	abaixal	↑ 28%	-	
<66	↑ 100%	*Gossypium hirsutum*	abaxial	↔	↔	Reddy et al., 1998[b]
			adaxial	↔	↔	
72	↑ 89%	*Lolium perenne*	adaxial	↑	*↓	Ferris et al., 1996[c]
80	↑ 100%	*Betula pendula*	abaxial	↔	↔	Wagner, 1998[b]

Experiment Length (days)	CO_2 Levels (relative to controls[a])	Species Used	Side of Leaf	Stomatal Density Response	Stomatal Index Response	Source
90	↑ 100%	*Quercus ilex*	abaxial	*↓ 27%	-	Paoletti et al., 1997[b]
90-120	↑ 100%	*Andropogon gerardii* (C_4)	abaxial	*↓ 28%	-	Knapp et al., 1994[c]
			adaxial	↑ 75%	-	
		Salvia pitcheri	abaxial	↑ 40%	-	
			adaxial	↑ 125%	-	
92	↑ 100%	*Populus trichocarpa*	abaxial	↔	↔	Radoglou and Jarvis, 1990[b]
			adaxial	↔	↔	
93	↓ 52%	*Oryza sativa*	abaxial	↓ 29%	-	Rowland-Bamford et al., 1990[b]
			adaxial	↓ 17%	-	
	↑ 173%	*Oryza sativa*	abaxial	↔	-	
			adaxial	↔	-	
105	↑ 186%	*Pelargonium hortorum*	abaxial	↔	-	Kelly et al., 1991[b]
			adaxial	↔	-	
114	↑ 87%	*Arachis hypogaea*	abaxial	*↓ 12%	↔	Clifford et al., 1995[b]
			adaxial	*↓ 16%	*↓ 8%	
120	↑ 757%	*Rhizophora mangle*	abaxial	*↓ 14%	-	Beerling, 1994[b]
		Laguncularia racemosa	abaxial	*↓ 31%	-	
		Musa apiculata	abaxial	↔	-	
			adaxial	↔	-	
120	↑ 100%	*Populus trichocarpa*	abaxial	*↓ 19%	*↓ 31%	Ceulemans et al., 1995[c]
			adaxial	↔	↔	
		Populus deltoides	abaxial	*↓ 27%	*↓ 36%	
			adaxial	*↓ 33%	↔	
120	↑ 100%	*Quercus petraea*	abaxial	*↓ 25%	*↓ 14%	Kürschner et al., 1998[b]
123	↑ 93%	*Pentaclethra macroloba*	abaxial	*↓ 7%	-	Oberbauer et al., 1985[b]
			adaxial	↔	-	

Experiment Length (days)	CO_2 Levels (relative to controls[a])	Species Used	Side of Leaf	Stomatal Density Response	Stomatal Index Response	Source
125	↑ 49%	*Triticum aestivum*	abaxial	↔	↔	Estiarte et al., 1994[c]
			adaxial	↔	↔	
135	↑ 100%	*Prunus avium*	abaxial	↔	-	Centritto et al., 1999[c]
150	↑ 100%	*Chlorophytum picturatum*	abaxial	*↓ 7%	*↓ 23%	Beerling and Woodward, 1995[b]
		Hedera helix	abaxial	*↓ 10%	*↓ 29%	
		Hypoestes variegata	abaxial	*↓ 9%	*↓ 6%	
217	↑ 100%	*Maranthes corymbosa*	abaxial	*↓ 14%	-	Eamus et al., 1993[b]
~240	↑ 98%	*Picea sitchensis*	abaxial	↔	-	Barton and Jarvis, 1999[b]
270	↑ 114%	*Pinus banksiana*	-	↔	-	Stewart and Hoddinott, 1993[b]
300	↑ 97%	*Eucalyptus tetrodonta*	abaxial	*↓ 20%	-	Berryman et al., 1994[b,c]
~365	↑ 71%	*Rumex obtusifolius*	abaxial	*↓ 8%	-	Pearson et al., 1995[b]
			adaxial	↔	-	
~400	↑ 100%	*Rhizophora mangle*	abaxial	*↓ 16%	↔	Farnsworth et al., 1996[b]
~425	↑ 71%	*Bromus erectus*	abaxial	↔	↔	Lauber and Körner, 1997[c]
			adaxial	↔	↔	
		Plantago media	abaxial	↔	↔	
			adaxial	↔	↔	
		Sanguisorba minor	abaxial	↔	↔	
570	↑ 100%	*Prunus avium*	abaxial	↔	-	Atkinson et al., 1997[b]
		Quercus robur	abaxial	↑ ~150%	-	
600	↑ 97%	*Pinus palustris*	-	↔	-	Pritchard et al., 1998[c]
~730	↑ 100%	*Picea abies*	-	↔	-	Dixon et al., 1995[c]
		Quercus rubra	abaxial	↑ 8%	-	
730	↑ 60%	*Tussilago farfara*	abaxial	-	*↓ 26%	Beerling and Woodward, 1997[b]

Experiment Length (days)	CO_2 Levels (relative to controls[a])	Species Used	Side of Leaf	Stomatal Density Response	Stomatal Index Response	Source
750	↑ 97%	*Mangifera indica*	abaxial	*↓ 17%	-	Goodfellow et al., 1997[b]
~840	↑ 99%	*Scirpus olneyi*	-	↔	-	Drake, 1992[c]
3 years	↑ 60%	*Pinus sylvestris*	abaxial adaxial	*↓ 16% *↓ 18%	- -	Beerling, 1997[b]
3 years	↑ 60%	*Ginkgo biloba*	abaxial	*↓ 20%	*↓ 7%	Beerling et al., 1998a[b]
1155	↑ 50%	*Pseudotsuga menziesii*	abaxial	↔	-	Apple et al., 2000[b]
~5 years	↑ ~82%	*Citrus aurantium*	abaxial	↔	↔	Estiarte et al., 1994[c]
meta-analysis		43 species (60% showed stomatal density reductions)		*↓ (9.0± 3.3% s.e.)	-	Woodward and Kelly, 1995

* Response inversely relates ($P < 0.05$) to CO_2 concentration
↔ No significant change ($P > 0.05$)
\- Not reported
[a] Typically between 340 and 360 ppmV
[b] Plants grown in enclosed greenhouses or chambers
[c] Plants grown in open-top chambers (OTCs)

APPENDIX 1.2

Subfossil Stomatal Responses

Age of Material (years)	CO_2 levels (relative to controls[a])	Species Used	Side of Leaf	Stomatal Density Response	Stomatal Index Response	Source
#	↓ 5%	*Salix herbacea*	abaxial	↔	-	Beerling et al., 1992
			adaxial	*↑ 83%	-	
#	↓ 13%	*Eucalyptus pauciflora*	combined	*↑ 26%	-	Körner and Cochrane, 1985
#	↓ 6%	*Griselinia littoralis*	combined	↔	-	Körner et al., 1986
	↓ 13%	*Nothofagus menziesii*	abaxial	*↑ 21%	-	
	↓ 8%	*Ranunculus grahamii*	combined	↔	-	
#	↓ 10%	*Vaccinium myrtillus*	abaxial	↓ 20%	-	Woodward, 1986
			adaxial	*↑ 425%	-	
#	↓ 6%	*Nardus stricta*	abaxial	↔	-	Woodward and Bazzaz, 1988
			adaxial	*↑ 19%	-	
@	↑ 194%	*Tussilago farfara*	abaxial	-	*↓ 65%	Beerling and Woodward, 1997
@	↑ 100%	*Scirpus lacustris*	-	*↓ 19%	-	Bettarini et al., 1997
@	↑ 100%	*Allium sphaerocephalon*	abaxial	↔	-	Bettarini et al., 1998
		Buxus sempervirens	abaxial	↔	↔	
		Convolvulus arvensis	abaxial	↔	↑ 26%	
		Convolvulus cantabrica	abaxial	↔	↔	
		Conyza canadensis	abaxial	*↓ 26%	↑ 21%	
		Fraxinus ornus	abaxial	*↓ 35%	↔	
		Geranium molle	abaxial	↔	↔	
		Globularia punctata	abaxial	↔	↔	
			adaxial	↔	↔	
		Hypericum perforatum	abaxial	↔	↔	
		Plantago lanceolata	abaxial	↔	↔	
			adaxial	↔	↔	

Age of Material (years)	CO_2 levels (relative to controls[a])	Species Used	Side of Leaf	Stomatal Density Response	Stomatal Index Response	Source
		Potentilla reptans	abaxial	↔	↔	
		Pulicaria sicula	abaxial	↔	↔	
		Ruscus aculeatus	abaxial	↔	-	
		Scabiosa columbaria	abaxial	↔	↔	
		Silene vulgaris	abaxial	↔	↔	
		Stachys recta	abaxial	*↓ 11%	↔	
		Trifolium pratense	abaxial	↔	↔	
@	↑~130%	*Bauhinia multinervia*	abaxial	↑ 62%	↑ 41%	Fernández et al., 1998
			adaxial	*↓ 71%	*↓ 73%	
		Spathiphyllum cannifolium	abaxial	↔	↔	
			adaxial	*↓ 72%	*↓ 85%	
@	↑ 40%	*Quercus pubescens*	abaxial	↔	↔	Miglietta and Rasci, 1993
@	↑ 515%	*Arbutus unedo*	abaxial	*↓ 29%	*↓ 20%	Jones et al., 1995
@	↑ 114%	*Quercus ilex*	abaxial	*↓ 26%	-	Paoletti et al., 1998
@	↑ 50%	*Boehmeria cylinderica*	-	↔	-	Woodward and Beerling, 1997
@	↑ ~71%	*Phragmites australis*	abaxial	↔	-	van Gardingen et al., 1997
			adaxial	*↓ 45%	-	
37	↑ 15%[b]	*Metasequoia glyptostroboides*	abaxial	↔	*↓ 17%	D.L. Royer, unpublished data
43	↑ 15%[b]	*Betula pendula*	abaxial	*↓ 30%	*↓ 32%	Wagner et al., 1996
70	↑ 18%[c]	*Acer campestre*	abaxial	↔	-	Beerling and Kelly, 1997
		Acer pseudoplatanus	abaxial	↔	-	
		Alliaria petiolata	abaxial	↑ 22%	-	
		Allium ursinum	abaxial	↔	-	
		Alnus glutinosa	abaxial	↑ 132%	-	
		Anemone nemorosa	abaxial	↔	-	
		Arum maculatum	abaxial	*↓ 61%	-	

Age of Material (years)	CO_2 levels (relative to controls[a])	Species Used	Side of Leaf	Stomatal Density Response	Stomatal Index Response	Source
			adaxial	*↓ 80%	-	
		Betula pendula	abaxial	*↓ 39%	-	
		Betula pendula	abaxial	*↓ 43%	-	
		Betula pubescens	abaxial	*↓ 56%	-	
		Carpinus betulus	abaxial	↑ 13%	-	
		Castanea sativa	abaxial	*↓ 24%	-	
		Chamaenerion angustifolium	abaxial	↔	-	
		Circaea lutetiana	abaxial	*↓ 25%	-	
		Cirsium palustre	abaxial	*↓ 22%	-	
		Cornus sanguinea	abaxial	*↓ 16%	-	
		Corylus avellana	abaxial	*↓ 50%	-	
		Crataegus monogyna	abaxial	*↓ 36%	-	
		Dipsacus fullonum	abaxial	↑ 54%	-	
			adaxial	↑ 550%	-	
		Epilobium montanum	abaxial	*↓ 28%	-	
			adaxial	↔	-	
		Fagus sylvatica	abaxial	↑ 33%	-	
		Fagus sylvatica	abaxial	↔	-	
		Fraxinus excelsior	abaxial	↑ 39%	-	
		Geranium dissectum	abaxial	↔	-	
		Geranium robertianum	abaxial	*↓ 58%	-	
			adaxial	↑	-	
		Geum urbanum	abaxial	*↓ 21%	-	
			adaxial	↔	-	
		Glechoma hederacea	abaxial	*↓ 23%	-	
		Hedera helix	abaxial	↑ 101%	-	
		Heracleum sphondylium	abaxial	*↓ 14%	-	
			adaxial	↔	-	
		Hyacinthoides non-scripta	abaxial	↑ 56%	-	
			adaxial	↔	-	

Age of Material (years)	CO_2 levels (relative to controls[a])	Species Used	Side of Leaf	Stomatal Density Response	Stomatal Index Response	Source
		Hypericum hirsutum	abaxial	*↓ 11%	-	
		Hypericum perforatum	abaxial	*↓ 56%	-	
		Ilex aquifolium	abaxial	↑ 31%	-	
		Lamiastrum galeobdolon	abaxial	↔	-	
		Lathyrus pratensis	abaxial	↔	-	
			adaxial	*↓ 38%	-	
		Ligustrum vulgare	abaxial	*↓ 67%	-	
		Lonicera periclymenum	abaxial	*↓ 27%	-	
		Luzula sylvatica	abaxial	*↓ 44%	-	
		Lysimachia nummularia	abaxial	*↓ 56%	-	
			adaxial	*↓ 67%	-	
		Mercurialis perennis	abaxial	*↓ 17%	-	
		Oxalis acetosella	abaxial	↔	-	
		Populus nigra	abaxial	↑ 46%	-	
		Primula vulgaris	abaxial	*↓ 14%	-	
		Prunella vulgaris	abaxial	*↓ 47%	-	
			adaxial	*↓ 55%	-	
		Prunus avium	abaxial	*↓ 20%	-	
		Pteridium aquilinum	abaxial	↔	-	
		Quercus petraea	abaxial	*↓ 14%	-	
		Quercus robur	abaxial	↔	-	
		Ranunculus ficaria	abaxial	*↓ 21%	-	
			adaxial	↔	-	
		Rosa canina	abaxial	*↓ 28%	-	
		Sambucus nigra (sun)	abaxial	↔	-	
		Sambucus nigra (shade)	abaxial	↔	-	
		Scrophularia nodosa	abaxial	*↓ 18%	-	
		Silene dioica	abaxial	↑ 49%	-	
			adaxial	*↓	-	
		Sorbus aucuparia	abaxial	↔	-	

Age of Material (years)	CO_2 levels (relative to controls[a])	Species Used	Side of Leaf	Stomatal Density Response	Stomatal Index Response	Source
		Stellaria holostea	abaxial	*↓ 28%	-	
		Taxus baccata	abaxial	↔	-	
		Tilia cordata	abaxial	*↓ 34%	-	
		Ulmus glabra	abaxial	↔	-	
		Vaccinium myrtillus	abaxial	↔	-	
			adaxial	↔	-	
		Vicia cracca	abaxial	*↓ 57%	-	
			adaxial	*↓ 20%	-	
		Vicia sepium	abaxial	*↓ 43%	-	
		Viola odorata	abaxial	↔	-	
91	↑ 20%[c]	*Betula nana*	abaxial	*↓ 29%	-	Beerling, 1993
98	↑ 24%[c]	*Salix herbacea*	combined	-	*↓ 21%	Rundgren and Beerling, 1999
110	↑ 25%[c]	*Betula pubescens*	abaxial	*↓ 45%	*↓ 35%	Kürschner, 1996
118	↑ 24%[c]	*Quercus petraea*	abaxial	-	*↓ 34%	van der Burgh et al., 1993
126	↑ 14%[c]	*Salix herbacea*	combined	*↓ 22%	-	Beerling et al., 1993
~127	↑ 24%[c]	*Salix cinerea*	abaxial	*↓ 22%	*↓ 17%	McElwain et al., 1995
144	↑ 23%[c]	*Salsola kali* (C_4)	abaxial	-	↔	Raven and Ramsden, 1988
144	↑ 27%[c]	*Ginkgo biloba*	abaxial	↔	*↓ 44%	D.L. Royer, unpublished data
150	↑ 14%[c]	*Salix herbacea*	combined	*↓ 26%	-	Beerling et al., 1995
151	↑ 27%[c]	*Quercus robur*	abaxial	*↓ 23%	-	Beerling and Chaloner, 1993b
173	↑ 25%[c]	*Olea europaea*	abaxial	*↓ 24%	-	Beerling and Chaloner, 1993c
181	↑ 26%[c]	*Fagus sylvatica*	abaxial	*↓ 43%	-	Paoletti and Gellini, 1993
		Quercus ilex	abaxial	*↓ 28%	-	
190	↑ 27%[c]	*Quercus petraea*	abaxial	*↓ 40%	*↓ 31%	Kürschner et al., 1996

Age of Material (years)	CO_2 levels (relative to controls[a])	Species Used	Side of Leaf	Stomatal Density Response	Stomatal Index Response	Source
200	↑ 24%[c]	*Acer pseudoplatanus, Carpinus betulus, Fagus sylvatica, Populus nigra, Quercus petraea, Q. robur, Rhamnus catharticus, Tilia cordata*	abaxial	*↓ 40% (mean)	-	Woodward, 1987
240	↑ 25%[c]	*Alnus glutinosa, Amaranthus caudatus, Betula pendula, Buxus sempervirens, Ceratonia siliqua, Cynodon dactylon, Gentiana alpina, Helleborus foetidus, Juniperus communis, Papaver alpinum, Pinus pinea, P. uncinata, Pistacia lentiscus, Rhododendron ferrugineum*	combined	*↓ 17% (mean)	↔ (mean)	Peñuelas and Matamala, 1990
3318	↑ 22%[d]	*Olea europaea*	abaxial	*↓ 33%	-	Beerling and Chaloner, 1993c

* Response inversely relates ($P < 0.05$) to CO_2 concentration
↔ No significant change ($P > 0.05$)
\- Not reported
[a] Typically between 340 and 360 ppmV; for herbarium studies, control corresponds with oldest material
[b] From direct measurements from Mauna Loa Observatory, Hawaii and South Pole (Keeling et al., 1995)
[c] From Siple Station ice core (Neftel et al., 1985; Friedli et al., 1986)
[d] From Taylor Dome ice core (Indermühle et al., 1999)
Data from an altitudinal study; thus, the 'age' is however long the population has existed at the sampled altitudes
@ Data from a natural CO_2 spring area; thus, the 'age' is however long the population has existed at the location, assuming constant CO_2 emissions

APPENDIX 1.3

Fossil Stomatal Responses

Age of Material (years)	CO_2 levels (relative to controls[a])	Species Used	Side of Leaf	Stomatal Density Response	Stomatal Index Response	Source
9000	↓ 25%[b,c]	*Salix herbacea*	combined	-	*↑ 55%	Rundgren and Beerling, 1999
9190	↓ 27%[b]	*Salix cinerea*	abaxial	*↑ 57%	*↑ 32%	McElwain et al., 1995
9800	↑ 20%[d,j]	*Betula pubescens, B. pendula*	abaxial	-	*↓ 32% (mean)	Wagner et al., 1999
10750 (Allerød/Y. Dryas)	↓ 25%[c,k]	*Salix herbacea*	combined	*↑ 27%	-	Beerling et al., 1995
11500	↓ 24%[b]	*Salix herbacea*	combined	↓ 46%	↔	Beerling et al., 1992
13000	↓ 29%[b]	*Betula nana*	abaxial	*↑ 60%	-	Beerling, 1993
16500	↓ 47%[b]	*Salix herbacea*	combined	*↑ 54%	*↑ 25%	Beerling et al., 1993
28000	↓ 46%[b]	*Pinus flexilis*	-	*↑ 31%	-	van de Water et al., 1994
140,000	↓ 47%[b]	*Salix herbacea*	combined	*↑ 73%	*↑ 39%	Beerling et al., 1993
2.5 m.y.	↑ 4%[e]	*Quercus petraea*	abaxial	-	*↓ 10%	van der Burgh et al., 1993; Kürschner et al., 1996
6.5 m.y.	↓ 20%[e] ↓ 24%[e,l]	*Quercus petraea* *Fagus attenuata*	abaxial abaxial	- -	*↑ 55% *↑ 41%	van der Burgh et al., 1993; Kürschner et al., 1996
6.5 m.y.	↓ 20%[d]	*Betula subpubescens*	abaxial	*↑ 72%	*↑ 45%	Kürschner, 1996
10 m.y.	↑ 4%[e]	*Quercus petraea*	abaxial	-	*↓ 9%	van der Burgh et al., 1993; Kürschner et al., 1996
10 m.y.	↔[d]	*Betula subpubescens*	abaxial	*↔	*↔	Kürschner, 1996

Age of Material (years)	CO_2 levels (relative to controls[a])	Species Used	Side of Leaf	Stomatal Density Response	Stomatal Index Response	Source
15.5 m.y.	↑[f]	*Chamaecyparis linguaefolia, Cunninghamia chaneyi, Metasequoia occidentalis, Pinus harneyana, Pinus* sp., *Taxodium dubium*	combined	*↓ (mean)	-	Huggins, 1985
44-50 m.y. (M. Eocene)	↑ 43%[g]	*Lindera cinnamomifolia, Lindera* sp.[n]	abaxial	*↓ 36% (mean)	*↓ 47% (mean)	McElwain, 1998
		Litsea bournensis, L. edwardsii, L. hirsuta[n]	abaxial	*↓ 27% (mean)	*↓ 38% (mean)	
160-185 m.y. (M. Jurassic)	↑ 149%[g]	*Brachyphyllum crucis*[n]	abaxial	*↓ 54%	*↓ 39%	McElwain and Chaloner, 1996
		B. mamillare[n]	abaxial	*↓ 39%	*↓ 52%	
		Ginkgo huttonii[n]	abaxial	*↓ 32%	-	
160-185 m.y. (M. Jurassic)	↑ 149%[g]	*Baeira furcata*[n]	abaxial	*↓ 44%	-	McElwain, 1998
			adaxial	*↓ 67%	-	
		Ctenis exilis, C. kaneharai, C. sulcicaulis[n]	abaxial	*↓ 46% (mean)	↑ 14% (mean)	
		Pagiophyllum kurrii, P. maculosum, P. ordinatum[n]	abaxial	*↓ 36% (mean)	*↓ 39% (mean)	

Age of Material (years)	CO_2 levels (relative to controls[a])	Species Used	Side of Leaf	Stomatal Density Response	Stomatal Index Response	Source
~205 m.y. (Latest Triassic)	↑ 69%[h]	*Baeira boeggildiana*[n]	abaxial	-	*↓ 44%	McElwain et al., 1999
		B. minuta[n]	abaxial	-	*↓ 49%	
		B. paucipartiata[n]	abaxial	-	*↓ 25%	
		Baeira sp.[n]	abaxial	-	*↓ 36%	
		Ctenis minuta, C. nilssonii[n]	abaxial	-	*↓ 43% (mean)	
		C. nilssonii[n]	abaxial	-	*↓ 21%	
		Ginkgo acosmica[n]	abaxial	-	*↓ 26%	
		G. obovatus[n]	abaxial	-	*↓ 57%	
~205 m.y. (Earliest Jurassic)	↑ 567%[h]	*Baeira longifolia*[n]	abaxial	-	*↓ 60%	
		B. spectabilis[n]	abaxial	-	*↓ 71%	
		Nilssonia polymorpha[n]	abaxial	-	*↓ 70%	
		Stenopteris dinosaurensis[n]	abaxial	-	*↓ 11%	
285-290 m.y. (E. Permian)	↔[g]	*Lebachia frondosa*[n]	abaxial	↑ 120%	*↔	McElwain and Chaloner, 1995
290-303 m.y. (L. Penn.)	↑[l]	*Neuropteris ovata*	abaxial	*↓ 40%	*↓ 27%	Cleal et al., 1999
310 m.y. (L. Penn.)	↔[g]	*Swillingtonia denticulata*[n]	abaxial	↑ 460%	*↔	McElwain and Chaloner, 1995
388-373 m.y. (M. Devonian)	↓ 61%[g,m]	*Drepanophycus spinaeformis*	-	*↑ 42%	*↑ 38%	Edwards et al., 1998
390-403 m.y. (E. Devonian)	↑ 657%[g]	*Aglaophyton major*[n]	combined	*↓ 99%	*↓ 84%	McElwain and Chaloner, 1995
		Sawdonia ornata[n]	combined	*↓ 98%	*↓ 78%	

* Response inversely relates ($P < 0.05$) to CO_2 concentration
↔ No significant change ($P > 0.05$)
\- Not reported
[a] Typically between 340 and 360 ppmV
[b] From Vostok (Barnola et al., 1987) and Taylor Dome (Indermühle et al., 1999) ice cores

[c] From stomatal response of recent *Salix herbacea*, where CO_2 concentrations are known; values match ice core data[b]
[d] From stomatal responses of recent *Betula pubescens* and *Betula pendula*, where CO_2 concentrations are known
[e] From stomatal response of recent *Quercus petraea*, where CO_2 concentrations are known; values correlate with temperature curve
[f] From Freeman and Hayes, 1992; Cerling et al., 1997 (c.f. Pagani et al., 1999a)
[g] From 'best estimate' of Berner (1994, 1998)
[h] From stomatal ratios (McElwain and Chaloner, 1995, 1996; McElwain, 1998)
[i] This likely CO_2 spike at the Westphalian/Stephanian boundary is corroborated by a warming interval in Gondwanan and Anfaran areas; the control group is the Westphalian material
[j] The control group is prior to the CO_2 spike (260 ppmV CO_2[d])
[k] The control group is the late Allerød material, prior to CO_2 drop (273 ppmV CO_2[c])
[l] The control group is the 10 Ma material (370 ppmV CO_2[e])
[m] The control group is the 388 Ma material (2600 ppmV CO_2[g])
[n] Stomatal responses compared with corresponding Nearest Living Equivalents (NLEs); method described in text

APPENDIX 2.1

Summary of sedimentology at ginkgo-bearing sites. W = Williston Basin (western North and South Dakota, USA); BHB = Bighorn Basin (Wyoming and Montana, USA); DB = Denver Basin (Colorado, USA); S = southwestern Spitsbergen (Norway); A = south-central Alberta (Canada); IM = Isle of Mull (Scotland); E = southwestern Ellesmere Island (Canada); ID = north-central Idaho (USA); MT = western Montana (USA). Sedimentological contexts with question marks not included in analysis.

Site #	Site name	Location	Age (Ma)	Sedimentary features	Interpretation
1	DMNH 571	W	65.9	sandstone-mudstone couplets	relief channel
2	DMNH 1492	W	65.9	tabular sand with root traces on top	crevasse splay
3	DMNH 572	W	65.8	sandstone-mudstone couplets	relief channel
4	DMNH 425	W	65.6	cross-bedded sandstone	channel
5	DMNH 2087	W	65.5	sandstone-mudstone couplets	relief channel
6	DMNH 568	W	65.5	cross-bedded sandstone	channel
7	DMNH 566	W	65.5	gleyed mudstone with abundant root traces	distal floodplain
8	DMNH 1489	W	65.4	sandstone-mudstone couplets	relief channel
9	KJ 83101 / 8415	BHB	64.5	tabular sand	crevasse splay
10	LJH 7423	BHB	64.5	sandstone-shale-lignite upward sequence; Ginkgo in sand	crevasse splay
11	LJH 7424c	BHB	64.5	ledgey cross-bedded sandstone	crevasse splay
12	LJH 7425 / 7653	BHB	64.5	ledgey cross-bedded sandstone	crevasse splay?
13	LJH 7659	BHB	64.5	siltstone (relief channel) at base of clay plug (abandoned cutoff)	relief channel
14	DMNH 2360	DB	64.1	gray claystone w/occasional fine/med sand partings	crevasse splay
15	Basilika	S	64	~8 m siltsontes/sandstones resting on ~30 cm pebble/cobble conglom.	relief channel
16	LJH 7861	BHB	64	siltstone/sandstone overlying lignite; Ginkgo in sand	crevasse splay
17	Joffre Bridge	A	58.5	carbonaceous mudstone; Ginkgo in hard mollusc layer	abandoned channel
18	Burbank	A	58.5	coarse sandstone bounded by shales	crevasse splay
19	SLW 0029	BHB	57.8	grey siltstone above carbonaceous shale	crevasse splay
20	SLW 0025	BHB	57.3	siltstone-mudstone couplets; Ginkgo mainly in siltstone	relief channel
21	LJH 72127	BHB	57	lignite-siltstone-sand sequence	crevasse splay
22	SLW 0019	BHB	56.7	cross-bedded medium to fine sandstone; large-scale crosscuts	channel
23	Chance	BHB	56.4	coarsening upwards sequence; Ginkgo in sand	crevasse splay
24	Almont	W	56	siliceous, iron-stained shale containing fish scales overlying fine sand	abandoned channel
25	SLW 993	BHB	55.9	base of channel fill directly above basal lag deposits (pebbles)	abandoned channel
26	SLW 992	BHB	55.9	interlaminated fine/coarse siltstones	abandoned channel
27	SLW 991	BHB	55.9	laminated gray siltstone	abandoned channel
28	SLW 0051	BHB	55.9	laminated siltstone and fine sandstone	crevasse splay
29	LJH 72141-1	BHB	55.8	3 m above brown fissile lignite	?

Site #	Site name	Location	Age (Ma)	Sedimentary features	Interpretation
30	SLW 9155	BHB	55.7	interlaminated siltstone-sandstone	crevasse splay
31	SLW 9427 / 9437	BHB	55.5	thinly bedded sandstone	crevasse splay
32	SLW 9411	BHB	55.5	interbedded siltstone and sandstone above a carbonaceous shale	crevasse splay
33	SLW 9412	BHB	55.5	laminated fine sand	distal floodplain
34	SLW 9438	BHB	55.5	thinly bedded sandstone	crevasse splay
35	SLW 9434	BHB	55.4	interlaminated cross-bedded siltstone-sandstone; Ginkgo in siltstone	crevasse splay
36	SLW 9050	BHB	55.3	interlaminated siltstone-sandstone	crevasse splay
37	SLW 9715 / 981	BHB	55.3	laminated fining upwards sequences; basal lag contains molluscs	relief channel
38	SLW 9936	BHB	55.3	siltstone overlying sandstone	?
39	SLW 8612	BHB	55.3	carbonaceous shale	backswamp
40	Ardtun Head	IM	55.2	white/grey clay in a clay/sandstone sequence interbedded with basalt	relief channel
41	SLW 9812	BHB	55.1	gray shale-mudstone couplets	relief channel
42	Stenkul Fiord	E	55	medium to fine cross-bedded sandstone with climbing ripples	channel
43	SLW 9911	BHB	54.8	mudstone/siltstone couplets; green sand at base	relief channel
44	SLW 9915	BHB	54.8	sandstone-carbonaceous shale-siltstone unit; Ginkgo in top siltstone	relief channel
45	SLW 841	BHB	54.3	carbonaceous shale	backswamp
46	SLW LB	BHB	53.9	coarse carbonaceous siltstone	relief channel
47	SLW H	BHB	53.5	sandy siltstone	relief channel
48	SLW near YPM 67	BHB	53.5		relief channel
49	LJH 9915	BHB	53.4	thin carbonaceous lenticular paper shale sandwiched between soils	relief channel
50	Beaver Creek	MT	36		lake
51	Juliaetta	ID	16.5	coarse sand; delta foresets	lake

APPENDIX 2.2

Summary of flora at ginkgo-bearing sites. Only those species that occur at ≥4 sites are tabulated here. *n* = number of occurrences for a given species. See Appendix 2.1 for full description of sites.

	Site name	DMNH 571	DMNH 572	DMNH 425	DMNH 2087	DMNH 568	DMNH 566	DMNH 1489	KJ 83101	LJH 7423	LJH 7424c	LJH 7425	LJH 7659	Basilika	LJH 7861	Joffre Bridge	Burbank
	Site #	1	3	4	5	6	7	8	9	10	11	12	13	15	16	17	18
	Age (Ma)	65.9	65.8	65.6	65.5	65.5	65.5	65.4	64.5	64.5	64.5	64.5	64.5	64	64	58.5	58.5
	Species richness	15	9	12	11	13	15	12	13	7	6	10	11	4	19	5	4
n	Taxon																
28	*Cercidiphyllum genetrix*		X		X				X	X	X	X	X	X	X		X
21	*Metasequoia occidentalis*	X	X				X		X	X	X	X	X	X	X	X	
20	*Platanus raynoldsii / guillelmae*								X	X	X	X	X		X		
14	*Glyptostrobus europaeus*	X							X			X	X		X	X	
8	*Dryophyllum subfalcata*	X	X	X	X	X	X	X							X		
8	*Menispermites parvareolatus*																
8	*Platanus nobilis / brownii*															X	
7	*Ampelopsis acerifolia*								X			X			X		
6	Betulaceae sp. 1																
6	*Ficus artocarpoides*								X			X	X		X		
6	*Ficus planicostata*										X						
6	*Erlingdorfia montana*	X	X	X		X	X	X									
6	*Leepierceia preartocarpoides*	X	X	X		X	X	X									
6	*Rhamnus cleburni*			X	X	X	X	X							X		
6	*Taxodium olrikii*	X		X		X	X	X					X				
6	*Vitis stantoni*	X	X		X		X				X				X		
5	*Corylus insignis*														X		
5	*Trochodendroides nebrascensis*	X		X		X	X	X									
5	*Viburnum cupanioides*														X		
5	*Zingiberopsis isonervosa*																
4	*Averrhoites affinis*																
4	*Aesculus hickeyi*														X		
4	*Nyssidium arcticum*	X		X			X										
4	*Paranymphea crassifolia*								X			X	X		X		
4	Platanaceae	X	X	X		X											

Appendix 2.2 continued

n	Site name	SLW 0029	SLW 0025	LJH 72127	SLW 0019	Chance	Almont	SLW 993	SLW 992	SLW 991	SLW 0051	LJH 72141	SLW 9155	SLW 9427	SLW 9411	SLW 9412	SLW 9438
	Site #	19	20	21	22	23	24	25	26	27	28	29	30	31	32	33	34
	Age (Ma)	57.8	57.3	57	56.7	56.4	56.0	55.9	55.9	55.9	55.9	55.8	55.7	55.5	55.5	55.5	55.5
	Species richness	3	3	10	8	11	11	6	4	5	5	12	4	8	4	4	11
n	Taxon																
28	*Cercidiphyllum genetrix*	X	X	X	X	X		X		X	X	X		X			X
21	*Metasequoia occidentalis*			X	X	X		X				X					X
20	*Platanus raynoldsii / guillelmae*		X		X	X		X			X		X	X		X	X
14	*Glyptostrobus europaeus*			X	X	X						X					
8	*Dryophyllum subfalcata*																
8	*Menispermites parvareolatus*				X			X		X							
8	*Platanus nobilis / brownii*													X		X	
7	*Ampelopsis acerifolia*	X		X		X											X
6	Betulaceae sp. 1												X	X			X
6	*Ficus artocarpoides*										X			X			
6	*Ficus planicostata*													X	X	X	X
6	*Erlingdorfia montana*																
6	*Leepierceia preartocarpoides*																
6	*Rhamnus cleburni*																
6	*Taxodium olrikii*																
6	*Vitis stantoni*																
5	*Corylus insignis*							X	X	X							
5	*Trochodendroides nebrascensis*																
5	*Viburnum cupanioides*			X					X	X							
5	*Zingiberopsis isonervosa*											X					
4	*Averrhoites affinis*								X								
4	*Aesculus hickeyi*			X								X					
4	*Nyssidium arcticum*						X										
4	*Paranymphea crassifolia*																
4	Platanaceae																

Appendix 2.2 continued

	Site name	SLW 9434	SLW 9050	SLW 9715	SLW 9936	SLW 8612	Ardtun Head	SLW 9812	SLW 9911	SLW 9915	SLW 841	SLW LB	SLW H	YPM 67	LJH 9915	Juliaetta
	Site #	35	36	37	38	39	40	41	43	44	45	46	47	48	49	50
	Age (Ma)	55.4	55.3	55.3	55.3	55.3	55.2	55.1	54.8	54.8	54.3	53.9	53.5	53.5	53.4	16.5
	Species richness	3	5	5	1	4	8	7	6	10	5	22	22	3	3	2
n	Taxon															
28	*Cercidiphyllum genetrix*							X	X	X	X	X	X		X	
21	*Metasequoia occidentalis*		X			X		X		X						
20	*Platanus raynoldsii / guillelmae*			X						X		X	X	X		
14	*Glyptostrobus europaeus*							X	X	X		X				
8	*Dryophyllum subfalcata*															
8	*Menispermites parvareolatus*			X					X	X		X	X			
8	*Platanus nobilis / brownii*	X		X					X	X			X			
7	*Ampelopsis acerifolia*															
6	Betulaceae sp. 1		X									X	X			
6	*Ficus artocarpoides*															
6	*Ficus planicostata*	X														
6	*Erlingdorfia montana*															
6	*Leepierceia preartocarpoides*															
6	*Rhamnus cleburni*															
6	*Taxodium olrikii*															
6	*Vitis stantoni*															
5	*Corylus insignis*			X												
5	*Trochodendroides nebrascensis*															
5	*Viburnum cupanioides*							X								
5	*Zingiberopsis isonervosa*										X	X	X		X	
4	*Averrhoites affinis*							X			X	X				
4	*Aesculus hickeyi*					X										
4	*Nyssidium arcticum*															
4	*Paranymphea crassifolia*															
4	Platanaceae															

APPENDIX 2.3

Complete list of species names with authors used in Chapter 2.

Acer silberlingii Brown

Aesculus hickeyi Manchester

Amentotaxus formosana Li

Amentotaxus gladifolia (Ludwig) Ferguson, Jähnichen, & Alvin

Archaeampelos acerifolia (Newberry) McIver & Basinger

Athyrium Felix-femina Linnaeus

Averrhoites affinis (Newberry) Hickey

Beringeaphyllum cupanoides (Newberry) Manchester, Crane & Golovneva

Betulaceae sp. 1

Cercidiphyllum genetrix (Newberry) Hickey

Cercidiphyllum japonicum Siebold & Zuccarini

Corylus insignis Heer

Dryophyllum subfalcata Lesquereux

Erlingdorfia montana Johnson

"Ficus" artocarpoides Lesquereux

"Ficus" planicostata Lesquereux

Gingko adiantoides (Unger) Heer

Gingko beckii Scott, Barghoorn & Prakash

Gingko biloba Linnaeus

Gingko coriacea Florin

Gingko digitata (Brongniart) Heer

Gingko gardnerii Florin

Gingko huttonii (Sternberg) Heer

Gingko spitzbergensis Manum

Gingko tigrensis Archangelsky

Gingko yimaensis Zhou & Zhang

Glyptostrobus europaeus (Brongniart) Heer

Leepierceia preartocarpoides Johnson

Metasequoia glyptostroboides H. H. Hu & Cheng

Metasequoia occidentalis (Newberry) Chaney

Nyssidium arcticum (Heer) Iljinskaya

Paranymphea crassifolia (Newberry) Berry

Platanaceae

Platanus X acerifolia Willdenow

Platanus brownii (Berry) MacGinitie

Platanus guillelmae Geoppert

Platanus mexicana Moricand

Platanus nobilis Newberry

Platanus occidentalis Linnaeus

Platanus orientalis Linnaeus

Platanus racemosa Nuttall

Platanus raynoldsii Newberry

Platanus wrightii Watson

“Rhamnus” cleburni Lesquereux

Taxodium olrikii (Heer) Brown

Trochodendroides nebrascensis (Newberry) Dorf

Vitis stantonii (Knowlton) Brown

Wardiaphyllum daturaefolia (Ward) Hickey

Zingiberopsis isonervosa Hickey

Zizyphoides flabella (Newberry) Crane, Manchester & Dilcher

APPENDIX 3.1

Voucher specimen information for historical collections used to construct training sets. All catalogued specimens are deposited at the Yale Peabody Museum (YPM) Herbarium. Permanent slides of *Ginkgo* were not prepared (see Table 4.3 for herbaria information).

Date	CO_2 (ppmV)	SI (%)	Source herbarium[a]	Source location of leaves	Cuticle accession number
				Metasequoia glyptostroboides	
1947	310	11.89	UC	E Szechuan / NW Hubei, China	dlr 00289-00293
1948	310	11.63	UC	E Szechuan / NW Hubei, China	dlr 00294-00298
1949	311	11.47	UC	Berkeley, CA	dlr 00299-00303
1950	311	11.62	UC	Bar Harbor, ME	dlr 00304-00308
1953	312	11.07	UC	San Rafael, CA	dlr 00309-00313
1961	317	10.56	UC	Tallahassee, FL	dlr 00314-00318
1962	318	11.49	YPM	Bethany, CT	(acetate peels) dlr 9924-9928
1964	319	10.20	MA	PA	(acetate peels) dlr 9931-9935
1965	320	10.81	UC	Washington DC	dlr 00319-00323
1968	323	9.44	UC	Fukuchiyama-city, Japan	dlr 00324-00328
1969	323	10.83	BBG	Brooklyn Botanical Garden, NY	(acetate peels) dlr 999-9913
1973	328	10.40	NA	Turlock, CA	(acetate peels) dlr 0064-0068
1975	331	10.16	UC	U of Oregon, Eugene, OR	dlr 00329-00333
1976	331	9.54	UC	U of Oregon, Eugene, OR	dlr 00334-00338
1980	338	9.73	UC	Western Hubei, China	dlr 00339-00343
1999	367	9.57	modern	New Haven, CT; London, UK	(various acetate peels)
				Platanus sp.	
1891	294	15.35	YPM	Stanley Co., NC (*P. occidentalis*)	dlr 0129-0134
1975	330	15.22	YPM	Gali Ali Beg, Iraq (*P. orientalis*)	dlr 0124-0128
2001	370	13.28	modern	New Haven, CT (*P.* x *acerfolia)*	dlr 0135-0138
2001	370	13.44	modern	New Haven, CT (*P. occidentalis*)	dlr 0139-0144

[a] YPM = Peabody Museum of Natural History (Yale University); NA = U.S. National Arboretum; BBG = Brooklyn Botanic Gardens; MA = Morris Arboretum (University of Pennsylvania); UC = University Herbarium (University of California, Berkeley); modern = collections of fresh leaves

APPENDIX 3.2

Voucher specimen information for experimental collections used to construct training sets. All catalogued specimens are deposited at the Yale Peabody Museum (YPM) Herbarium.

CO_2 (ppmV)	SI (%)	Plant age (yr)	Cuticle accession number
		Ginkgo biloba	
431	8.70	6	dlr 00203-00218
	8.73	1	dlr 00226-00233
446	8.13	7	dlr 0172-0179
	8.00	2	dlr 0164-0171
791	7.16	6	dlr 00187-00202
	6.84	1	dlr 00219-00225
801	6.99	7	dlr 0156-0163
	6.67	2	dlr 0148-0155
		Metasequoia glyptostroboides	
431	9.04	1	dlr 00349-00364
446	9.31	2	dlr 0180-0183
791	7.84	1	dlr 00365-00380
801	7.96	2	dlr 0184-0187

APPENDIX 3.3

Voucher specimen information for fossils used in CO_2 reconstruction.

Age (Ma)	SI (%)	Site	Depository[a]	Rock accession number[b]	Cuticle accession number
		Ginkgo sp.[c]			
168	4.46	[d]Andøya, Norway [*G. dahlii*]	PMO	PMO-PA 4450	PMO 167.552-167.555
120	7.97	[d]Lapasha #14 (DMNH 1913) [*G. pluripartita*]	DMNS	DMNH EPI.14283(1)	DMNH EPI.14283(1)-(3)
75	9.24	[d]First Good Location (DMNH 894) [*G. dissecta*]	DMNS		dlr 0051-0055
65.9	7.03	[d]Little Mound of Glee (DMNH 571)	DMNS	DMNH 18880(1)	DMNH 18880(1)
65.8	7.09	[d]KJ 87134	YPM	YPM 7114a	YPM 46833
				YPM 7112	YPM 46859
				YPM 7111a,b	YPM 46828
65.5	8.32	Ginkgo Salad (DMNH 566)	DMNS	DMNH 20644(1)-(6)	DMNH 20644(1)-(6)
				DMNH 20642(1)-(2)	DMNH 20642(1)-(2)
				DMNH 20638(1)-(3)	DMNH 20638(1)-(3)
				DMNH 20645(1)-(2)	DMNH 20645(1)-(2)
				DMNH 20631(1)	DMNH 20631(1)
				DMNH 20643(1),(3)	DMNH 20643(1),(3)
				DMNH 20636(1)	DMNH 20636(1)
				DMNH 20635(1)	DMNH 20635(1)
				DMNH 13663(1)	DMNH 13663(1)
				DMNH 20632(1)	DMNH 20632(1)
				DMNH 20640(1)-(2)	DMNH 20640(1)-(2)
				DMNH 20634(1)	DMNH 20634(1)
				DMNH 20633(1)	DMNH 20633(1)
				DMNH 20641(1)	DMNH 20641(1)
				DMNH 20693(1)	DMNH 20693(1)
				DMNH 20692(1)	DMNH 20692(1)
				DMNH 20690(1)	DMNH 20690(1)
				DMNH 20695(1)	DMNH 20695(1)
				DMNH 20697(1)	DMNH 20697(1)
				DMNH 20698(1)	DMNH 20698(1)

Age (Ma)	SI (%)	Site	Depository[a]	Rock accession number[b]	Cuticle accession number
65.4	8.42	[d]Wet Butte (DMNH 1489)	DMNS	DMNH 20613(1)	DMNH 20613(1)
				DMNH 20610(1)	DMNH 20610(1)
64.5	9.48	Ginkgo (LJH 7423)	USNM		USNM 519346-519350
64.5	9.32	Debeya (LJH 7659)	YPM		YPM 40794-40800
					YPM 45166-45173
64.1	9.90	Eat My Ginkgo (DMNH 2360)	DMNS	DMNH 23071-23075	DMNH 23071-23075
64	9.42	Spitsbergen (Basilika Fm.)	PMO		PMO PA164.991
					PMO PA164.992
					PMO PA164.998
					PMO PA165.003
					PMO PA167.556
					PMO PA167.557
			YPM		YPM 45128
63	8.60	[d]? (coll. by E. Dorf)	YPM		YPM 45127
58.5	7.55	Burbank (Paskapoo Fm.)	UA	S17775	dlr 00129
				S17778	dlr 00130
				S17777	dlr 00131
				S24573B	dlr 00132
				S17764	dlr 00133
				S17779	dlr 00134
				S51314	dlr 00135
58.5	7.96	Joffre Bridge (Paskapoo Fm.)	UA	S39561	dlr 00136
				S39559	dlr 00137
				S39552	dlr 00138
				S39555	dlr 00139
				S39549	dlr 00140
58	11.24	[d]Linch (UF 18255)	FMNH	UF 25310	UF 25310
				UF 25313-25314	UF 25313-25314
57.3	9.01	SLW 0025	USNM		USNM 519351-519357
56.4	8.75	Chance (LJH 7132/72118; USNM 14184)	YPM	USNM 511364	USNM 511364
					YPM 45196
					YPM 45914
					YPM 45197-45198
56	8.86	[d]LB 2373 (coll. By E.L. Simons)	YPM		YPM 40013
56	8.89	[d]Almont/Sentinel Butte (DMNH 907)	DMNS		dlr 0057-0058

Age (Ma)	SI (%)	Site	Depository[a]	Rock accession number[b]	Cuticle accession number
55.9	10.97	SLW 991	USNM		USNM 519358-519362
55.9	10.80	SLW 992	USNM		dlr 00115-00117
					USNM 519363-519367
55.9	11.43	SLW 993	USNM		USNM 516616-516622
55.8	10.63	Powell dump / J.P. Reiss (LJH 72141-1)	YPM		YPM 45129
					YPM 45130
			USNM		dlr 9952-9954
					dlr 9945-9946
55.7	11.21	SLW 9155	USNM		USNM 519368-519377
55.6	11.5	SLW 9411	USNM		USNM 519378-519385
55.4	12.23	SLW 9434	USNM		USNM 519386-519392
55.3	8.23	SLW 9715/981	USNM		dlr 0071-0075
					dlr 0081-0085
					dlr 00100-00101
55.3	12.18	SLW 9050	USNM		dlr 00110-00114
55.3	11.77	SLW 9936	USNM		dlr 9960-9964
					dlr 9939-9942
					dlr 9955-9959
55.3	12.41	SLW 8612	USNM		dlr 9947-9951
					dlr 9943-9944
55.2	6.54	Isle of Mull, Scotland [*G. gardneri*]	PMO		PMO PA165.018
					PMO PA165.020
					PMO PA165.022
			YPM		YPM 45126
			BNHM		PA 2997
					PA 2999
55.1	8.53	SLW 9812	USNM		dlr 0076-0080
					dlr 0096-0097
					dlr 00104
					dlr 0086-0090
					dlr 00102-00103
					dlr 0091-0095
					dlr 0098-0099
55	8.29	[d]Stenkul Fiord (LJH 8411)	YPM		YPM 45199
					YPM 48913

Age (Ma)	SI (%)	Site	Depository[a]	Rock accession number[b]	Cuticle accession number
54.8	8.83	SLW 9915	USNM		dlr 9961-9962
					USNM 519393-519397
53.9	9.29	SLW LB	USNM		USNM 519399-519403
53.5	10.22	SLW H	USNM		USNM 519404-519412
53.4	9.38	LJH 9915	YPM		YPM 48029
					YPM 48002
					YPM 40776
					YPM 40777
					YPM 40778
					YPM 47747
					YPM 47754
					YPM 47780
					YPM 47753
					YPM 47802
					YPM 47833
					YPM 47942
					YPM 47971
					YPM 47939
48	8.49	[d]Yellowstone Nat'l Park (coll. by E. Dorf)	YPM		YPM 20691
16.5	8.14	Juliaetta (P6 / LJH 0012)	YPM		YPM 45174-45185
			UI		2 slides from W. Rember (UI)
2	12.29	[d]Klärbecken (near Frankfurt)	BMNH		BMNH v.17168
		Metasequoia occidentalis			
15.2	10.95	Emerald Creek (P37a)	YPM		YPM 45189
					YPM 45190
					YPM 45191-45192
15.3	10.94	Clarkia fossil bowl (P33b)	YPM		YPM 45193
					YPM 45194
					YPM 45195
15.3	11.59	Clarkia fossil bowl (P33a)	YPM		YPM 45186-45187
					YPM 45188
		Platanus guillelmae			
53.5	12.89	SLW H	USNM		USNM 519413-519419

[a] PMO = Oslo Paleontological Museum; DMNS = Denver Museum of Nature and Science; YPM = Yale Peabody Museum; USNM = National Museum of Natural History, Smithsonian Institution; FMNH = Florida Museum of Natural History; UA = University of Alberta; BNHM = British Natural History Museum; UI = University of Idaho
[b] Accession number of rock from which cuticle was removed
[c] *Ginkgo adiantoides* unless noted otherwise
[d] Data not used in CO_2 reconstruction (i.e., Figs. 3.2 and 4.3)

LITERATURE CITED

Abrams, M.D., 1994. Genotypic and phenotypic variation as stress adaptations in temperate tree species: a review of several case studies. Tree Physiology, 14: 833-842.

Ahn, Y.-J., Kwon, M., Park, H.M., Han, C.K., 1997. Potent insecticidal activity of *Ginkgo biloba* derived trilactone terpenes against *Nilaparvata lugens*. Phytochemicals for Pest Control, 658: 90-105.

Allen, J.R.L., 1964. Studies in fluviatile sedimentation: six cyclothems from the lower Old Red Sandstone, Anglo-Welsh Basin. Sedimentology, 3: 164-198.

Allen, J.R.L., 1965. A review of the origins and characteristics of Recent alluvial sediments. Sedimentology, 5: 89-91.

Andrews, J.E., Tandon, S.K., Dennis, P.F., 1995. Concentrations of carbon dioxide in the Late Cretaceous atmosphere. Journal of the Geological Society, London, 152: 1-3.

Apple, M.E., Olszyk, D.M., Ormrod, D.P., Lewis, J., Southworth, D., Tingey, D.T., 2000. Morphology and stomatal function of Douglas fir needles exposed to climate change: elevated CO_2 and temperature. International Journal of Plant Science, 161: 127-132.

Arnold, C.A., 1947. An Introduction to Paleobotany. McGraw, New York.

Arnott, H.J., 1959. Anastomoses in the venation of *Ginkgo biloba*. American Journal of Botany, 46: 405-411.

Ashton, P.M.S., Berlyn, G.P., 1994. A comparison of leaf physiology and anatomy of *Quercus* (section *Erythrobalanus*-Fagaceae) species in different light environments. American Journal of Botany, 81: 589-597.

Atkinson, C.J., Taylor, J.M., Wilkins, D., Besford, R.T., 1997. Effects of elevated CO_2 on chloroplast components, gas exchange and growth of oak and cherry. Tree Physiology, 17: 319-325.

Atzmon, N., Henkin, Z., 1998. Establishing forest tree species on peatland in a reflooded area of the Huleh Valley, Israel. Forestry, 71: 141-146.

Bains, S., Corfield, R.M., Norris, R.D., 1999. Mechanisms of climate warming at the end of the Paleocene. Science, 285: 724-727.

Barnett, T.P., Pierce, D.W., Schnur, R., 2001. Detection of anthropogenic climate change in the world's oceans. Science, 292: 270-274.

Barnola, J.M., Raynaud, D., Korotkevich, Y.S., Lorius, C., 1987. Vostok ice core provides 160,000-year record of atmospheric CO_2. Nature, 329: 408-414.

Barron, E.J., 1987. Eocene equator-to-pole surface ocean temperatures: A significant climate problem? Paleoceanography, 2: 729-739.

Beerling, D.J., 1993. Changes in the stomatal density of *Betula nana* leaves in response to increases in atmospheric carbon dioxide concentration since the late-glacial. Special Papers in Palaeontology, 49: 181-187.

Beerling, D.J., 1994. Palaeo-ecophysiological studies on Cretaceous and Tertiary fossil floras. In: Boulter, M.C., Fisher, H.C. (Eds.), Cenozoic Plants and Climates of the Arctic. Springer-Verlag, Berlin, pp. 23-33.

Beerling, D.J., 1997. Carbon isotope discrimination and stomatal responses of mature *Pinus sylvestris* L. trees exposed *in situ* for three years to elevated CO_2 and temperature. Acta Œcologica, 18: 697-712.

Beerling, D.J., 1999. Stomatal density and index: Theory and application. In: Jones, T.P., Rowe, N.P. (Eds.), Fossil Plants and Spores: Modern Techniques. The Geological Society, London, pp. 251-256.

Beerling, D.J., 2000. Increased terrestrial carbon storage across the Palaeocene-Eocene boundary. Palaeogeography, Palaeoclimatology, Palaeoecology, 161: 395-405.

Beerling, D.J., Chaloner, W.G., 1992. Stomatal density as an indicator of atmospheric CO_2 concentration. The Holocene, 2: 71-78.

Beerling, D.J., Chaloner, W.G., 1993a. Evolutionary responses of stomatal density to global CO_2 change. Biological Journal of the Linnean Society, 48: 343-353.

Beerling, D.J., Chaloner, W.G., 1993b. The impact of atmospheric CO_2 and temperature change on stomatal density: observations from *Quercus robur* lammas leaves. Annals of Botany, 71: 231-235.

Beerling, D.J., Chaloner, W.G., 1993c. Stomatal density responses of Egyptian *Olea europaea* L. leaves to CO_2 change since 1327 B.C. Annals of Botany, 71: 431-435.

Beerling, D.J., Chaloner, W.G., 1994. Atmospheric CO_2 changes since the last glacial maximum: evidence from the stomatal density record of fossil leaves. Review of Palaeobotany and Palynology, 81: 11-17.

Beerling, D.J., Kelly, C.K., 1997. Stomatal density responses of temperate woodland plants over the past seven decades of CO_2 increase: a comparison of Salisbury (1927) with contemporary data. American Journal of Botany, 84: 1572-1583.

Beerling, D.J., Osborne, C.P., 2002. Physiological ecology of Mesozoic polar forests in a high CO_2 environment. Annals of Botany, in press.

Beerling, D.J., Royer, D.L., 2002a. Fossil plants as indicators of the Phanerozoic global carbon cycle. Annual Review of Earth and Planetary Sciences, in press.

Beerling, D.J., Royer, D.L., 2002b. Reading a CO_2 signal from fossil stomata: New Phytologist, in press.

Beerling, D.J., Woodward, F.I., 1995. Stomatal responses of variegated leaves to CO_2 enrichment. Annals of Botany, 75: 507-511.

Beerling, D.J., Woodward, F.I., 1996. Palaeo-ecophysiological perspectives on plant responses to global change. Trends in Ecology and Evolution, 11: 20-23.

Beerling, D.J., Woodward, F.I., 1997. Changes in land plant function over the Phanerozoic: reconstructions based on the fossil record. Botanical Journal of the Linnean Society, 124: 137-153.

Beerling, D.J., Chaloner, W.G., Huntley, B., Pearson, J.A., Tooley, M.J., 1991. Tracking stomatal densities through a glacial cycle: their significance for predicting the response of plants to changing atmospheric CO_2 concentrations. Global Ecology and Biogeography Letters, 1: 136-142.

Beerling, D.J., Chaloner, W.G., Huntley, B., Pearson, J.A., Tooley, M.J., Woodward, F.I., 1992. Variations in the stomatal density of *Salix herbacea* L. under the changing atmospheric CO_2 concentrations of late- and post-glacial time. Philosophical Transactions of the Royal Society of London, B336: 215-224.

Beerling, D.J., Chaloner, W.G., Huntley, B., Pearson, J.A., Tooley, M.J., 1993. Stomatal density responds to the glacial cycle of environmental change. Proceedings of the Royal Society London, B251: 133-138.

Beerling, D.J., Birks, H.H., Woodward, F.I., 1995. Rapid late-glacial atmospheric CO_2 changes reconstructed from the stomatal density record of fossil leaves. Journal of Quaternary Science, 10: 379-384.

Beerling, D.J., McElwain, J.C., Osborne, C.P., 1998a. Stomatal responses of the 'living fossil' *Ginkgo biloba* L. to changes in atmospheric CO_2 concentrations. Journal of Experimental Botany, 49: 1603-1607.

Beerling, D.J., Woodward, F.I., Lomas, M.R., Wills, M.A., Quick, W.P., Valdes, P.J., 1998b. The influence of Carboniferous palaeoatmospheres on plant function: an experimental and modelling assessment. Philosophical Transactions of the Royal Society of London, B353: 131-140.

Beerling D.J., Lomax, B.H., Royer, D.L., Upchurch, G.R., Kump, L.R., 2002. An atmospheric pCO_2 reconstruction across the Cretaceous-Tertiary boundary from leaf megafossils. Proceedings of the National Academy of Sciences USA, in press.

Berger, D., Altmann, T., 2000. A subtilisin-like serine protease involved in the regulation of stomatal density and distribution in *Arabidopsis thaliana*. Genes & Development, 14: 1119-1131.

Bell, D.T., 1980. Gradient trends in the streamside forest of central Illinois. Bulletin of the Torrey Botanical Club, 107: 172-180.

Berner, R.A., 1994. GEOCARB II: a revised model of atmospheric CO_2 over Phanerozoic time. American Journal of Science, 294: 56-91.

Berner, R.A., 1998. Sensitivity of Phanerozoic atmospheric CO_2 to paleogeographically induced changes in land temperature and runoff. In: Crowley, T.J., Burke, K.C. (Eds.), Tectonic Boundary Conditions for Climate Reconstructions. Oxford University Press, New York, pp. 251-260.

Berner, R.A., Canfield, D., 1989. A new model for atmospheric oxygen over Phanerozoic time. American Journal of Science, 289: 333-361.

Berner, R.A., Kothavala, Z., 2001. GEOCARB III: a revised model of atmospheric CO_2 over Phanerozoic time. American Journal of Science, 301: 182-204.

Berner, R.A., Petsch, S.T., Lake, J.A., Beerling, D.J., Popp, B.N., Lane, R.S., Laws, E.A., Westley, M.B., Cassar, N., Woodward, F.I., Quick, W.P., 2000. Isotope fractionation and atmospheric oxygen: implications for Phanerozoic O_2 evolution. Science, 287: 1630-1633.

Berryman, C.A., Eamus, D., Duff, G.A., 1994. Stomatal responses to a range of variables in tree species grown with CO_2 enrichment. Journal of Experimental Botany, 45: 539-546.

Bettarini, I., Miglietta, F., Raschi, A., 1997. Studying morpho-physiological responses of *Scirpus lacustris* from naturally CO_2-enriched environments. In: Raschi, A., Miglietta, F., Tognetti, R., van Gardingen, P.R. (Eds.), Plant Responses to Elevated CO_2. Cambridge University Press, Cambridge, pp. 134-147.

Bettarini, I., Vaccari, F.P., Miglietta, F., 1998. Elevated CO_2 concentrations and stomatal density: observations from 17 plant species growing in a CO_2 spring in central Italy. Global Change Biology, 4: 17-22.

Boetsch, J., Chin, J., Ling, M., Croxdale, J., 1996. Elevated carbon dioxide affects the patterning of subsidiary cells in *Tradescantia* stomatal complexes. Journal of Experimental Botany, 47: 925-931.

Boulter, M.C., Kvaček, Z., 1989. The Palaeocene flora of the Isle of Mull. Special Papers in Palaeontology, 42: 1-149.

Boivin, R., Richard, M., Beauseigle, D., Bousquet, J., Bellemare, G., 1996. Phylogenetic inferences from chloroplast chlB gene sequences of *Nephrolepis exaltata* (Filicopsida), *Ephedra altissima* (Gnetopsida), and diverse land plants. Molecular Phylogenetics and Evolution, 6: 19-29.

Bowen, G.J., Koch, P.L., Gingerich, P.D., Norris, R.D., Bains, S., Corfield, R.M., 2001. Refined isotope stratigraphy across the continental Paleocene-Eocene boundary on Polecat Bench in the northern Bighorn Basin. In: Gingerich, P.D. (ed.), Paleocene-Eocene Stratigraphy and Biotic Change in the Bighorn and Clarks Fork Basins, Wyoming. University of Michigan Papers on Paleontology, 33: 73-88.

Bristow, J.M., Looi, A.-S., 1968. Effects of carbon dioxide on the growth and morphogenesis of *Marsilea*. American Journal of Botany, 55: 884-889.

Bryant, J., Taylor, G., Frehner, M., 1998. Photosynthetic acclimation to elevated CO_2 is modified by source:sink balance in three component species of chalk grassland swards grown in a free air carbon dioxide enrichment (FACE) experiment. Plant, Cell and Environment, 21: 159-168.

Burnham, R.J., 1994. Paleoecological and floristic heterogeneity in the plant fossil record: an analysis based on the Eocene of Washington. United States Geological Survey Bulletin, 2085B: 1-36.

Case, A.L., Curtis, P.S., Snow, A.A., 1998. Heritable variation in stomatal responses to elevated CO_2 in wild radish, *Raphanus raphanistrum* (Brassicaceae). American Journal of Botany, 85: 253-258.

Centritto, M., Maonani, F., Lee, H.S.J., Jarvis, P.G., 1999. Interactive effects of elevated [CO_2] and drought on cherry (*Prunus avium*) seedlings. II. Photosynthetic capacity and water relations. New Phytologist, 141: 141-153.

Cerling, T.E., 1991. Carbon dioxide in the atmosphere: evidence from Cenozoic and Mesozoic paleosols. American Journal of Science, 291: 377-400.

Cerling, T.E., 1992. Use of carbon isotopes in paleosols as an indicator of the P(CO_2) of the paleoatmosphere. Global Biogeochemical Cycles, 6: 307-314.

Cerling, T.E., Harris, J.M., MacFadden, B.J., Leakey, M.G., Quade, J., Eisenmann, V., Ehleringer, J.R., 1997. Global vegetation change through the Miocene/Pliocene boundary. Nature, 389: 153-158.

Ceulemans, R., van Praet, L., Jiang, X.N., 1995. Effects of CO_2 enrichment, leaf position and clone on stomatal index and epidermal cell density in poplar (*Populus*). New Phytologist, 131: 99-107.

Chamberlain, C.J., 1935. Gymnosperms: Structure and Evolution. University of Chicago Press, Chicago.

Chaney, R.W., 1951. A revision of fossil *Sequoia* and *Taxodium* in western North America based on the recent discovery of *Metasequoia*. Transactions of the American Philosophical Society, 40: 171-263.

Chase, C.G., Gregory-Wodzicki, K.M., Parrish, J.T., DeCelles, P.G., 1998. Topographic history of the Western Cordillera of North America and controls on climate. In: Crowley, T.J., Burke, K.C. (Eds.), Tectonic Boundary Conditions for Climate Reconstructions. Oxford Monographs on Geology and Geophysics, 39: 73-99.

Chaw, S.M., Long, H., Wang, B.S., Zharkikh, A., Li, W.H., 1993. The phylogenetic position of Taxaceae based on 18S ribosomal-RNA sequences. Journal of Molecular Evolution, 37: 624-630.

Chaw, S.M., Zharkikh, A., Sung, H.M., Lau, T.C., Li, W.H., 1997. Molecular phylogeny of extant gymnosperms and seed plant evolution: Analysis of nuclear 18S rRNA sequences. Molecular Biology and Evolution, 14: 56-68.

Chen, L.-Q., Cheng-Sen, L., Chaloner, W.G., Beerling, D.J., Sun, Q.-G., Collinson, M.E., Mitchell, P.L., 2001. Assessing the potential for the stomatal characters of extant and fossil *Ginkgo* leaves to signal atmospheric CO_2 change. American Journal of Botany, 88: 1309-1315.

Christensen, T.G., Sproston, T., 1972. Phytoalexin production in *Ginkgo biloba* in relation to inhibition of fungal penetration. Phytopathology, 62: 493-494.

Christophel, D.C., 1976. Fossil floras of the Smoky Tower locality, Alberta, Canada. Palaeontographica, B157: 1-43.

Critchfield, W.B., 1970. Shoot growth and heterophylly in *Ginkgo biloba*. Botanical Gazette, 131: 150-162.

Chu, K.-L., Cooper, W.S., 1950. An ecological reconnaissance in the native home of *Metasequoia glyptostroboides*. Ecology, 31: 260-278.

Cleal, C.J., James, R.M., Zodrow, E.L., 1999. Variation in stomatal density in the Late Carboniferous gymnosperm frond *Neuropteris ovata*. Palaios, 14: 180-185.

Clifford, S.C., Black, C.R., Roberts, J.A., Stronach, I.M., Singleton-Jones, P.R., Mohamed, A.D., Azam-Ali, S.N., 1995. The effect of elevated atmospheric CO_2 and drought on stomatal frequency in groundnut (*Arachis hypogaea* (L.)). Journal of Experimental Botany, 46: 847-852.

Coley, P.D., Bryant, J.P., Chapin, F.S., 1985. Resource availability and plant antiherbivore defense. Science, 230: 895-899.

Cox, J.E., Railsback, L.B., Gordon, E.A., 2001. Evidence from Catskill pedogenic carbonates for a rapid Late Devonian decrease in atmospheric carbon dioxide concentrations. Northeastern Geology and Environmental Sciences, 23: 91-102.

Crane, P.R., 1985. Phylogenetic analysis of seed plants and the origin of angiosperms. Annals of the Missouri Botanical Garden, 72: 716-793.

Crane, P.R., Manchester, S.R. Dilcher, D.L., 1990. A preliminary survey of fossil leaves and well-preserved reproductive structures from the Sentinel Butte Formation (Paleocene) near Almont, North Dakota. Fieldiana (Geology), 20: 1-63.

Critchfield, W.B., 1970. Shoot growth and heterophylly in *Ginkgo biloba*. Botanical Gazette, 131: 150-162.

Crowley, T.J., 2000. Causes of climate change over the past 1000 years. Science, 289: 270-277.

Crowley, T.J., Berner, R.A., 2001. Carbon dioxide and paleoclimate over the Phanerozoic. Science, 292: 870-872.

Curtis, P.S., Wang, X., 1998. A meta-analysis of elevated CO_2 effects on woody plant mass, form, and physiology. Oecologia, 113: 299-313.

DeConto, R.M., Hay, W.W., Thomson, S.L., Bergengren, J., 1999. Late Cretaceous climate and vegetation interactions: Cold continental interior paradox. In: Barrera, E., Johnson, C.C. (Eds.), Evolution of the Cretaceous Ocean-Climate System. Geological Society of America Special Paper, 332: 391-406.

Del Tredici, P., 1989. *Ginkgos* and multituberculates: evolutionary interactions in the Tertiary. BioSystems, 22: 327-339.

Del Tredici, P., 1992. Natural regeneration of *Ginkgo biloba* from downward growing cotyledonary buds (basal chichi). American Journal of Botany, 79: 522-530.

Del Tredici, P., Ling, H., Yang, G., 1992. The *Ginkgos* of Tian Mu Shan. Conservation Biology, 6: 202-209.

DiMichele, W.A., Wing, S.L. (Eds.), 1988. Methods and Applications of Plant Paleoecology. Paleontological Society Special Publication No. 3, Knoxville.

de Queiroz, K., Gauthier, J., 1990. Phylogeny as a central principle in taxonomy: phylogenetic definitions of taxon names. Systematic Zoology, 39: 307-322.

Dickens, G.R., 2001. Modeling the global carbon cycle with a gas hydrate capacitor: Significance for the Latest Paleocene Thermal Maximum. In: Paull, C.K., Dillon, W.P. (Eds.), Natural Gas Hydrates: Occurrence, Distribution, and Detection. Geophysical Monograph Series, 124: 19-38.

Dickens, G.R., O'Neil, J.R., Rea, D.K., Owen, R.M., 1995. Dissociation of oceanic methane hydrate as a cause of the carbon isotope excursion at the end of the Paleocene. Paleoceanography, 10: 965-971.

Dixon, M., Le Thiec, D., Garrec, J.-P., 1995. The growth and gas exchange response of soil-planted Norway spruce [*Picea abies* (L.) Karst.] and red oak (*Quercus rubra* L.) exposed to elevated CO_2 and to naturally occurring drought. New Phytologist, 129: 265-273.

Doyle, J.A., Donoghue, M.J., 1986. Seed plant phylogeny and origin of angiosperms: an experimental cladistic approach. Botanical Review, 52: 321-431.

Doyle, J.A., Donoghue, M.J., 1987. The origin of angiosperms: a cladistic approach. In: Friis, E.M., Chaloner, W.G., Crane, P.R. (Eds.), The Origins of Angiosperms and Their Biological Consequences. Cambridge University Press, Cambridge, pp. 17-49.

Doyle, J.A., Hickey, L.J., 1976. Pollen and leaves from the mid-Cretaceous Potomac Group and their bearing on early angiosperm evolution. In: Beck, C.B. (Ed.), Origin and Early Evolution of Angiosperms. Columbia University Press, New York, pp. 139-206.

Drake, B.G., 1992. A field study of the effects of elevated CO_2 on ecosystem processes in a Chesapeake Bay Wetland. Australian Journal of Botany, 40: 579-595.

Eamus, D., Berryman, C.A., Duff, G.A., 1993. Assimilation, stomatal conductance, specific leaf area and chlorophyll responses to elevated CO_2 of *Maranthes corymbosa*, a tropical monsoon rain forest species. Australian Journal of Plant Physiology, 20: 741-755.

Edwards, D., Kerp, H., Hass, H., 1998. Stomata in early land plants: an anatomical and ecophysiological approach. Journal of Experimental Botany, 49: 255-278.

Ehleringer, J.R., Cerling, T.E., 1995. Atmospheric CO_2 and the ratio of intercellular to ambient CO_2 concentrations in plants. Plant Physiology, 15: 105-111.

Ekart, D.D., Cerling, T.E., Montañez, I.P., Tabor, N.J., 1999. A 400 million year carbon isotope record of pedogenic carbonate: implications for paleoatmospheric carbon dioxide. American Journal of Science, 299: 805-827.

Elick, J.M., Mora, C.I., Driese, S.G., 1999. Elevated atmospheric CO_2 levels and expansion of early vascular land plants: stable isotope evidence from the Battery Point Fm. (Early to Middle Devonian), Gaspé Bay, Canada. GSA Abstracts with Programs, 31: A-159.

Eriksson, O. 1993., Dynamics of genets in clonal plants. Trends in Ecology and Evolution, 8: 313-316.

Eriksson, O., Bremer, B., 1992. Pollination systems, dispersal modes, life forms, and diversification rates in angiosperm families. Evolution, 46: 258-266.

Estiarte, M., Peñuelas, J., Kimball, B.A., Idso, S.B., LaMorte, R.L., Pinter, P.J., Wall, G.W., Garcia, R.L., 1994. Elevated CO_2 effects on stomatal density of wheat and sour orange trees. Journal of Experimental Botany, 45: 1665-1668.

Everitt, B.L., 1968. Use of cottonwood in an investigation of the recent history of a flood plain. American Journal of Science, 266: 417-439.

Everson, D.A., Boucher, D.H., 1998. Tree species-richness and topographic complexity along the riparian edge of the Potomac River. Forest Ecology and Management, 109: 305-314.

Falcon-Lang, H.J., Cantrill, D.J. Nichols, G.J., 2001. Biodiversity and terrestrial ecology of a mid-Cretaceous, high-latitude floodplain, Alexander Island, Antarctica. Journal of the Geological Society, London, 158: 709-724.

Falder, A.B., Stockey, R.A., Rothwell, G.W., 1999. In situ fossil seedlings of a *Metasequoia*-like taxodiaceous conifer from Paleocene river floodplain deposits of central Alberta, Canada. American Journal of Botany, 86: 900-902.

Farnsworth, E.J., Ellison, A.M., Gong, W.K., 1996. Elevated CO_2 alters anatomy, physiology, growth, and reproduction of red mangrove (*Rhizophora mangle* L.). Oecologia, 108: 599-609.

Farquhar, G.D., von Caemmerer, S., Berry, J.A., 1980. A biochemical model of photosynthetic CO_2 assimilation in leaves of C_3 species. Planta, 149: 78-90.

Fernández, M.D., Pieters, A., Donoso, C., Tezara, W., Azkue, M., Herrera, C., Rengifo, E., Herrera, A., 1998. Effects of a natural source of very high CO_2 concentration on the leaf gas exchange, xylem water potential and stomatal characteristics of plants of *Spatiphylum cannifolium* and *Bauhinia multinervia*. New Phytologist, 138: 689-697.

Ferris, R., Taylor, G., 1994. Stomatal characteristics of four native herbs following exposure to elevated CO_2. Annals of Botany, 73: 447-453.

Ferris, R., Nijs, I., Behaeghe, T., Impens, I., 1996. Elevated CO_2 and temperature have different effects on leaf anatomy of perennial ryegrass in spring and summer. Annals of Botany, 78: 489-497.

Fox, R.C., 1990. The succession of Paleocene mammals in western Canada. In: Bown, T.M., Rose, K.D. (Eds.), Dawn of the Age of Mammals in the Northern Part of the

Rocky Mountain Interior, North America. Geological Society of America Special Publication, 243: 51-70.

Franklin, A.H., 1959. *Ginkgo biloba* L: Historical summary and bibliography. The Virginia Journal of Science, 10: 131-176.

Freeman, K.H., Hayes, J.M., 1992. Fractionation of carbon isotopes by phytoplankton and estimates of ancient CO_2 levels. Global Biogeochemical Cycles, 6: 185-198.

Frey, B., Scheidegger, C., Günthardt-Goerg, M.S., Matyssek, R., 1996. The effects of ozone and nutrient supply on stomatal response in birch (*Betula pendula*) leaves as determined by digital image-analysis and X-ray microanalysis. New Phytologist, 132: 135-143.

Friedli, H., Lötscher, H., Oeschger, H., Siegenthaler, U., Stauffer, B., 1986. Ice core record of the $^{13}C/^{12}C$ ratio of atmospheric CO_2 in the past two centuries. Nature, 324: 237-238.

Frye, C.I., 1969. Stratigraphy of the Hell Creek Formation in North Dakota. North Dakota Geological Survey Bulletin, 54: 1-65.

Fujii, K., 1895. On the nature and origin of so-called "chichi" (nipple) of *Ginkgo biloba* L. Botanical Magazine (Tokyo), 9: 444-450.

Furukawa, A., 1997. Stomatal frequency of *Quercus myrsinaefolia* grown under different irradiances. Photosynthetica, 34: 195-199.

Gastaldo, R.A., Bearce, S.C., Degges, C.W., Hunt, R.J., Peebles, M.W., Violette, D.L., 1989. Biostratinomy of a Holocene oxbow lake: a backswamp to mid-channel transect. Review of Palaeobotany and Palynology, 58: 47-59 .

Gaudillère, J.P., Mousseau, M., 1989. Short term effect of CO_2 on leaf development and gas exchange of young poplars (*Populus euramericana* cv. I 214). Oecologia Plantarum, 10: 95-105.

Gay, A.P., Hauck, B., 1994. Acclimation of *Lolium temulentum* to enhanced carbon dioxide concentration. Journal of Experimental Botany, 45: 1133-1141.

Gay, A.P., Hurd, R.G., 1975. The influence of light on stomatal density in the tomato. New Phytologist, 75: 37-46.

Ghosh, P., Bhattacharya, S.K., Jani, R.A., 1995. Palaeoclimate and palaeovegetation in central India during the Upper Cretaceous based on stable isotope composition of the palaeosol carbonates. Palaeogeography, Palaeoclimatology, Palaeoecology, 114: 285-296.

Ghosh, P., Ghosh, P., Bhattacharya, S.K., 2001. CO_2 levels in the Late Palaeozoic and Mesozoic atmosphere from soil carbonate and organic matter, Satpura basin, Central India. Palaeogeography, Palaeoclimatology, Palaeoecology, 170: 219-236.

Gifford, E.M., Foster, A.S., 1989. Morphology and Evolution of Vascular Plants. W.H. Freeman, New York.

Gingerich, P.D., 2000. Paleocene/Eocene boundary and continental vertebrate faunas of Europe and North America. GFF, 122: 57-59.

Goodfellow, J., Eamus, D., Duff, G., 1997. Diurnal and seasonal changes in the impact on CO_2 enrichment on assimilation, stomatal conductance and growth in a long-term study of *Mangifera indica* in the wet-dry tropics of Australia. Tree Physiology, 17: 291-299.

Gray, J.E., Holroyd, G.H., van der Lee, F.M., Bahrami, A.R., Sijmons, P.C., Woodward, F.I., Schuch, W., Hetherington, A.M., 2000. The *HIC* signalling pathway links CO_2 perception to stomatal development. Nature, 408: 713-716.

Greenwood, D.R., Wing, S.L., 1995. Eocene continental climates and latitudinal temperature gradients. Geology, 23: 1044-1048.

Grime, J.P., 2001. Plant Strategies, Vegetation Processes, and Ecosystem Properties (2nd edition). John Wiley, Chichester.

Handa, M., Iizuka, Y., Fujiwara, N., 1997. *Ginkgo* landscapes. In: Hori, T., Ridge, R.W., Tulecke, W., Del Tredici, P., Trémouillaux-Guiller, J., Tobe, H. (Eds.), *Ginkgo biloba*—A Global Treasure. Springer, Tokyo, pp. 259-283.

Harper, J.L., Lovell, P.H., Moore, K.G., 1970. The shapes and sizes of seeds. Annual Review of Ecology and Systematics, 1: 327-356.

Harries, J.E., Brindley, H.E., Sagoo, P.J., Bantges, R.J., 2001. Increases in greenhouse forcing inferred from the outgoing longwave radiation spectra of the Earth in 1970 and 1997. Nature, 410: 355-357.

Hasebe, M., 1997. Molecular phylogeny of *Ginkgo biloba*: Close relationships between *Ginkgo biloba* and cycads. In: Hori, T., Ridge, R.W., Tulecke, W., Del Tredici, P., Trémouillaux-Guiller, J., Tobe, H. (Eds.), *Ginkgo biloba*—A Global Treasure. Springer, Tokyo, pp. 173-181.

He, S.-A., Yin, G., Pang, Z.-J., 1997. Resources and prospects of *Ginkgo biloba* in China. In: Hori, T., Ridge, R.W., Tulecke, W., Del Tredici, P., Trémouillaux-Guiller, J., Tobe, H. (Eds.), *Ginkgo biloba*—A Global Treasure. Springer, Tokyo, pp. 373-383.

Heckenberger, U., Roggatz, U., Schurr, U., 1998. Effect of drought stress on the cytological status in *Ricinus communis*. Journal of Experimental Botany, 49: 181-189.

Hickey, L.J., 1977. Stratigraphy and paleobotany of the Golden Valley Formation (early Tertiary) of western North Dakota. Geological Society of America Memoir, 150: 1-181.

Hickey, L.J., 1980. Paleocene stratigraphy and flora of the Clark's Fork Basin. In: Gingerich, P.D. (Ed.), Early Cenozoic Paleontology and Stratigraphy of the Bighorn Basin, Wyoming. University of Michigan Papers on Paleontology, 24: 33-49.

Hickey, L.J., 1996. A new proposal for seed plant phylogeny. Abstract Volume of the Fifth Quadrenniial Conference of the International Organization of Palaeobotany, Santa Barbara, California, June 30th - July 5th, 1996, p. 43.

Hickey, L.J., Doyle, J.A., 1977. Early Cretaceous evidence for angiosperm evolution. Botanical Review, 42: 3-105.

Hicks, J.F., Johnson, K.R. Tauxe, L., Clark, D., Obradovich, J.D., 2002. Magnetostratigraphy and geochronology of the Hell Creek and basal Fort Union Formations of southwestern North Dakota and a recalibration of the Cretaceous-Tertiary boundary. In: Hartman, J., Johnson, K.R., Nichols, D.J. (Eds.), The Hell Creek Formation and the Cretaceous-Tertiary Boundary in the Northern Great Plains: An Integrated Continental Record of the End of the Cretaceous. Geological Society of American Special Paper, 348, in press.

Hoffman, G.L., Stockey, R.A., 1999. Geological setting and paleobotany of the Joffre Bridge roadcut fossil locality (Late Paleocene), Red Deer Valley, Alberta. Canadian Journal of Earth Science, 36: 2073-2084.

Honda, H. 1997. *Ginkgo* and insects. In: Hori, T., Ridge, R.W., Tulecke, W., Del Tredici, P., Trémouillaux-Guiller, J., Tobe, H. (Eds.), *Ginkgo biloba*—A Global Treasure. Springer, Tokyo, pp. 243-250.

Houghton, J.T., Meira Filho, L.G., Callander, B.A., Harris, N., Kattenberg, A., Maskell, K., 1995. Climate Change. The IPCC Scientific Assessment. Cambridge University Press, Cambridge.

Huber, M., Sloan, L.C., 1999. Warm climate transitions: A general circulation modeling study of the Late Paleocene Thermal Maximum (~56 Ma). Journal of Geophysical Research, 104: 16633-16655.

Huggins, L.M., 1985. Cuticular analyses and preliminary comparisons of some Miocene conifers from Clarkia, Idaho. In: Smiley, C.J. (Ed.), Late Cenozoic history of the Pacific Northwest. American Association for the Advancement of Science, San Francisco, pp. 113-138.

Hughes, N.F., 1976. Palaeobotany of Angiosperm Origins: Problems of Mesozoic Seed-plant Evolution. Cambridge University Press, Cambridge.

Hutchison, J.H., 1982. Turtle, crocodilian, and champsosaur diversity changes in the Cenozoic of the north-central region of western United States. Palaeogeography, Palaeoclimatology, Palaeoecology, 37: 149-164.

Indermühle, A., Stocker, T.F., Joos, F., Fischer, H., Smith, H.J., Wahlen, M., Deck, B., Mastroianni, D., Tschumi, J., Blunier, T., Meyer, R., Stauffer, B., 1999. Holocene carbon-cycle dynamics based on CO_2 trapped in ice at Taylor Dome, Antarctica. Nature, 398: 121-126.

Ishizuka, M., Sugawara, S., 1989. Composition and structure of natural mixed forests in central Hokkaido (II) Effect of disturbances on the forest vegetation patterns along the topographic moisture gradients. Journal of the Japanese Forestry Society, 71: 89-98.

Jiang, M.Y., Jin, Y., Zhang, Q., 1990. A preliminary study on *Ginkgo biloba* in Dahongshan region, Hubei. Journal of Wuhan Botanical Research, 8: 191-193 (in Chinese).

Johnson, K.R., 2002. Overview of the Cretaceous-Tertiary (K/T) megaflora of the Hell Creek and lower Fort Union Formations in southwestern North Dakota and northwestern South Dakota: Biostratigraphy and paleoecology of the end-Cretaceous terrestrial vegetation. In: Hartman, J., Johnson, K.R., Nichols, D.J. (Eds.), The Hell Creek Formation and the Cretaceous-Tertiary Boundary in the Northern Great Plains: An Integrated Continental Record of the End of the Cretaceous. Geological Society of American Special Paper, 348, in press.

Jones, M.B., Brown, J.C., Raschi, A., Miglietta, F., 1995. The effects on *Arbutus unedo* L. of long-term exposure to elevated CO_2. Global Change Biology, 1: 295-302.

Kalkreuth, W.D., Riediger, C.L., McIntyre, D.J., Richardson, R.J.H., Fowler, M.G., Marchioni, D., 1996. Petrological, palynological and geochemical characteristics of Eureka Sound Group coals (Stenkul Fiord, southern Ellesmere Island, Arctic Canada). International Journal of Coal Geology, 30: 151-182.

Katz, M.E., Pak, D.K., Dickens, G.R., Miller, K.G., 1999. The source and fate of massive carbon input during the latest Paleocene thermal maximum. Science, 286: 1531-1533.

Keeling, C.D., Whorf, T.P., Wahlen, M., van der Plicht, J., 1995. Interannual extremes in the rate of atmospheric carbon dioxide since 1980. Nature, 375: 666-670. [see http://www.cmdl.noaa.gov/ccg/figures/co2mm_mlo.gif for update].

Kelly, D.W., Hicklenton, P.R., Reekie, E.G., 1991. Photosynthetic response of geranium to elevated CO_2 as affected by leaf age and time of CO_2 exposure. Canadian Journal of Botany, 69: 2482-2488.

Kennett, J.P., Stott, L.D., 1991. Abrupt deep-sea warming, palaeoceanographic changes and benthic extinctions at the end of the Palaeocene. Nature, 353: 225-229.

Kim, Y.S., Lee, J.K., 1990. Chemical and structural characteristics of conifer needles exposed to ambient air pollution. European Journal of Forest Pathology, 20: 193-200.

Kim, Y.S., Lee, J.K., Chung, G.C., 1997. Tolerance and susceptibility of *Ginkgo* to air pollution. In: Hori, T., Ridge, R.W., Tulecke, W., Del Tredici, P., Trémouillaux-Guiller, J., Tobe, H. (Eds.), *Ginkgo biloba*—A Global Treasure. Springer, Tokyo, pp. 233-242.

King, D.C., 1998. Interpretation of stable isotope compositions of pedogenic carbonate in Late Silurian to Late Devonian paleosols, Appalachian basin. Unpublished ms Thesis. University of Tennessee, Knoxville, 123 p.

Knapp, A.K., Cocke, M., Hamerlynck, E.P., Owensby, C.E., 1994. Effect of elevated CO_2 on stomatal density and distribution in a C_4 grass and a C_4 forb under field conditions. Annals of Botany, 74: 595-599.

Koch, P.L., Zachos, J.C., Gingerich, P.D., 1992. Correlation between isotope records in marine and continental carbon reservoirs near the Palaeocene/Eocene boundary. Nature, 358: 319-322.

Körner, Ch., 1988. Does global increase of CO_2 alter stomatal density? Flora, 181: 253-257.

Körner, Ch., Cochrane, P.M., 1985. Stomatal responses and water relations of *Eucalyptus pauciflora* in summer along an elevational gradient. Oecologia, 66: 443-455.

Körner, Ch., Bannister, P., Mark, A.F., 1986. Altitudinal variation in stomatal conductance, nitrogen content and leaf anatomy in different plant life forms in New Zealand. Oecologia, 69: 577-588.

Kothavala, Z., Oglesby, R.J., Saltzman, B., 1999. Sensitivity of equilibrium surface temperature of CCM3 to systematic changes in atmospheric CO_2. Geophysical Research Letters, 26: 209-212.

Kovar-Eder, J., Givulsecu, R., Hably, L., Kvaček, Z., Mihajlovic, D., Teslenko, J., Walther, H., Zastawniak, E., 1994. Floristic changes in the areas surrounding the Paratethys during Neogene time. In: Boulter, M.C., Fisher, H.C. (Eds.), Cenozoic Plants and Climates of the Arctic. Springer, Berlin, pp. 347-369.

Kump, L.R., Arthur, M.A., Patzkowsky, M.E., Gibbs, M.T., Pinkus, D.S., Sheehan, P.M., 1999. A weathering hypothesis for glaciation at high atmospheric pCO_2 during the Late Ordovician. Palaeogeography, Palaeoclimatology, Palaeoecology, 152: 173-187.

Kürschner, W.M., 1996. Leaf stomata as biosensors of paleoatmospheric CO_2 levels. LPP Contributions Series, 5: 1-153.

Kürschner, W.M., 1997. The anatomical diversity of recent and fossil leaves of the durmast oak (*Quercus petraea* Lieblein/*Q. pseudocastanea* Goeppert)--implications for their use as biosensors of palaeoatmospheric CO_2 levels. Review of Palaeobotany and Palynology, 96: 1-30.

Kürschner, W.M., van der Burgh, J., Visscher, H., Dilcher, D.L., 1996. Oak leaves as biosensors of late Neogene and early Pleistocene paleoatmospheric CO_2 concentrations. Marine Micropaleontology, 27: 299-312.

Kürschner, W.M., Wagner, F., Visscher, E.H., Visscher, H., 1997. Predicting the response of leaf stomatal frequency to a future CO_2-enriched atmosphere: constraints from historical observations. Geologische Rundschau, 86: 512-517.

Kürschner, W.M., Stulen, I., Wagner, F., Kuiper, P.J.C., 1998. Comparison of palaeobotanical observations with experimental data on the leaf anatomy of durmast oak [*Quercus petraea* (Fagaceae)] in response to environmental change. Annals of Botany, 81: 657-664.

Kürschner, W.M., Wagner, F., Dilcher, D.L, Visscher, H., 2001. Using fossil leaves for the reconstruction of Cenozoic paleoatmospheric CO_2 concentrations. In: Gerhard, L.C., Harrison, W.E., Hanson, B.M. (Eds.), Geological Perspectives of Global Climate Change. AAPG Studies in Geology 47, pp. 169-189.

Kvaček, Z., Manum, S.B., Boulter, M.C., 1994. Angiosperms from the Palaeogene of Spitsbergen, including an unfinished work by A. G. Nathorst. Palaeontographica, B232: 103-128.

Kwon, M., Ahn, Y.-J., Yoo, J.-K., Choi, B.-R., 1996. Potent insecticidal activity of extracts from *Ginkgo biloba* leaves against *Nilaparvata lugens* (Homoptera: Delphacidae). Applied Entomology and Zoology, 31: 162-166.

Lake, J.A., Quick, W.P., Beerling, D.J., Woodward, F.I., 2001. Signals from mature to new leaves. Nature, 411: 154.

Lambers, H., Chapin, F.S., Pons, T.L., 1998. Plant Physiological Ecology. Springer-Verlag, New York.

Lauber, W., Körner, Ch., 1997. *In situ* stomatal responses to long-term CO_2 enrichment in calcareous grassland plants. Acta Œcologica, 18: 221-229.

Lear, C.H., Elderfield, H., Wilson, P.A., 2000. Cenozoic deep-sea temperatures and global ice volumes from Mg/Ca in benthic foraminiferal calcite. Science, 287: 269-272.

Lee, Y.I., 1999. Stable isotopic composition of calcic paleosols of the Early Cretaceous Hasandong Formation, southeastern Korea. Palaeogeography, Palaeoclimatology, Palaeoecology, 150: 123-133.

Lee, Y.I., Hisada, K., 1999. Stable isotopic composition of pedogenic carbonates of the Early Cretaceous Shimonoseki Subgroup, western Honshu, Japan. Palaeogeography, Palaeoclimatology, Palaeoecology, 153: 127-138.

Lemarchand, D., Gaillardet, J., Lewin, É., Allègre, C.J., 2000. The influence of rivers on marine boron isotopes and implications for reconstructing past ocean pH. Nature, 408: 951-954.

Levitus, S., Antonov, J.I., Wang, J., Delworth, T.L., Dixon, K.W., Broccoli, A.J., 2001. Anthropogenic warming of Earth's climate system. Science, 292: 267-270.

Li, H.-L., 1956. A horticultural and botanical history of *Ginkgo*. Morris Arboretum Bulletin, 7: 3-12.

Ligard, S., Crane, P.R., 1990. Angiosperm diversification and Cretaceous floristic trends: a comparison of palynofloras and leaf macrofloras. Paleobiology, 16: 77-93.

Liu, Y.-J., Li, C.-S., Wang, Y.-F., 1999. Studies on fossil *Metasequoia* from north-east China and their taxonomic implications. Botanical Journal of the Linnean Society, 130: 267-297.

Long, S.P., Osborne, C.P., Humphries, S.W., 1996. Photosynthesis, rising atmospheric carbon dioxide concentration and climate change. In: Breymeyer, A.I., Hall, D.O., Melillo, J.M., Ågren, G.I. (Eds.), Global Change: Effects on Coniferous Forests and Grasslands. John Wiley & Sons, New York, pp. 121-159.

Lupia, R., Lidgard, S., Crane, P.R., 1999. Comparing palynological abundance and diversity: implications for biotic replacement during the Cretaceous angiosperm radiation. Paleobiology, 25: 305-340.

Madsen, E., 1973. Effect of CO_2-concentration on the morphological, histological and cytological changes in tomato plants. Acta Agriculturæ Scandinavica, 23: 241-246.

Mai, D.H., 1994. Two conifers—*Tetraclinis* Mast. (Cupressaceae) and *Metasequoia* Miki (Taxodiaceae)—relicts or palaeoclimatic indicators of the past. In: Boulter, M.C., Fisher, H.C. (Eds.), Cenozoic Plants and Climates of the Arctic. Springer-Verlag, Berlin, pp. 199-214.

Major, R.T., 1967. The *Ginkgo*, the most ancient living tree. Science, 157: 1270-1273.

Major, R.T., Marchini, P., Sproston, T., 1960. Isolation from *Ginkgo biloba* L. of an inhibitor of fungus growth. The Journal of Biological Chemistry, 235: 3298-3299.

Malone, S.R., Mayeux, H.S., Johnson, H.B., Polley, H.W., 1993. Stomatal density and aperture length in four plant species grown across a subambient CO_2 gradient. American Journal of Botany, 80: 1413-1418.

Mann, M.E., Bradley, R.S., Hughes, M.K., 1998. Global-scale temperature patterns and climate forcing over the past six centuries. Nature, 392: 779-787.

Mann, M.E., Bradley, R.S., Hughes, M.K., 1999. Northern hemisphere temperatures during the past millennium: inferences, uncertainties, and limitations. Geophysical Research Letters, 26: 759-762.

Manum, S., 1963. Notes on the Cretaceous-Tertiary boundary in Basilikaen, Vestspitsbergen, and a new record of *Ginkgo* from the Spitsbergen Tertiary. Norsk Polarinstitutt-Årbok 1962: 149-152.

Manum, S., 1966. *Ginkgo spitsbergensis* n. sp. from the Paleocene of Spitsbergen and a discussion of certain Tertiary species of *Ginkgo* from Europe and North America. Norsk Polarinstitutt-Årbok 1965: 49-58.

Markwick, P.J., 1994. "Equability," continentality, and Tertiary "climate": the crocodilian perspective. Geology, 22: 613-616.

Markwick, P.J., 1998. Fossil crocodilians as indicators of Late Cretaceous and Cenozoic climates: implications for using palaeontological data in reconstructing palaeoclimate. Palaeogeography, Palaeoclimatology, Palaeoecology, 137: 205-271.

Masterson, J., 1994. Stomatal size in fossil plants: evidence for polyploidy in majority of angiosperms. Science, 264: 421-424.

Mastrogiuseppe, J.D., Cridland, A.A., Bogyo, T.P., 1970. Multivariate comparison of fossil and Recent *Ginkgo* wood. Lethaia, 3: 271-277.

Mazzanti, G., Mascellino, M.T., Battinelli, L., Coluccia, D., Manganaro, M., Saso, L., 2000. Antimicrobial investigation of semipurified fractions of *Ginkgo biloba* leaves. Journal of Ethnopharmacology, 71: 83-88.

McClain, W.E., Jenkins, M.A., Jenkins, S.E., Ebinger, J.E., 1993. Changes in the woody vegetation of a bur oak savanna remnant in central Illinois. Natural Areas Journal, 13: 108-114.

McElwain, J.C., 1998. Do fossil plants signal palaeoatmospheric CO_2 concentration in the geological past? Philosophical Transactions of the Royal Society London, B353: 83-96.

McElwain, J.C., Chaloner, W.G., 1995. Stomatal density and index of fossil plants track atmospheric carbon dioxide in the Palaeozoic. Annals of Botany, 76: 389-395.

McElwain, J.C., Chaloner, W.G., 1996. The fossil cuticle as a skeletal record of environmental change. Palaios, 11: 376-388.

McElwain, J., Mitchell, F.J.G., Jones, M.B., 1995. Relationship of stomatal density and index of *Salix cinerea* to atmospheric carbon dioxide concentrations in the Holocene. The Holocene, 5: 216-219.

McElwain, J.C., Beerling, D.J., Woodward, F.I., 1999. Fossil plants and global warming at the Triassic-Jurassic boundary. Science, 285: 1386-1390.

Meyen, S.V., 1984. Basic features of gymnosperm systematics and phylogeny as evidenced by the fossil record. Botanical Review, 50: 1-111.

Meyen, S.V., 1987. Fundamentals of Palaeobotany. Chapman and Hall, London.

Miall, A.D., 1992. Alluvial deposits. In: Walker, R.G., James, N.P. (Eds.), Facies models: response to sea level change. Geological Association of Canada, St. John's, pp. 119-142.

Miglietta, F., Raschi, A., 1993. Studying the effect of elevated CO_2 in the open in a naturally enriched environment in central Italy. Vegetatio, 104/105: 391-400.

Miller, C.N., 1977. Mesozoic conifers. Botanical Review, 43: 217-280.

Minnocci, A., Panicucci, A., Sebastiani, L., Lorenzini, G., Vitagliano, C., 1999. Physiological and morphological responses of olive plants to ozone exposure during a growing season. Tree Physiology, 19: 391-397.

Mishra, M.K., 1997. Stomatal characteristics at different ploidy levels in *Coffea* L. Annals of Botany, 80: 689-692.

Mitchell, J.F.B., Karoly, D.J., Hegerl, G.C., Zwiers, F.W., Allen, M.R., Marengo, J., 2001. Detection of climate change and attribution of causes. In: Houghton, J.T., Ding, Y., Griggs, D.J., Noguer, M., van der Linden, P.J., Xiaosu, D., Maskell, K., Johnson, C.A. (Eds.), Climate Change 2001: The Scientific Basis. Contribution of Working Group I to the Third Assessment Report of the Intergovernmental Panel on Climate Change. Cambridge University Press, Cambridge, 881 pp.

Momohara, A., 1994. Paleoecology and Paleobiogeography of *Metasequoia*. Fossils, 57: 24-30 (in Japanese).

Montañez, I.P., Tabor, N.J., Ekart, D., Collister, J.W., 1999. Evolution of Permian atmospheric pCO_2 as derived from latest Carboniferous through Permian paleosol carbonates, Midland and Paradox Basins, U.S.A. and northern Italian Alps. GSA Abstracts with Programs, 31: A-326.

Mora, C.I., Driese, S.G., Seager, P.G., 1991. Carbon dioxide in the Paleozoic atmosphere: evidence from carbon-isotope compositions of pedogenic carbonate. Geology, 19: 1017-1020.

Mora, C.I., Driese, S.G., Colarusso, L.A., 1996. Middle and Late Paleozoic atmospheric CO_2 levels from soil carbonate and organic matter. Science, 271: 1105-1107.

Mösle, B., Collinson, M.E., Finch, P., Stankiewicz, A., Scott, A.C., Wilson, R., 1998. Factors influencing the preservation of plant cuticles: A comparison of morphology and chemical composition of modern and fossil examples. Organic Geochemistry, 29: 1369-1380.

Muchez, P., Peeters, C., Keppens, E., Viaene, W.A., 1993. Stable isotopic composition of paleosols in the Lower Visan of eastern Belgium: evidence of evaporation and soil-gas CO_2. Chemical Geology, 106: 389-396.

Murphy, E.C., Hoganson, J.W., Johnson, K.R., Hartman, J.H., 1999. Lithostratigraphy of the Hell Creek Formation in North Dakota. Geological Society of America Abstracts with Programs, 31 (7): A70-71.

Neftel, A., Moor, E., Oeschger, H., Stauffer, B., 1985. Evidence from polar ice cores for the increase in atmospheric CO_2 in the past two centuries. Nature, 315: 45-47.

Norris, R.D., Röhl, U., 1999. Carbon cycling and chronology of climate warming during the Palaeocene/Eocene transition. Nature, 401: 775-778.

Oberbauer, S.F., Strain, B.R., 1986. Effects of canopy position and irradiance on the leaf physiology and morphology of *Pentaclethra macroloba* (Mimosaceae). American Journal of Botany, 73: 409-416.

Oberbauer, S.F., Strain, B.R., Fetcher, N., 1985. Effect of CO_2-enrichment on seedling physiology and growth of two tropical tree species. Physiologia Plantarum, 65: 352-356.

O'Connell, S., Chandler, M.A., Ruedy, R., 1996. Implications for the creation of warm saline deep water: Late Paleocene reconstructions and global climate model simulations. Geological Society of America Bulletin, 108: 270-284.

O'Leary, J.W., Knecht, G.N., 1981. Elevated CO_2 concentration increases stomate numbers in *Phaseolus vulgaris* leaves. Botanical Gazette, 142: 438-441.

Otto-Bliesner, B.L., Upchurch, G.R., 1997. Vegetation-induced warming of high-latitude regions during the Late Cretaceous period. Nature, 385: 804-807.

Pääkkönen, E., Vahala, J., Pohjola, M., Holopainen, T., Kärenlampi, L., 1998. Physiological, stomatal and ultrastructural ozone responses in birch (*Betula pendula* Roth.) are modified by water stress. Plant, Cell and Environment, 21:671-684.

Pagani, M., Arthur, M.A., Freeman, K.H., 1999a. Miocene evolution of atmospheric carbon dioxide. Paleoceanography, 14: 273-292.

Pagani, M., Freeman, K.H., Arthur, M.A., 1999b. Late Miocene atmospheric CO_2 concentrations and the expansion of C_4 grasses. Science, 285: 876-879.

Page, C.N., 1990. Cephalotaxaceae. In: Kramer, K.U., Green, P.S. (Eds.), The Families and Genera of Vascular Plants; vol. I: Pteridophytes and Gymnosperms. Springer, Berlin, pp. 299-302.

Pant, D.D., 1977. Early conifers and conifer allies. Journal of the Indian Botanical Society, 56: 23-37.

Paoletti, E., Gellini, R., 1993. Stomatal density variation in beech and holm oak leaves collected over the last 200 years. Acta Œcologica, 14: 173-178.

Paoletti, E., Miglietta, F., Raschi, A., Manes, F., Grossoni, P., 1997. Stomatal numbers in holm oak (*Quercus ilex* L.) leaves grown in naturally and artificially CO_2-enriched environments. In: Raschi, A., Miglietta, F., Tognetti, R., van Gardingen, P.R. (Eds.), Plant Responses to Elevated CO_2. Cambridge University Press, Cambridge, pp. 197-208.

Paoletti, E., Nourrison, G., Garrec, J.P., Raschi, A., 1998. Modifications of the leaf surface structures of *Quercus ilex* L. in open, naturally CO_2-enriched environments. Plant, Cell and Environment, 21: 1071-1075.

Pearson, M., Davies, W.J., Mansfield, T.A., 1995. Asymmetric responses of adaxial and abaxial stomata to elevated CO_2: impacts on the control of gas exchange by leaves. Plant, Cell and Environment, 18: 837-843.

Pearson, P.N., Palmer, M.R., 1999. Middle Eocene seawater pH and atmospheric carbon dioxide concentrations. Science, 284: 1824-1826.

Pearson, P.N., Palmer, M.R., 2000. Atmospheric carbon dioxide concentrations over the past 60 million years. Nature, 406: 695-699.

Pelzer, G., Riegel, W., Wilde, V., 1992. Depositional controls on the Lower Cretaceous Wealden coals of Northwest Germany. In: Parrish, J.T., McCabe, P.J. (Eds.), Controls on the Distribution and Quality of Cretaceous Coals. Geological Society of America Special Paper, 267: 227-244.

Peñuelas, J., Matamala, R., 1990. Changes in N and S leaf content, stomatal density and specific leaf area in 14 plant species during the last three centuries. Journal of Experimental Botany, 41: 1119-1124.

Petit, J.R., Jouzel, J., Raynaud, D., Barkov, N.I., Barnola, J.-M., Basile, I., Bender, M., Chappellaz, J., Davis, M., Delaygue, G., Delmotte, M., Kotlyakov, V.M., Legrand, M., Lipenkov, V.Y., Lorius, C., Pépin, L., Ritz, C., Saltzman, E., Stievenard, M., 1999. Climate and atmospheric history of the past 420,000 years from the Vostok ice core, Antarctica. Nature, 399: 429-436.

Pickett, S.T.A., White, P.S. (Eds.), 1985. The Ecology of Natural Disturbance and Patch Dynamics. Academic Press, Orlando.

Platt, N.H., 1989. Lacustrine carbonates and pedogenesis: sedimentology and origin of palustrine deposits from the Early Cretaceous Rupelo Formation, W. Cameros Basin, N. Spain. Sedimentology, 36: 665-684.

Polley, H.W., Johnson, H.B., Mayeux, H.S., 1992. Growth and gas exchange of oats (*Avena sativa*) and wild mustard (*Brassica kaber*) at subambient CO_2 concentrations. International Journal of Plant Science, 153: 453-461.

Polley, H.W., Johnson, H.B., Marino, B.D., Mayeux, H.S., 1993. Increase in C_3 plant water-use efficiency and biomass over Glacial to present CO_2 concentrations. Nature, 361: 61-64.

Poole, I., Weyers, J.D.B., Lawson, T., Raven, J.A., 1996. Variations in stomatal density and index: implications for palaeoclimatic reconstructions. Plant, Cell and Environment, 19: 705-712.

Popp, B.N., Anderson, T.F., Sandberg, P.A., 1986. Brachiopods as indicators of original isotopic composition in some Paleozoic limestones. Bulletin of the Geological Society of America, 97: 1262-1269.

Pritchard, S.G., Mosjidis, C., Peterson, C.M., Runion, G.B., Rogers, H.H., 1998. Anatomical and morphological alterations in longleaf pine needles resulting from growth in elevated CO_2: interactions with soil resource availability. International Journal of Plant Sciences, 159: 1002-1009.

Radoglou, K.M., Jarvis, P.G., 1990. Effects of CO_2 enrichment on four poplar clones. II. Leaf structure properties. Annals of Botany, 65: 627-632.

Radoglou, K.M., Jarvis, P.G., 1992. The effects of CO_2 enrichment and nutrient supply on growth, morphology and anatomy of *Phaseolus vulgaris* L. seedlings. Annals of Botany, 70: 245-256.

Radoglou, K.M., Jarvis, P.G., 1993. Effects of atmospheric CO_2 enrichment on early growth of *Vivia faba*, a plant with large cotyledons. Plant, Cell and Environment, 16: 93-98.

Rahim, M.A., Fordham, R., 1991. Effect of shade on leaf and cell size and number of epidermal cells in garlic (*Allium sativum*). Annals of Botany, 67: 167-171.

Ranasinghe, S., Taylor, G., 1996. Mechanism for increased leaf growth in elevated CO_2. Journal of Experimental Botany, 47: 349-358.

Raubeson, L.A, Jansen, R.K., 1992. Chloroplast DNA evidence on the ancient evolutionary split in vascular land plants. Science, 255: 1697-1699.

Raven, J.A., Ramsden, H.J., 1988. Similarity of stomatal index in the C_4 plant *Salsola kali* L. in material collected in 1843 and 1987: relevance to changes in atmospheric CO_2 content. Transaction of the Botanical Society of Edinburgh, 45: 223-233.

Raynolds, R.G.H., Johnson, K.R., Arnold, L.R., Farnham, T.M., Fleming, R.F., Hicks, J.F., Kelley, S.A., Lapey, L.A., Nichols, D.J., Obradovich, J.D., Wilson, M.D., 2001. The Kiowa core, a continuous drill core through the Denver Basin bedrock aquifers at Kiowa, Elbert County, Colorado. U.S. Geological Survey Open-File Report 01-185, Boulder. [http://geology.cr.usgs.gov/pub/open-file-reports/ofr-01-0185/].

Reddy, K.R., Robana, R.R., Hodges, H.F., Liu, X.J., McKinion, J.M., 1998. Interactions of CO_2 enrichment and temperature on cotton growth and leaf characteristics. Environmental and Experimental Botany, 39: 117-129.

Reidel, S.P., Fecht, K.R., 1986. The Huntziger flow: evidence of surface mixing of the Columbia River Basalt and its petrogenetic implications. Geological Society of America Bulletin, 98: 664-677.

Retallack, G.J., 1997. Early forest soils and their role in Devonian global change. Science, 276: 583-585.

Retallack, G.J., 2001. A 300-million-year record of atmospheric carbon dioxide from fossil plant cuticles. Nature, 411: 287-290.

Robinson, J.M., 1994. Speculations on carbon dioxide starvation, Late Tertiary evolution of stomatal regulation and floristic modernization. Plant, Cell and Environment, 17: 345-354.

Rothwell, G.W., Serbet, R., 1994. Lignophyte phylogeny and the evolution of spermatophytes—a numerical cladistic-analysis. Systematic Botany, 19: 443-482.

Rowland-Bamford, A.J., Nordenbrock, C., Baker, J.T., Bowes, G., Allen, L.H., 1990. Changes in stomatal density in rice grown under various CO_2 regimes with natural solar radiation. Environmental and Experimental Botany, 30: 175-180.

Rowson, J.M., 1946. The significance of stomatal index as a differential character. Part III. Studies in the genera *Atropa, Datura, Digitalis, Phytolacca* and in polyploid leaves. Quarterly Journal of Pharmacy and Pharmaceuticals, 19: 136-143.

Royer, D.L., Berner, R.A., Beerling, D.J., 2001. Phanerozoic atmospheric CO_2 change: evaluating geochemical and paleobiological approaches. Earth-Science Reviews, 54: 349-392.

Rundgren, M., Beerling, D., 1999. A Holocene CO_2 record from the stomatal index of sub-fossil *Salix herbacea* L. leaves from northern Sweden. The Holocene, 9: 509-513.

Ryle, G.J.A., Stanley, J., 1992. Effect of elevated CO_2 on stomatal size and distribution in perennial ryegrass. Annals of Botany, 69: 563-565.

Salisbury, E.J., 1927. On the causes and ecological significance of stomatal frequency, with special reference to the woodland flora. Philosophical Transactions of the Royal Society of London, B216: 1-65.

Santamour, F.S., He, S., Ewert, T.E., 1983. Growth, survival and sex expression in *Ginkgo*. Journal of Arboriculture, 9: 170-171.

Savin, S.M., Douglas, R.G., Stehli, F.G., 1975. Tertiary marine paleotemperatures. Geological Society of America Bulletin, 86: 1499-1510.

Schettino, A., Scotese, C.R., 2001. New internet software aids paleomagnetic analysis and plate tectonic reconstructions. Eos (Transactions, American Geophysical Union), 82 (45) (software available at: http://www.itis-molinari.mi.it/plot.htm).

Schoch, P.G., Zinsou, C., Sibi, M., 1980. Dependence of the stomatal index on environmental factors during stomatal differentiation in leaves of *Vigna sinensis* L. I. Effect of light intensity. Journal of Experimental Botany, 31: 1211-1216.

Scott, R.A., Barghoorn, E.S., Prakash, U., 1962. Wood of *Ginkgo* in the Tertiary of western North America. American Journal of Botany, 49: 1095-1101.

Seiwa, K., Kikuzwa, K., 1996. Importance of seed size for the establishment of seedlings of five deciduous broad-leaved tree species. Vegetatio, 123: 51-64.

Sewall, J.O., Sloan, L.C., Huber, M., Wing, S., 2000. Climate sensitivity to changes in land surface characteristics. Global and Planetary Change, 26: 445-465.

Seward, A.C., 1919. Fossil Plants. IV. Ginkgoales, Coniferales, Gnetales. Cambridge University Press, Cambridge.

Shackleton, N.J., 2000. The 100,000-year ice-age cycle identified and found to lag temperature, carbon dioxide, and orbital eccentricity. Science, 289: 1897-1902.

Shaparenko, K., 1935. *Ginkgo adiantoides* (Unger) Heer: Contemporary and fossil forms. The Philippine Journal of Science, 57: 1-28.

Sharma, G.K., Dunn, D.B., 1968. Effect of environment on the cuticular features in *Kalanchoe fedschenkoi*. Bulletin of the Torrey Botanical Club, 95: 464-473.

Sharma, G.K., Dunn, D.B., 1969. Environmental modifications of leaf surface traits in *Datura stramonium*. Canadian Journal of Botany, 47: 1211-1216.

Sinha, A., Stott, L.D., 1994. New atmospheric pCO_2 estimates from paleosols during the late Paleocene / early Eocene global warming interval. Global and Planetary Change, 9: 297-307.

Sloan, L.C., Barron, E.J., 1990. "Equable" climates during Earth history? Geology, 18: 489-492.

Sloan, L.C., Barron, E.J., 1992. A comparison of Eocene climate model results to quantified paleoclimatic interpretations. Palaeogeography, Palaeoclimatology, Palaeoecology, 93: 183-202.

Sloan, L.C., Pollard, D., 1998. Polar stratospheric clouds: a high latitude warming mechanism in an ancient greenhouse world. Geophysical Research Letters, 25: 3517-3520.

Sloan, L.C., Rea, D.K., 1995. Atmospheric carbon dioxide and early Eocene climate: A general circulation modeling sensitivity study. Palaeogeography, Palaeoclimatology, Palaeoecology, 119: 275-292.

Sloan, L.C., Walker, J.C.G., Moore, T.C., 1995. Possible role of oceanic heat transport in early Eocene climate. Paleoceanography, 10: 347-356.

Sloan, L.C., Huber, M., Crowley, T.J., Sewall, J.O., Baum, S., 2001. Effect of sea surface temperature configuration on model simulations of "equable" climate in the Early Eocene. Palaeogeography, Palaeoclimatology, Palaeoecology, 167: 321-335.

Smith, S., Weyers, J.D.B., Berry, W.G., 1989. Variation in stomatal characteristics over the lower surface of *Commelina communis* leaves. Plant, Cell and Environment, 12: 653-659.

Sokal, R.R, Rohlf, F.J., 1995. Biometry. Third Edition. W. . Freeman, New York.

Solárová, J., Pospíšilová, J., 1988. Stomatal frequencies in the adaxial and abaxial epidermes of primary bean leaves affected by growing irradiances. Acta Universitatis Carolinae--Biologica, 31: 101-105.

Speirs, B., 1982. Fossil collecting in Alberta, Canada. Fossils Quarterly, 1(3): 10-16.

Spicer, R.A., 1980. The importance of depositional sorting to the biostratigraphy of plant megafossils. In: Dilcher, D.L., Taylor, T.N. (Eds.), Biostratigraphy of Fossil Plants. Dowden, Hutchinson and Ross, Stroudsburg, pp. 171-183.

Spicer, R.A., Greer, A.G., 1986. Plant taphonomy in fluvial and lacustrine systems. In: Broadhead, T. (Ed.), Land Plants. University of Tennessee Department of Geological Sciences Studies in Geology, 15:10-26.

Spicer, R.A., Herman, A.B., 2001. The Albian-Cenomanian flora of the Kukpowruk River, western North Slope, Alaska: stratigraphy, palaeofloristics, and plant communities. Cretaceous Research, 22: 1-40.

Spicer, R.A., Parrish, J.T., 1990. Late Cretaceous-early Tertiary palaeoclimates of northern high latitudes: A quantitative view. Journal of the Geological Society, London, 147: 329-341.

Stancato, G.C., Mazzoni-Viveiros, S.C., Luchi, A.E., 1999. Stomatal characteristics in different habitat forms of Brazilian species of *Epidendrum* (Orchidaceae). Nordic Journal of Botany, 19: 271-275.

Stewart, J.D., Hoddinott, J., 1993. Photosynthetic acclimation to elevated atmospheric carbon dioxide and UV irradiation in *Pinus banksiana*. Physiologia Plantarum, 88: 493-500.

Stewart, W.N., 1983. Paleobotany and the evolution of plants. Cambridge University Press, Cambridge.

Stott, L.D., 1992. Higher temperatures and lower oceanic pCO_2: a climate enigma at the end of the Paleocene epoch. Paleoceanography, 7: 395-404.

Suchecky, R.K., Hubert, J.F., Birney de Wit, C.C., 1988. Isotopic imprint of climate and hydrogeochemistry on terrestrial strata of the Triassic-Jurassic Hartford and Fundy Rift Basins. Journal of Sedimentary Petrology, 58: 801-811.

Tajika, E., 1998. Climate change during the last 150 million years: reconstruction from a carbon cycle model. Earth and Planetary Science Letters, 160: 695-707.

Tang, C.Q., Ohsawa, M., 1997. Zonal transition of evergreen, deciduous, and coniferous forests along the altitudinal gradient on a humid subtropical mountain, Mt. Emei, Sichuan, China. Plant Ecology, 133: 63-78.

Tang, Z.C., Kozlowski, T.T., 1982. Physiological, morphological, and growth responses of *Platanus occidentalis* seedlings to flooding. Plant and Soil, 66: 243-255.

Taylor, D.W., Hickey, L.J., 1996. Evidence for and implications of an herbaceous origin for angiosperms. In: Taylor, D.W., Hickey, L.J. (Eds.), Flowering Plant Origin, Evolution, and Phylogeny. Chapman and Hall, New York, pp. 232-266.

Thiry, M., Sinha, A., Stott, L.D., 1998. Chemostratigraphy. In: Thiry, M., Dupuis, C. (Eds.), The Palaeocene/Eocene Boundary in the Paris Basin. Memoires des Sciences de la Terre, 34: 21-27.

Thomas, B., Spicer, R.a., 1987. The evolution and paleobotany of land plants. Croom Helm, Kent.

Thomas, J.F., Harvey, C.N., 1983. Leaf anatomy of four species grown under continuous CO_2 enrichment. Botanical Gazette, 144: 303-309.

Thomas, R.L., Anderson, R.C., 1993. Influence of topography on stand composition in a midwestern ravine forest. The American Midland Naturalist, 130: 1-12.

Tichá, I., 1982. Photosynthetic characteristics during ontogenesis of leaves. 7. Stomata density and sizes. Photosynthetica, 16: 375-471.

Tipping, C., Murray, D.R., 1999. Effects of elevated atmospheric CO_2 concentration on leaf anatomy and morphology in *Panicum* species representing different photosynthetic modes. International Journal of Plant Science, 160: 1063-1073.

Tralau, H., 1967. The phytogeographic evolution of the genus *Ginkgo* L. Botaniska Notiser, 120: 409-422.

Tralau, H., 1968. Evolutionary trends in the genus *Ginkgo*. Lethaia, 1: 63-101.

Tsukahara, H., Kozlowski, T.T., 1985. Importance of adventitious roots to growth of flooded *Platanus occidentalis* seedlings. Plant and Soil, 88: 123-132.

Uemura, K., 1997. Cenozoic history of *Ginkgo* in east Asia. In: Hori, T., Ridge, R.W., Tulecke, W., Del Tredici, P., Trémouillaux-Guiller, J., Tobe, H. (Eds.), *Ginkgo biloba*—A Global Treasure. Springer, Tokyo, pp. 207-221.

Upchurch, G.R., Otto-Bliesner, B.L., Scotese, C.R., 1999. Terrestrial vegetation and its effects on climate during the latest Cretaceous. In: Barrera, E., Johnson, C.C. (Eds.), Evolution of the Cretaceous Ocean-Climate System. Geological Society of America Special Paper, 332: 407-426.

Vakhrameev, V.A., 1991. Jurassic and Cretaceous floras and climates of the Earth. English ed. (Translated by Litvinov, J.V.; Edited by Hughes, N.F.) Cambridge University Press, Cambridge.

Van der Burgh, J., Visscher, H., Dilcher, D.L., Kürschner, W.M., 1993. Paleoatmospheric signatures in Neogene fossil leaves. Science, 260: 1788-1790.

Van de Water, P.K., Leavitt, S.W., Betancourt, J.L., 1994. Trends in stomatal density and $^{13}C/^{12}C$ ratios of *Pinus flexilis* needles during last glacial-interglacial cycle. Science, 264: 239-243.

Van Gardingen, P.R., Grace, J., Jeffree, C.E., Byari, S.H., Miglietta, F., Raschi, A., Bettarini, I., 1997. Long-term effects of enhanced CO_2-concentrations on leaf gas exchange: research opportunities using CO_2 springs. In: Raschi, A., Miglietta, F., Tognetti, R., van Gardingen, P.R. (Eds.), Plant Responses to Elevated CO_2. Cambrige University Press, Cambridge, pp. 69-86.

Van Konijnenburg-van Cittert, J.H.A., 1971. *In situ* gymnosperm pollen from the Middle Jurassic of Yorkshire. Botanica Neerlandica, 20: 1-96.

Vasilevskaya, N.D., 1963. Poryakod 2. Ginkgoales, Obshchaya Chast'. In: Takhtajahn, A.L., Vachrameev, V.A., Radchenko, G.P. (Eds.), Osnovy Paleontologii-Golosemennye i Pokrytosemennye. (Spravochnik delya Paleontologov i Geologov SSSR.) Akademiya Nauk SSSR, Moscow, pp. 168-182.

Vasilevskaya, N.D., Kara-Murza, Z.H., 1963. Spetsial'naya Chast', Semeistov Ginkgoaceae. In: Takhtajahn, A.L., Vachrameev, V.A., Radchenko, G.P. (Eds.), Osnovy Paleontologii-Golosemennye i Pokrytosemennye. (Spravochnik delya Paleontologov i Geologov SSSR.) Akademiya Nauk SSSR, Moscow, pp. 182-184.

Veizer, J., Ala, D., Azmy, K., Bruckschen, P., Buhl, D., Bruhn, F., Carden, G.A.F., Diener, A., Ebneth, S., Godderis, Y., Jasper, T., Korte, C., Pawellek, F., Podlaha, O.G., Strauss, H., 1999. $^{87}Sr/^{86}Sr$, $\delta^{13}C$ and $\delta^{18}O$ evolution of Phanerozoic seawater. Chemical Geology, 161: 59-88.

Villar de Seoane, L., 1997. Comparative study between *Ginkgoites tigrensis* Archangelsky and *Ginkgo biloba* Linn. leaves. The Palaeobotanist, 46: 1-12.

Wagner, F., 1998. The influence of environment on the stomatal frequency in *Betula*. LPP Contributions Series, 9: 1-102.

Wagner, F., Below, R., De Klerk, P., Dilcher, D.L., Joosten, H., Kürschner, W.M., Visscher, H., 1996. A natural experiment on plant acclimation: lifetime stomatal frequency response of an individual tree to annual atmospheric CO_2 increase. Proceedings of the National Academy of Sciences USA, 93: 11705-11708.

Wagner, F., Bohncke, S.J.P., Dilcher, D.L., Kürschner, W.M., van Geel, B., Visscher, H., 1999. Century-scale shifts in early Holocene atmospheric CO_2 concentration. Science, 284: 1971-1973.

Wallmann, K., 2001. Controls on the Cretaceous and Cenozoic evolution of seawater composition, atmospheric CO_2 and climate. Geochimica et Cosmochimica Acta, 65: 3005-3025.

Wang, C.-W., 1961. The Forests of China. Maria Moors Cabot Foundation, Cambridge.

Ware, S., Redfearn, P.L., Pyrah, G.L., Weber, W.R., 1992. Soil pH, topography and forest vegetation in the central Ozarks. The American Midland Naturalist, 128: 40-52.

Westoby, M., Jurado, E., Leishman, M., 1992. Comparative evolutionary ecology of seed size. Trends in Ecology and Evolution, 7: 368-372.

White, J.M., Ager, T.A., Adam, D.P., Leopold, E.B., Liu, G., Jetté, H., Schweger, C.E., 1997. An 18 million year record of vegetation and climate change in northwestern

Canada and Alaska: tectonic and global climatic correlates. Palaeogeogrpahy, Palaeoclimatology, Palaeoecology, 130: 293-306.

Wilf, P., 2000. Late Paleocene-early Eocene climate changes in southwestern Wyoming: paleobotanical analysis. Geological Society of America Bulletin, 112: 292-307.

Wiltshire, J.J.J., Wright, C.J., Colls, J.J., Craigon, J., Unsworth, M.H., 1996. Some foliar characteristics of ash trees (*Fraxinus excelsior*) exposed to ozone episodes. New Phytologist, 134: 623-630.

Wing, S.L., 1984. Relation of paleovegetation to geometry and cyclicity of some fluvial carbonaceous deposits. Journal of Sedimentary Petrology, 54: 52-66.

Wing, S.L., 1991. "Equable" climates during Earth history?: Comment. Geology, 19: 539-540.

Wing, S.L., Boucher, L.D., 1998. Ecological aspects of the Cretaceous flowering plant radiation. Annual Review in Earth and Planetary Sciences, 26: 379-421.

Wing, S.L., Greenwood, D.R., 1993. Fossils and fossil climate: The case for equable continental interiors in the Eocene. Philosophical Transactions of the Royal Society London, B341: 243-252.

Wing, S.L., Alroy, J., Hickey, L.J., 1995. Plant and mammal diversity in the Paleocene to Early Eocene of the Bighorn Basin. Palaeogeography, Palaeoclimatology, Palaeoecology, 115: 117-155.

Wing, S.L., Bao, H., Koch, P.L., 2000. An early Eocene cool period? Evidence for continental cooling during the warmest part of the Cenozoic. In: Huber, B.T., MacLeod, K.G., Wing, S.L. (Eds.), Warm Climates in Earth History. Cambridge University Press, Cambridge, pp. 197-237.

Wolfe, J.A., 1977. Paleogene floras from the Gulf of Alaska region. U.S. Geological Survey Professional Paper, 997: 1-108.

Wolfe, J.A., 1994. Tertiary climatic changes at middle latitudes of western North America. Palaeogeography, Palaeoclimatology, Palaeoecology, 108: 195-205.

Woodward, F.I., 1986. Ecophysiological studies on the shrub *Vaccinium myrtillus* L. taken from a wide altitudinal range. Oecologia, 70: 580-586.

Woodward, F.I., 1987. Stomatal numbers are sensitive to increases in CO_2 from pre-industrial levels. Nature, 327: 617-618.

Woodward, F.I., 1988. The responses of stomata to changes in atmospheric levels of CO_2. Plants Today, 1: 132-135.

Woodward, F.I., Bazzaz, F.A., 1988. The responses of stomatal density to CO_2 partial pressure. Journal of Experimental Botany, 39: 1771-1781.

Woodward, F.I., Beerling, D.J., 1997. Plant-CO_2 responses in the long term: plants from CO_2 springs in Florida and tombs in Egypt. In: Raschi, A., Miglietta, F., Tognetti, R., van Gardingen, P.R. (Eds.), Plant Responses to Elevated CO_2. Cambridge University Press, Cambridge, pp. 103-113.

Woodward, F.I., Kelly, C.K., 1995. The influence of CO_2 concentration on stomatal density. New Phytologist, 131: 311-327.

Wyman, D., 1965. *Ginkgo biloba fastigiata*. American Nurseryman, 121(11): 37.

Yapp, C.J., Poths, H., 1992. Ancient atmospheric CO_2 pressures inferred from natural goethites. Nature, 355: 342-344.

Yapp, C.J., Poths, H., 1996. Carbon isotopes in continental weathering environments and variations in ancient atmospheric CO_2 pressure. Earth and Planetary Science Letters, 137: 71-82.

Yoshitama, K., 1997. Flavonoids of *Ginkgo biloba*. In: Hori, T., Ridge, R.W., Tulecke, W., Del Tredici, P., Trémouillaux-Guiller, J., Tobe, H. (Eds.), *Ginkgo biloba*—A Global Treasure. Springer, Tokyo, pp. 287-299.

Zacchini, M., Morini, S., Vitagliano, C., 1997. Effect of photoperiod on some stomatal characteristics of *in vitro* cultured fruit tree shoots. Plant, Cell, Tissue and Organ Culture, 49: 195-200.

Zachos, J.C., Stott, L.D., Lohmann, K.C., 1994. Evolution of early Cenozoic marine temperatures. Paleoceanography, 9: 353-387.

Zachos, J., Pagani, M., Sloan, L., Thomas, E., Billups, K., 2001. Trends, rhythms, and aberrations in global climate 65 Ma to present. Science, 292: 686-693.

Zhang, S.T., Zeng, Y.Y., Xie, W.B., 1992. The distribution and production of *Ginkgo* in Hunan province. In: Bulletin of the First National Symposium on *Ginkgo*. Hubei Science and Technology Press, Wuhan.

Zhou, Z., 1993. Comparative ultrastructure of fossil and living ginkgoacean megasporemembranes. Review of Palaeobotany and Palynology, 78: 167-182.